

New Ideas for the Penalty Method

by

Xihui Xie

B.S. in Mathematics, Shanghai Jiao Tong University, 2015

M.A. in Mathematics, University of Wisconsin, 2016

Submitted to the Graduate Faculty of
the Dietrich School of Arts and Sciences in partial fulfillment
of the requirements for the degree of
Doctor of Philosophy

University of Pittsburgh

2022

UNIVERSITY OF PITTSBURGH
DIETRICH SCHOOL OF ARTS AND SCIENCES

This dissertation was presented

by

Xihui Xie

It was defended on

July 12th 2022

and approved by

William Layton, Professor of Mathematics, University of Pittsburgh

Michael Neilan, Professor of Mathematics, University of Pittsburgh

Catalin Trenchea, Professor of Mathematics, University of Pittsburgh

Hessam Babaei, Assistant Professor of Engineering, University of Pittsburgh

Dissertation Director: William Layton, Professor of Mathematics, University of Pittsburgh

New Ideas for the Penalty Method

Xihui Xie, PhD

University of Pittsburgh, 2022

My research is directed at accurate predictions of the flow of fluids and what the fluid transports. This is essential for many critical engineering and scientific applications, including climate change and energy efficiency optimization. For example, 85% of the energy in the US is generated by combustion, for which accurate simulation of turbulent mixing is critical for energy efficiency optimization. To address these, my research develops algorithms that have the potential to break current barriers in accuracy, reliability and efficiency in CFD, and a rigorous mathematical foundation addressing when they work and how they fail, at the crossroads of theory and practical computation.

My research considers the adaptivity of the penalty parameter ϵ both in space and in time. In the first project, I consider the ϵ -adaptive penalty methods for the Navier-Stokes equation. The unconditional stability is proven for velocity when adapting ϵ . The stability of the velocity time derivative under conditions on the rate of change of the penalty parameter is also analyzed. The analysis and tests show that adapting ϵ in response to $\|\nabla \cdot u\|$ removes the problem of picking ϵ and yields good approximations for the velocity. The adaptive penalty parameter method is supplemented by also adapting the time-step. The penalty parameter ϵ and time-step are adapted independently.

The second project proposes and analyzes a new adaptive penalty scheme, which picks the penalty parameter ϵ element by element small where $\|\nabla \cdot u\|$ is large. The research starts by analyzing and testing the new scheme in the most simple but interesting setting, the Stokes problem. Finally, this adaptive method is extended and tested on the incompressible Navier-Stokes equation on complex flow problems. The scheme is developed in the penalty method but also can be used to pick a grad-div stabilization parameter.

Table of Contents

Preface	ix
1.0 Introduction	1
1.1 The Incompressible Navier-Stokes Equations	4
1.2 The Penalty Method	7
1.3 Notation and preliminaries	7
2.0 Adapting ϵ in time	13
2.1 Introduction	13
2.1.1 Review of a Common Penalty Method	14
2.1.2 Related work	16
2.1.3 Motivation For Choice of Estimator for ϵ	16
2.2 Stability of Backward Euler	17
2.2.1 Stability of the velocity	18
2.2.2 Stability of $\ u_t\ $ for the linear Stokes problem	19
2.3 Error Analysis	23
2.4 Algorithms	29
2.5 Numerical Experiments	36
2.5.1 Modified Taylor-Green vortex, taken from [18]	36
2.5.1.1 Modified test 1	36
2.5.1.2 Modified test 2	39
2.5.2 A test with exact solution, taken from [17]	44
2.5.2.1 Constant time-step, variable ϵ test	45
2.5.2.2 Double Adaptive	48
2.5.3 Flow Between Offset Circles, taken from [48]	49
3.0 Adapting ϵ in space	53
3.1 Introduction	53
3.1.1 Previous Work	55

3.1.2 Formulation	55
3.2 Analysis	58
3.2.1 Stability	58
3.2.2 Error analysis	61
3.3 Algorithm	66
3.4 Numerical Tests	69
3.4.1 Test 1: An exact solution problem, taken from Burman and Hansbo [12]	69
3.4.2 Test 2: Flow between offset cylinders, taken from Layton and McLaugh-	
lin [48]	71
3.4.3 Test3. Comparison test between constant penalty and elementwise	
penalty see Layton and Xu [52]	73
3.4.4 Test4: Flow around a cylinder, see Ingram [33], John, Matthies and	
Rang [40]	75
3.4.4.1 Comparison with constant penalty methods	77
4.0 Conclusions and future perspectives	83
Bibliography	85

List of Tables

1	Comparison of velocity error $\ u - u^h\ _{L_2 L_2}$	39
2	Constant time-step variable ϵ error comparison	46
3	Variable time-step error comparison	48
4	numerical error $\ u - u^h\ _{L^2}$ and convergence rate of elementwise penalty (compared with coupled system (54))	71
5	numerical error $\ \nabla(u - u^h)\ _{L^2}$ and convergence rate of elementwise penalty (compared with coupled system (54))	72
6	numerical error $\ \nabla \cdot (u - u^h)\ _{L^4}^2$ and convergence rate of elementwise penalty (compared with coupled system (54))	72
7	$\ \nabla \cdot u^h\ ^2$ numerical result of Test 1	72
8	numerical result $\ \nabla \cdot u^h\ ^2$ of Test 2 Stokes problem	73
9	comparison of $\ \nabla \cdot u^h\ ^2$ and average value of ϵ between constant penalty and elementwise penalty (Algorithm 1)	75
10	Comparison of $\Delta p(8)$, method 1) by solving system $\nabla \cdot u^h + \epsilon_\Delta p^h = 0$, method 2) by direct calculating $p^h = -1/\epsilon_\Delta(\nabla \cdot u^h)$	82

List of Figures

1	plot of the differentiable function $F(t)$ over time interval $[0, 25]$	37
2	Test1: Comparison between adaptive penalty (Algorithm 1) and two constant penalty methods, tests are done with 100 mesh points per side and $\Delta t = 0.005$.	38
3	Test1: Pressure error comparison between adaptive penalty (Algorithm 1) and two constant penalty methods, tests are done with 100 mesh points per side and $\Delta t = 0.005$	39
4	Test2: Comparison of $\ \nabla \cdot u\ $ and discrete $\ u_t\ $ between adaptive penalty (Algorithm 1) and two constant penalty methods, tests are done with 100 mesh points per side and $\Delta t = 0.005$	40
5	Test2: Zoomed in comparison of $\ \nabla \cdot u\ $ and discrete $\ u_t\ $ between adaptive penalty (Algorithm 1) and constant penalty $\epsilon = 10^{-8}\nu$, tests are done with 100 mesh points per side and $\Delta t = 0.005$	41
6	Test2: Evolution of $\ \nabla \cdot u\ $ of constant penalty $\epsilon = 10^{-8}\nu$, tests are done with 100 mesh points per side and $\Delta t = 0.005$	42
7	Test2: Evolution of ϵ and $\ u - u^h\ $ between adaptive penalty (Algorithm 1) and two constant penalty methods, tests are done with 100 mesh points per side and $\Delta t = 0.005$	43
8	Test2: Comparison of $\ p - p^h\ $ and discrete $\ p^h\ $ between adaptive penalty (Algorithm 1) and two constant penalty methods, tests are done with 100 mesh points per side and $\Delta t = 0.005$	44
9	$\ (u - u^h)(10)\ $ with constant time-step and different values of penalty parameter ϵ	45
10	Comparison of results with different Δt of variable ϵ , constant time-step method (Algorithm 1)	46
11	log-log plot, log of velocity error at final step $T=10$ $\ (u - u^h)(10)\ $ v.s. $\log \Delta t$ using variable ϵ constant time-step method (Algorithm 1). Slope of plot $\ (u - u^h)(10)\ $ is close to 2.	47

12	Comparison of variable time-step, variable ϵ method (Algorithm 2,3,4)	49
13	$\ u_t\ $ plot of variable time-step, variable ϵ method (Algorithm 2,3,4) The spikes show at the time when ϵ decrease too fast (violation of (34))	50
14	Comparison between different estimators $\ \nabla \cdot u\ $ and $\ \nabla \cdot u\ /\ \nabla u\ $, $Re = 100$, $\Delta t =$ 0.005 with Algorithm 1 (constant time-step, variable ϵ). No penalty uses Back- ward Euler with grad-div stabilization (41) with $\Delta t = 0.001$. Tests without penalty use 320 mesh points around the outer circle and 80 mesh points around the inner circle. The finite element discretization has a maximal mesh width of $h_{max} = 0.0347224$	51
15	$ \nabla \cdot u^h _{\Delta}^2/ \Delta $ with 10 mesh points on each side	70
16	$ \nabla \cdot u^h _{\Delta}^2/ \Delta $ with 20 mesh points on each side	70
17	$ \nabla \cdot u^h _{\Delta}^2/ \Delta $ with 40 mesh points on each side	71
18	$\ \nabla \cdot u^h\ _{\Delta}^2/ \Delta $ of Test 2, comparison between coupled (54) and elementwise penalty system (Algorithm 5) (Note the scale in two plots are different. Cou- pled Stokes problem $\max_{\Delta} \ \nabla \cdot u^h\ _{\Delta}^2 = \mathcal{O}(10^2)$, elementwise penalty method $\max_{\Delta} \ \nabla \cdot u^h\ _{\Delta}^2 = \mathcal{O}(10^{-17})$)	74
19	velocity plot of Test 2, comparison between coupled (54) and elementwise penalty system (Algorithm 5)	75
20	magnitude of velocity field at $T = 2, 4, 5, 6, 7, 8$ of Test 4 Algorithm 6 for NSE, $\Delta t = 0.005$	77
21	Plot of $\ \nabla \cdot u^h\ ^2$ from $T=0$ to $T=8$	78
22	result of Test 4 Algorithm 6 for NSE, $\Delta t = 0.005$	79
23	Comparison of $\ \nabla \cdot u^h\ $ using Algorithm 6 and constant penalty methods	80
24	Comparison of drag and lift coefficients, pressure recovery by solving system $\nabla \cdot u^h + \epsilon_{\Delta} p^h = 0$	81
25	Comparison of drag and lift coefficients, pressure recovery by direct calculating $p^h = -1/\epsilon_{\Delta}(\nabla \cdot u^h)$	81

Preface

I would like to thank a number of people for their help and support during the production of this thesis.

First and foremost I am extremely grateful to my advisor, Prof. William Layton for his invaluable advice, continuous support and guidance during all the time of research. I could not have imagined having a better advisor for my Ph.D. study.

I also could not undertaken this journey without my thesis committee members, Prof. Michael Neilan, Prof. Catalin Trenchea and Prof. Hessam Babaei, who generously provided immense knowledge and suggestions.

Moreover, I would like to thank all the faculties and staff members, my friends in the math department who helped and inspired me.

Lastly, I would like to thank my family, especially my parents. Their unconditional support has kept me motivated during this process.

1.0 Introduction

My research considers the adaptivity of the penalty parameter ϵ both in space and in time. The penalty method on NSE decouples velocity and pressure and makes it easier to solve the system. However, the penalty method is sensitive to the penalty parameter ϵ value and also has some accuracy issues throughout the time. We want to find an automatic epsilon self-adaptive algorithm that is time efficient and also costs low storage of memory.

The method with the lowest space and computational complexity is based on penalization of incompressibility and elimination of the pressure. This method has difficulties with its high sensitivity to the precise choice of the penalization parameter. My research is inspired by the observation of von Neumann that sensitivity makes prediction hard but control easy. I thus consider the penalty parameter as a control for the incompressibility error, so the algorithms act like an AI system which automatically selects near-optimal epsilons.

In the first project, I consider the ϵ -adaptive penalty methods for the Navier-Stokes equation (NSE).

Let u denote the fluid velocity, p pressure, ν viscosity and f the external force:

$$u_t - \nu \Delta u + u \cdot \nabla u + \nabla p = f, \quad \nabla \cdot u = 0. \quad (1)$$

The velocity and pressure are coupled together by the incompressibility constraint $\nabla \cdot u = 0$. Coupled systems require more memory to store and are more expensive to solve. Penalty methods replace $\nabla \cdot u = 0$ with $\nabla \cdot u + \epsilon(t)p = 0$ where $0 < \epsilon \ll 1$. The pressure can be eliminated using $\nabla p = -\nabla(1/\epsilon(t)\nabla \cdot u)$. This results in a system of u only, which takes less computing time and less storage memory to solve than (1):

$$u_{\epsilon,t} - \nu \Delta u_\epsilon + u_\epsilon \cdot \nabla u_\epsilon + \frac{1}{2}(\nabla \cdot u_\epsilon)u_\epsilon - \nabla\left(\frac{1}{\epsilon(t)}\nabla \cdot u_\epsilon\right) = f. \quad (2)$$

Here $u_\epsilon \cdot \nabla u_\epsilon + \frac{1}{2}(\nabla \cdot u_\epsilon)u_\epsilon$ is the modified bilinear term introduced by Temam [63]. This bilinear term ensures the dissipativity of the system (28). The unconditional stability is proven for velocity when adapting ϵ . The stability of the velocity time derivative under conditions on the rate of change of the penalty parameter is also analyzed. The stability

conditions on ϵ that are derived from the linear Stokes problem are necessary for the case of nonlinear NSE. The analysis shows that we could increase ϵ arbitrarily in each time step but could not decrease too much. The analysis and tests also show that adapting ϵ in response to the norm of $\|\nabla \cdot u\|$ removes the problem of picking ϵ and yields good approximations for the velocity. The adaptive penalty parameter method is supplemented by also adapting the time-step with the help of time-filter [26, 48]. The penalty parameter ϵ and time-step are adapted independently.

In the second project, a new adaptive penalty scheme is proposed and analyzed, which picks the penalty parameter ϵ element by element small where the norm of $\|\nabla \cdot u\|$ is large. The research starts by analyzing and testing the new scheme in the most simple but interesting setting, the Stokes problem.

Let u denote the fluid velocity, p pressure, ν viscosity and f the external force:

$$-\nu\Delta u + \nabla p = f(x), \quad \nabla \cdot u = 0. \quad (3)$$

On a bounded, open polyhedral domain Ω subject to no-slip boundary conditions $u = 0$ on $\partial\Omega$. Penalty methods replace $\nabla \cdot u = 0$ with $\nabla \cdot u + \epsilon p = 0$ where $0 < \epsilon \ll 1$. The pressure can be eliminated using $\nabla p = -\nabla(1/\epsilon \nabla \cdot u)$. Here we consider ϵ as a function of finite elements Δ .

Hence, the penalty approximation we considered is: find $u^h \in X^h$ such that

$$\nu(\nabla u_\epsilon^h, \nabla v^h) + \sum_{\Delta} \int_{\Delta} \epsilon_{\Delta}^{-1} \nabla \cdot u_\epsilon^h \nabla \cdot v^h \, dx = (f, v^h). \quad (4)$$

Next, we localize the global tolerance TOL for $\|\nabla \cdot u_\epsilon^h\|$ and define the local tolerance as

$$\text{LocTol}_{\Delta} := \frac{1}{2} \frac{TOL^2}{|\Omega|} |\Delta|.$$

And here we have two options for ϵ_{Δ} :

Option 1. Elementwise Penalty (EP)

$$\epsilon_{\Delta} := \frac{\text{LocTol}_{\Delta}}{\|\nabla \cdot u_\epsilon^h\|_{\Delta}^2}.$$

Such that the variational form becomes: find $u_\epsilon^h \in X^h$ such that

$$\int_{\Omega} \nu \nabla u_\epsilon^h : \nabla v^h \, dx + \sum_{\Delta} \frac{1}{LocTol_{\Delta}} \|\nabla \cdot u_\epsilon^h\|_{\Delta}^2 \int_{\Delta} \nabla \cdot u_\epsilon^h \nabla \cdot v^h \, dx = \int_{\Omega} f \cdot v^h \, dx. \quad (5)$$

Option 2. Pointwise Penalty (PP)

$$\epsilon_{\Delta}(x) := \frac{LocTol_{\Delta}}{|\nabla \cdot u_\epsilon^h(x)|^2}.$$

Such that the variational form becomes: find $u_\epsilon^h \in X^h$ such that

$$\int_{\Omega} \nu \nabla u_\epsilon^h : \nabla v^h \, dx + \sum_{\Delta} \frac{1}{LocTol_{\Delta}} \int_{\Delta} |\nabla \cdot u_\epsilon^h|^2 \nabla \cdot u_\epsilon^h \nabla \cdot v^h \, dx = \int_{\Omega} f \cdot v^h \, dx. \quad (6)$$

We focus herein on the analysis of option 2 (PP) and the numerical results of option 1 (EP). In option 2 (PP), the resulting nonlinearity is both strongly monotone and locally Lipschitz continuous, sharing structures with the p-Laplacian. Then, there is a well-trodden analytical path to be adapted here. We proved the stability for both PP and EP. Also, error analysis of PP using strong monotonicity and local Lipschitz continuity is given in Chapter 3.

Finally, this adaptive method is extended and tested on the incompressible time-dependent Navier-Stokes equation on complex flow problems. The scheme is developed in the penalty method but also can be used to pick a grad-div stabilization parameter.

In the following few sections of Chapter 1, the Navier-Stokes equations, notations and preliminaries are introduced. Chapter 2 is based on paper *A Doubly Adaptive Penalty Method for the Navier-Stokes Equations* [42]. In Chapter 2, we present an overview of penalty methods and our results of time-adaptive penalty methods. Chapter 3 is based on paper *On Adaptive Grad-Div Parameter Selection* [65]. In Chapter 3, a new space-adaptive was developed and tested on the Stokes and the Navier-Stokes equations. Finally, conclusions and future perspectives are presented in Chapter 4.

1.1 The Incompressible Navier-Stokes Equations

There have been plenty of work on details of derivation of the Navier-Stokes equations [60, 64, 25, 37, 22, 30, 10, 24, 57, 19]. We refer the reader to [39, 47] for a more comprehensive explanation. The derivation herein is derived from these two books.

Let Ω be an open domain in \mathbb{R}^d ($d = 2, 3$) with boundary $\partial\Omega$. We denote by \mathbf{x} the spatial variable, ρ the density of the fluid, u is the velocity, and p is the pressure of the flow. The equation describing the conservation of mass is called the continuity equation. We let the mass of the fluid equal

$$m(t) = \int_{\Omega} \rho \, d\mathbf{x}.$$

If mass is conserved, the rate of change of mass in Ω equal the net mass flux across $\partial\Omega$:

$$\frac{d}{dt} \int_{\Omega} \rho \, d\mathbf{x} = - \int_{\partial\Omega} (\rho u) \cdot \mathbf{n} \, dS.$$

The Divergence Theorem then implies:

$$- \int_{\partial\Omega} (\rho u) \cdot \mathbf{n} \, dS = - \int_{\Omega} \nabla \cdot (\rho u) \, d\mathbf{x}.$$

Rearranging, we have

$$\int_{\Omega} \frac{\partial \rho}{\partial t} + \nabla \cdot (\rho u) \, d\mathbf{x} = 0.$$

Shrinking Ω to a point yields

$$\frac{\partial \rho}{\partial t} + \nabla \cdot (\rho u) = 0.$$

If the fluid is incompressible and homogeneous, $\rho(\mathbf{x}, t) \equiv \rho_0$ and conservation of mass reduces to:

$$\nabla \cdot u = 0, \tag{7}$$

which is the incompressible condition on the fluid velocity u we used for the rest of our thesis.

Conservation of momentum states that the rate of change of linear momentum equals the net forces acting on a collection of fluid particles, i.e., *force = mass \times acceleration*. Let us consider a fluid particle. At position \mathbf{x} , time t and after Δt it moved to $(\mathbf{x} + u\Delta t, t + \Delta t)$. The acceleration is therefore:

$$\lim_{\Delta t \rightarrow 0} \frac{u(\mathbf{x} + u\Delta t, t + \Delta t) - u(\mathbf{x}, t)}{\Delta t} = u_t + (u \cdot \nabla)u.$$

Then, *mass* \times *acceleration* in Ω is

$$\int_{\Omega} \rho(u_t + u \cdot \nabla u) \, d\mathbf{x},$$

and by the conservation of momentum this need to be balanced by forces (both internal and external).

Let f be the external forces acting on the fluid. Internal forces of a fluid are contact forces that act on the surface of the fluid. Then the net contribution of the external force on Ω is

$$\int_{\Omega} f \, d\mathbf{x}.$$

Let \vec{t} denote the internal force called Cauchy stress vector or traction vector, then the net contribution of the internal forces on Ω is

$$\int_{\partial\Omega} \vec{t} \, dS.$$

Thus, the equation for conservation of momentum is

$$\int_{\Omega} \rho(u_t + u \cdot \nabla u) \, d\mathbf{x} = \int_{\Omega} f \, d\mathbf{x} + \int_{\partial\Omega} \vec{t} \, dS.$$

Cauchy proved that if linear momentum is conserved then \vec{t} is a linear function of the normal vector \mathbf{n} . Thus,

$$\vec{t}(\mathbf{n}) = \mathbf{n} \cdot \Pi,$$

where Π is a matrix called the stress tensor. Rearranging,

$$\int_{\Omega} \rho(u_t + u \cdot \nabla u) - \nabla \cdot \Pi \, d\mathbf{x} = \int_{\Omega} f \, d\mathbf{x}.$$

Shrinking Ω to a point yields

$$\rho(u_t + u \cdot \nabla u) - \nabla \cdot \Pi = f.$$

There are two main types of internal forces: pressure forces and viscous forces. The pressure forces act on a surface purely normal to the surface. Therefore we define the pressure in

an incompressible flow is $p := \frac{1}{3}(\Pi_{11} + \Pi_{22} + \Pi_{33})$. Thus the pressure force is $-p\mathbb{I}\mathbf{n}$. The non-pressure part of the stress tensor is the viscous stress tensor \mathbb{V} :

$$\mathbb{V} := \Pi + p\mathbb{I}.$$

The system is not closed until \mathbb{V} is related to the fluid velocity. The internal force depends on local velocity differences, so \mathbb{V} depends on some combination of derivatives of u . The combination is denoted by \mathbb{D} , called the deformation tensor. We assume here the fluid follows the linear stress-deformation relation: $\mathbb{D} = \frac{1}{2}(\nabla u + \nabla u^t)$. And considering here we are dealing with the incompressible flow, the relation between Cauchy stress tensor and deformation tensor is given by

$$\mathbb{V} = 2\mu\mathbb{D},$$

where μ is the viscosity coefficient. The momentum equation then becomes,

$$\rho(u_t + u \cdot \nabla u) - \nabla \cdot (2\mu\mathbb{D} - p\mathbb{I}) = f.$$

Here $\nabla \cdot (p\mathbb{I}) = \nabla \cdot p$ and $\nabla \cdot (2\mu\mathbb{D}) = \mu\Delta u$. Dividing by the density ρ , the momentum equation then reduce to

$$u_t + u \cdot \nabla u - \frac{\mu}{\rho}\Delta u + \nabla \left(\frac{p}{\rho} \right) = \frac{f}{\rho}.$$

Now redefine the pressure p, f to be $p/\rho, f/\rho$ respectively and let $\mu/\rho =: \nu$ the kinematic viscosity. Coupling with the incompressible condition (7), we then have the incompressible Navier-Stokes Equation: $\nabla \cdot u = 0$ and

$$u_t + u \cdot \nabla u - \nu\Delta u + \nabla p = f.$$

1.2 The Penalty Method

Consider the incompressible Navier-Stokes Equations,

$$u_t - \nu \Delta u + u \cdot \nabla u + \nabla p = f, \quad \nabla \cdot u = 0. \quad (8)$$

The velocity and pressure are coupled together by the incompressibility constraint $\nabla \cdot u = 0$. Coupled systems require more memory to store and are more expensive to solve. There are many strategies to overcome this difficulty; one popular approach is to relax the incompressible constraint. Among these are the penalty method and the artificial compressibility method, the pressure stabilization method and the projection method, see [14, 15, 62, 63, 61, 11, 58, 59, 55, 43, 44]. Here we consider the Penalty method.

Penalty methods replace $\nabla \cdot u = 0$ with $\nabla \cdot u + \epsilon(t)p = 0$ where $0 < \epsilon \ll 1$. The pressure can be eliminated using $\nabla p = -\nabla(1/\epsilon \nabla \cdot u)$. This results in a system of u only, which is easier to solve than (8):

$$u_{\epsilon,t} - \nu \Delta u_{\epsilon} + u_{\epsilon} \cdot \nabla u_{\epsilon} + \frac{1}{2}(\nabla \cdot u_{\epsilon})u_{\epsilon} - \nabla \left(\frac{1}{\epsilon} \nabla \cdot u_{\epsilon} \right) = f. \quad (9)$$

Here $u_{\epsilon} \cdot \nabla u_{\epsilon} + \frac{1}{2}(\nabla \cdot u_{\epsilon})u_{\epsilon}$ in the modified nonlinear term introduced by Temam [63].

1.3 Notation and preliminaries

We denote by $\|\cdot\|$ and (\cdot, \cdot) the $L^2(\Omega)$ norm and inner product, respectively. We denote by $\|\cdot\|_{L^p}$ the $L^p(\Omega)$ norm. The velocity space X and pressure space Q are:

$$X := (H_0^1(\Omega))^d, \text{ where } H_0^1(\Omega) = \{v \in L^2(\Omega) : \nabla v \in L^2(\Omega) \text{ and } v = 0 \text{ on } \partial\Omega\},$$

$$Q := L_0^2(\Omega) = \{q \in L^2(\Omega) : \int_{\Omega} q \, dx = 0\}.$$

Let $X^h \subset X$ be the finite element velocity space and $Q^h \subset Q$ be the finite element pressure space. We assume that (X^h, Q^h) are conforming and satisfy the following approximation properties and Condition 1.3.1:

$$\begin{aligned} \inf_{v \in X^h} \|u - v\| &\leq Ch^{m+1}|u|_{m+1}, \quad u \in H^{m+1}(\Omega)^d, \\ \inf_{v \in X^h} \|\nabla(u - v)\| &\leq Ch^m|u|_{m+1}, \quad u \in H^{m+1}(\Omega)^d, \\ \inf_{q \in Q^h} \|p - q\| &\leq Ch^m|p|_m, \quad p \in H^m(\Omega). \end{aligned} \quad (10)$$

Condition 1.3.1. (The Ladyzhenskaya-Babuska-Brezzi Condition (LBB^h) see [22], p.62 [47]).

Suppose (X^h, Q^h) satisfies:

$$\inf_{q^h \in Q^h} \sup_{v^h \in X^h} \frac{(q^h, \nabla \cdot v^h)}{\|\nabla v^h\| \|q^h\|} \geq \beta^h > 0, \quad (11)$$

where β^h is bounded away from zero uniformly in h .

The (LBB^h) condition is equivalent to:

$$\beta^h \|q^h\| \leq \sup_{v^h \in X^h} \frac{(q^h, \nabla \cdot v^h)}{\|\nabla v^h\|}, \quad \forall q \in Q^h.$$

The space $H^{-1}(\Omega)$ denotes the dual space of bounded linear functional defined on $H_0^1(\Omega)$.

This space is equipped with the norm:

$$\|f\|_{-1} = \sup_{0 \neq v \in X} \frac{(f, v)}{\|\nabla v\|}.$$

Let I^h denote the interpolation in the space of C^0 piecewise linears, suppose the following interpolation estimate in $H^{-1}(\Omega)$ holds (see p.160 [47], p.146 of Theorem of Brenner and Scott [9])

$$\|u - I^h(u)\|_{H^{-1}(\Omega)} \leq Ch\|u - I^h(u)\|. \quad (12)$$

Denote by $b^*(u, v, w)$, the skew-symmetric trilinear form, is

$$b^*(u, v, w) := \frac{1}{2}(u \cdot \nabla v, w) - \frac{1}{2}(u \cdot \nabla w, v) \quad \forall u, v, w \in [H^1(\Omega)]^d.$$

A weak formulation of the penalty NSE is: find $u : (0, T] \rightarrow X$ such that

$$\begin{aligned} (u_t, v) + b^*(u, u, v) + \nu(\nabla u, \nabla v) + \frac{1}{\epsilon}(\nabla \cdot u, \nabla \cdot v) &= (f, v), \quad \forall v \in X, \\ u(\mathbf{x}, 0) &= u^0(\mathbf{x}). \end{aligned}$$

Lemma 1.3.2. (*skew-symmetry see p.123 p.155 [47], upper bound for the product of three functions see p.11 [47]*) There exists C_1 and C_2 such that for all $u, v, w \in X$, $b^*(u, v, w)$ satisfies

$$\begin{aligned} b^*(u, v, w) &= (u \cdot \nabla v, w) + \frac{1}{2}((\nabla \cdot u)v, w), \\ b^*(u, v, w) &\leq C_1 \|\nabla u\| \|\nabla v\| \|\nabla w\|, \\ b^*(u, v, w) &\leq C_2 \sqrt{\|u\| \|\nabla u\|} \|\nabla v\| \|\nabla w\|. \end{aligned}$$

Moreover, if $v \in H^2(\Omega)$, then there exists C_3 such that

$$b^*(u, v, w) \leq C_3 (\|u\| \|v\|_2 \|\nabla w\| + \|\nabla \cdot u\| \|\nabla v\| \|\nabla w\|).$$

Further, if $v \in H^2(\Omega) \cap L^\infty(\Omega)$, then

$$b^*(u, v, w) \leq (C_3 \|v\|_2 + \|v\|_\infty) \|u\| \|\nabla w\|.$$

Lemma 1.3.3. (*The Poincaré-Friedrichs' inequality see [46], p.9 [47]*) There is a positive constant $C_{PF} = C_{PF}(\Omega)$ such that

$$\|u\| \leq C_{PF} \|\nabla u\| \quad \forall u \in X. \quad (13)$$

Lemma 1.3.4. (*A Sobolev inequality see [2], [47]*) Let Ω be a bounded open set and suppose $\nabla u \in L^p(\Omega)$ with $u = 0$ on a subset of $\partial\Omega$ with positive measure. Then there is a $C = C(\Omega, p)$ such that for $1 \leq p < \infty$,

$$\begin{aligned} \|u\|_{L_{p^*}} &\leq C \|\nabla u\|_{L^p}, \\ \text{where } \frac{1}{p^*} &= \frac{1}{p} - \frac{1}{\dim(\Omega)} \text{ if } p < \dim(\Omega). \end{aligned}$$

For example, with $p = 2$, for $1 \leq p^* < \infty$ in $2d$ and $1 \leq p^* \leq 6$ in $3d$,

$$\|u\|_{L_{p^*}} \leq C \|\nabla u\|. \quad (14)$$

Lemma 1.3.5. (Useful inequalities see [7], p.7 [47], polarization identity) The L^2 inner product satisfies the Hölder's and Young's inequalities: for any $u, v \in X$, for any δ , $0 < \delta < \infty$ and $\frac{1}{p} + \frac{1}{q} = 1$, $1 \leq p, q \leq \infty$,

$$(u, v) \leq \|u\|_{L^p} \|v\|_{L^q}, \text{ and } (u, v) \leq \frac{\delta}{p} \|u\|_{L^p}^p + \frac{\delta^{-q/p}}{q} \|v\|_{L^q}^q. \quad (15)$$

Further, for any $u, v, w \in X$, for any p, q, r , $1 \leq p, q, r \leq \infty$, with $\frac{1}{p} + \frac{1}{q} + \frac{1}{r} = 1$,

$$\int_{\Omega} |u| |v| |w| dx \leq \|u\|_{L^p} \|v\|_{L^q} \|w\|_{L^r}. \quad (16)$$

Polarization identity: for any $u, v \in X$

$$(u, v) = \frac{1}{2} \|u\|^2 + \frac{1}{2} \|v\|^2 - \frac{1}{2} \|u - v\|^2. \quad (17)$$

Proposition 1.3.6. (see p.173 of [8]) Let $W^{m,p}(\Omega)$ denote the Sobolev space, d denote the dimension of space Ω , let $p \in [1, +\infty]$ and $q \in [p, p^*]$. There is a $C > 0$ such that

$$\|u\|_{L^q} \leq C \|u\|_{L^p}^{1+d/q-d/p} \|u\|_{W^{1,p}}^{d/p-d/q}, \quad \forall u \in W^{1,p}(\Omega) \quad (18)$$

Lemma 1.3.7. (A $L^p - L^2$ type inverse inequality see Lemma 2.1 of Layton [53] also similar result of p.112 Theorem of Brenner and Scott [9]) Let θ_0 be the minimum angle in the triangulation and $M^k = \{v(x) : v(x)|_e \in \mathcal{P}_k(e) \forall e \in \mathcal{T}^h(\Omega)\}$, \mathcal{P}_k being the polynomials of degree $\leq k$. Then, for ∇^h the elementwise defined gradient operator, there is a $C = C(\theta_0, p, k)$ such that for $2 \leq p < \infty$, $d = 2, 3$ and all $v \in M^k$,

$$\|\nabla^h v\|_{L^p(\Omega)} \leq Ch^{\frac{d}{2}(\frac{2-p}{p})} \|\nabla^h v\|. \quad (19)$$

Proposition 1.3.8. (The continuous inf-sup condition see p.58 [47]) There is a constant $\beta > 0$ such that

$$\inf_{q \in Q} \sup_{v \in X} \frac{(q, \nabla \cdot v)}{\|\nabla v\| \|q\|} \geq \beta > 0. \quad (20)$$

Lemma 1.3.9. (A Discrete Gronwall lemma see Lemma 5.1 p.369 [31]) Let $\Delta t, B, a_n, b_n, c_n, d_n$ be non-negative numbers such that for $l \geq 1$

$$a_l + \Delta t \sum_{n=0}^l b_n \leq \Delta t \sum_{n=0}^{l-1} d_n a_n + \Delta t \sum_{n=0}^l c_n + B, \quad \text{for } l \geq 0,$$

then for all $\Delta t > 0$,

$$a_l + \Delta t \sum_{n=0}^l b_n \leq \exp\left(\Delta t \sum_{n=0}^{l-1} d_n\right) \left(\Delta t \sum_{n=0}^l c_n + B\right), \quad \text{for } l \geq 0.$$

We will use the next lemma in Chapter 3 to analyze the space-adaptive penalty method. On each mesh element Δ denote $(\phi, \psi)_\Delta = \int_\Delta \phi \cdot \psi \, dx$. The nonlinear term satisfies the following, often called Strong Monotonicity, and Local Lipschitz continuity.

Lemma 1.3.10. (Strong Monotonicity and Local Lipschitz continuity) Let $u, v, w \in X$, on each mesh element Δ , then there exist constants C_1, C_2 such that the following inequalities hold:

$$(|\nabla \cdot u|^2 \nabla \cdot u - |\nabla \cdot w|^2 \nabla \cdot w, \nabla \cdot (u - w))_\Delta \geq C_1 \|\nabla \cdot (u - w)\|_{L^4(\Delta)}^4, \quad (21)$$

$$(|\nabla \cdot u|^2 \nabla \cdot u - |\nabla \cdot w|^2 \nabla \cdot w, \nabla \cdot v)_\Delta \leq C_2 r^2 \|\nabla \cdot (u - w)\|_{L^4(\Delta)} \|\nabla \cdot v\|_{L^4(\Delta)}, \quad (22)$$

$$\text{where } r = \max\{\|\nabla \cdot u\|_{L^4(\Delta)}, \|\nabla \cdot w\|_{L^4(\Delta)}\}.$$

Proof. (of Local Lipschitz continuity)

$$\begin{aligned} & (|\nabla \cdot u|^2 \nabla \cdot u - |\nabla \cdot w|^2 \nabla \cdot w, \nabla \cdot v)_\Delta \\ &= (|\nabla \cdot u|^2 \nabla \cdot u - |\nabla \cdot u|^2 \nabla \cdot w, \nabla \cdot v)_\Delta + (|\nabla \cdot u|^2 \nabla \cdot w - |\nabla \cdot w|^2 \nabla \cdot w, \nabla \cdot v)_\Delta \\ &= \int_\Delta |\nabla \cdot u|^2 \nabla \cdot (u - w) \nabla \cdot v \, dx + \int_\Delta \nabla \cdot w (\nabla \cdot u + \nabla \cdot w) (\nabla \cdot u - \nabla \cdot w) \nabla \cdot v \, dx \\ &= \int_\Delta \nabla \cdot (u - w) \nabla \cdot v (|\nabla \cdot u|^2 + \nabla \cdot u \nabla \cdot w + |\nabla \cdot w|^2) \, dx \\ &\leq \int_\Delta |\nabla \cdot (u - w)| |\nabla \cdot v| (|\nabla \cdot u| + |\nabla \cdot w|)^2 \, dx \\ &\leq \|\nabla \cdot (u - w)\|_{L^4(\Delta)} \|\nabla \cdot v\|_{L^4(\Delta)} \left(\int_\Delta (|\nabla \cdot u| + |\nabla \cdot w|)^4 \, dx \right)^{1/2}, \end{aligned}$$

Denote $r = \max(\|\nabla \cdot u\|_{L^4(\Delta)}, \|\nabla \cdot w\|_{L^4(\Delta)})$, then we have

$$(|\nabla \cdot u|^2 \nabla \cdot u - |\nabla \cdot w|^2 \nabla \cdot w, \nabla \cdot v)_\Delta \leq C_2 r^2 \|\nabla \cdot (u - w)\|_{L^4(\Delta)} \|\nabla \cdot v\|_{L^4(\Delta)}.$$

The proof of Strong Monotonicity follows similarly to the p-Laplacian in Barrett and Liu [3], Glowinski and Marroco [23], so we omit the part here. \square

2.0 Adapting ϵ in time

We develop, analyze and test adaptive penalty parameter methods. We prove unconditional stability for velocity when adapting the penalty parameter, ϵ , and stability of the velocity time derivative under a condition on the change of the penalty parameter, $\epsilon(t_{n+1}) - \epsilon(t_n)$. The analysis and tests show that adapting $\epsilon(t_{n+1})$ in response to $\nabla \cdot u(t_n)$ removes the problem of picking ϵ and yields good approximations for the velocity. We provide error analysis and numerical tests to support these results. We supplement the adaptive- ϵ method by also adapting the time-step. The penalty parameter ϵ and time-step are adapted independently. We further compare first, second, and variable order time-step algorithms. Accurate recovery of pressure remains an open problem.

2.1 Introduction

The velocity and pressure of an incompressible, viscous fluid are given by the Navier-Stokes equations. Let u denote the fluid velocity, p the pressure, ν the kinematic viscosity and f an external force:

$$u_t - \nu \Delta u + u \cdot \nabla u + \nabla p = f, \quad \nabla \cdot u = 0, \quad \forall (\mathbf{x}, t) \in \Omega \times (0, T]. \quad (23)$$

The velocity and pressure are coupled together by the incompressibility constraint $\nabla \cdot u = 0$. Coupled systems require more memory to store and are more expensive to solve. Penalty methods and artificial compression methods relax the incompressibility condition and result in a pseudo-compressible system. This allows us to uncouple velocity and pressure, which will reduce storage space and computational complexity. Penalty methods that allow complete elimination of the pressure variable are the simplest and fastest and will be studied herein.

Penalty methods replace $\nabla \cdot u = 0$ with $\nabla \cdot u + \epsilon p = 0$ where $0 < \epsilon \ll 1$. The pressure can be eliminated using $\nabla p = -\nabla(1/\epsilon \nabla \cdot u)$. As the pressure is entirely eliminated from the system, we do not need to solve for it at every time-step, leading to further increases

in speed. The accuracy of penalty methods is known to be very sensitive to the choice of ϵ (see Fig. 6.1). This sensitivity suggests considering ϵ as a control and picking ϵ through a self-adaptive algorithm. This problem of determining ϵ self-adaptively is considered herein.

When adapting the parameter, ϵ , $\|\nabla \cdot u\|$ is monitored and used to adjust ϵ . The stability of the standard penalty method with variable ϵ is examined in Section 2.2. No condition on the rate of change of ϵ is required for the stability of $\|u\|$. However, the stability of $\|u_t\|$ is not unconditional. There is no restriction on the increase of ϵ , however decreasing ϵ quickly will lead to growth in $\|u_t\|$. In Section 2.2.2, we derive condition (34)

$$(1 - k\alpha)\epsilon_n \leq \epsilon_{n+1} \text{ for some } \alpha > 0,$$

where k is the step-size. This condition is required for stability of $\|u_t\|$. Figure 13 of Section 2.5.2.2 confirms that violating this condition leads to spikes of catastrophic growth in $\|u_t\|$.

The utility of penalty methods lies in accurate velocity approximation at low cost by simple methods. Consistent with this intent, we couple the adaptive ϵ algorithm with simple, low-cost time-stepping methods based on the backward Euler method. Simple time filters allow us to implement an effective variable order, variable time-step adaptive scheme, developing further an algorithm of [26]. The self-adaptive ϵ penalty method can be easily implemented for both constant time-step and variable time-step methods. We develop, analyze and test these new algorithms that independently adapt the time-step k and the penalty parameter ϵ .

In addition to adapting the time-step, we adapt the order of the method between the first and second order. This variable time-step variable order (VSVO) method performed better than both first and second-order methods in our tests (see Figure 12).

2.1.1 Review of a Common Penalty Method

Recall the incompressible Navier-Stokes equations,

$$u_t - \nu \Delta u + u \cdot \nabla u + \nabla p = f, \quad \nabla \cdot u = 0, \quad \forall (\mathbf{x}, t) \in \Omega \times (0, T], \quad (24)$$

$$u = 0 \quad \forall (\mathbf{x}, t) \in \partial\Omega \times (0, T], \quad u(\mathbf{x}, 0) = u_0(\mathbf{x}) \quad \forall \mathbf{x} \in \Omega. \quad (25)$$

Perturbing the continuity equation by adding a penalty term to the incompressibility condition and explicitly skew-symmetrizing the nonlinear term in the momentum equation in (24) results in the penalty Navier-Stokes equations:

$$u_t - \nu \Delta u + u \cdot \nabla u + \frac{1}{2}(\nabla \cdot u)u + \nabla p = f, \quad (26)$$

$$\nabla \cdot u + \epsilon p = 0. \quad (27)$$

Here $u \cdot \nabla u + \frac{1}{2}(\nabla \cdot u)u$ is the modified bilinear term introduced by Temam [61]. This bilinear term ensures the dissipativity of the system (26)-(27). By (27), $p = (-1/\epsilon)\nabla \cdot u$. Inserting this into (26) results in a system of u only, which is easier to solve than (24):

$$u_{\epsilon,t} - \nu \Delta u_{\epsilon} + u_{\epsilon} \cdot \nabla u_{\epsilon} + \frac{1}{2}(\nabla \cdot u_{\epsilon})u_{\epsilon} - \nabla \left(\frac{1}{\epsilon} \nabla \cdot u_{\epsilon} \right) = f. \quad (28)$$

From Theorem 1.2 p.120 of Temam [61] we know $\lim_{\epsilon \rightarrow 0} (u_{\epsilon}(t), p_{\epsilon}(t)) = (u(t), p(t))$. And later the error bound of $(u_{\epsilon}, p_{\epsilon})$ to (u, p) provided by Shen [59] indicates:

$$\sup_{0 \leq t \leq T} (\tau^{1/2}(t)) \|u(t) - u_{\epsilon}(t)\|_{L^2} + \tau(t) \|u(t) - u_{\epsilon}(t)\|_{H^1} + \left(\int_0^T \tau^2(t) \|p - p_{\epsilon}\|_{L^2}^2 dt \right)^{1/2} \leq \kappa \epsilon,$$

where $\tau(t) = \min(t, 1)$ and κ is a positive constant depending on data (ν, Ω, u_0, f, T) .

Consider the first-order discretization of (26)-(27). k_n is the n^{th} time-step, ϵ_n is the parameter ϵ at n^{th} time-step, $t_0 = 0, t_n = t_{n-1} + k_n$. Let u^* denote the standard (second order) linear extrapolation of u at t_{n+1} :

$$u^* = \left(1 + \frac{k_{n+1}}{k_n} \right) u^n - \frac{k_{n+1}}{k_n} u^{n-1}.$$

The backward Euler time discretization gives us

$$\frac{u^{n+1} - u^n}{k_{n+1}} + u^* \cdot \nabla u^{n+1} + \frac{1}{2}(\nabla \cdot u^*)u^{n+1} + \nabla p^{n+1} - \nu \Delta u^{n+1} = f^{n+1}, \quad (29)$$

$$\nabla \cdot u^{n+1} + \epsilon_{n+1} p^{n+1} = 0. \quad (30)$$

As before, we use $p^{n+1} = ((-1/\epsilon_{n+1})\nabla \cdot u^{n+1})$, to uncouple (29)-(30) into the following time discrete, velocity only equation

$$\frac{u^{n+1} - u^n}{k_{n+1}} + u^* \cdot \nabla u^{n+1} + \frac{1}{2}(\nabla \cdot u^*)u^{n+1} - \nu \Delta u^{n+1} - \nabla \left(\frac{1}{\epsilon_{n+1}} \nabla \cdot u^{n+1} \right) = f^{n+1}. \quad (31)$$

For constant $\epsilon_{n+1} = \epsilon, k_{n+1} = k$, (31) is unconditionally stable by Theorem 4.1 of He and Li [28]. The analysis of the stability of the variable ϵ , constant k method see Theorem 2.2.1. Analysis of stability of acceleration u_t for linear Stokes problem can be found in Section 2.2.2.

2.1.2 Related work

Penalty methods were first introduced by Courant in 1943 [16]. They were first applied to the unsteady Navier-Stokes equations by Teman [61]. Error estimates for continuous time, constant ϵ , (28) were proved by Shen in Theorem 4.1 p.395 [59]. In Theorem 5.1 p.397, Shen further proved error estimates for the backward Euler time discretization of the penalty Navier-Stokes equations. This analysis suggests a choice of $\epsilon = k$. Shen [58] studied higher-order projection schemes in the semi-discrete form and proposed a penalty-projection scheme with improved error estimates. Prohl [56] suggested a new analytical approach to the penalty method. He [27], He and Li [28] studied fully discrete penalty finite element methods and proved optimal error estimates with conditions on $\epsilon, \Delta t$ and mesh size h .

Bercovier and Engelman showed that the velocity error of penalty methods is sensitive to the choice of ϵ , see [4]. If ϵ is too large, it will poorly model incompressible flow. Choosing ϵ too small will cause numerical conditioning problems, see Hughes, Liu and Brooks [32]. The optimal choice of the penalty parameter also varies depending on the time and space discretization schemes used, see Shen [59]. [32] introduced a theory for determining the penalty parameter, which only depends on the Reynolds number Re and viscosity ν .

The penalty method gives inaccurate pressure (see Table 2 and Table 3), and we focus on the velocity accuracy in this thesis. However, pressure recovery is essential when calculating quantities based on stresses, e.g., lift and drag coefficients. The easiest way is by using $\nabla \cdot u + \epsilon p = 0$ and solving for pressure. There are also other possibilities to recover pressure, e.g., Pressure Poisson equations and momentum equations, see Kean and Schneier [41].

2.1.3 Motivation For Choice of Estimator for ϵ

We choose an estimator to control the residual in the continuity equation, $\|\nabla \cdot u_\epsilon\|$. The immediate choice is to adapt ϵ based on the size of $\|\nabla \cdot u_\epsilon\|$. However, controlling the relative, not the absolute error, is a more logical choice.

Taking L^2 inner product of (28) with u_ϵ , we get:

$$\frac{1}{2} \frac{d}{dt} \|u_\epsilon\|^2 + \nu \|\nabla u_\epsilon\|^2 + \frac{1}{\epsilon} \|\nabla \cdot u_\epsilon\|^2 = (f, u_\epsilon).$$

We aim to ensure $\nu\|\nabla u_\epsilon\|^2$ does not dominate $\frac{1}{\epsilon}\|\nabla \cdot u_\epsilon\|^2$. This suggests an upper bound for ϵ :

$$\frac{1}{\epsilon}\|\nabla \cdot u_\epsilon\|^2 \geq \nu\|\nabla u_\epsilon\|^2 \implies \epsilon \leq \frac{1}{\nu} \left(\frac{\|\nabla \cdot u_\epsilon\|}{\|\nabla u_\epsilon\|} \right)^2.$$

This motivates the choice of the estimator to be $\|\nabla \cdot u_\epsilon\|/\|\nabla u_\epsilon\|$, the relative residual. This has the additional benefits of being non-dimensional and independent of the size of u_ϵ . Since ν is constant, scaling by $1/\nu$ is just a change of adaptive tolerance. The comparison of absolute and relative residual estimators is presented in Section 2.5.3.

The rest of this chapter is organized as follows. In Section 2.2, stabilities of $\|u\|$ and $\|u_t\|$ for the variable ϵ penalty method with constant time-step are presented. Section 2.3 presents an error estimate of the semi-discrete, variable ϵ method. Using this, we develop an effective algorithm that adapts ϵ and k independently, presented in Section 2.4. We introduce four different algorithms, including the constant time-step and variable time-step variable ϵ method. Numerical tests are shown in Section 2.5.

2.2 Stability of Backward Euler

This section establishes conditions for stability for the variable ϵ first-order method with constant time-step:

$$\frac{u^{n+1} - u^n}{k} + u^* \cdot \nabla u^{n+1} + \frac{1}{2}(\nabla \cdot u^*)u^{n+1} - \nu \Delta u^{n+1} - \nabla \left(\frac{1}{\epsilon_{n+1}} \nabla \cdot u^{n+1} \right) = f^{n+1}. \quad (32)$$

We prove that the velocity is unconditionally stable, but $\|u_t\|$ is stable with restrictions on the change of ϵ .

2.2.1 Stability of the velocity

Theorem 2.2.1. (Stability of variable ϵ penalty method). The variable ϵ first-order method (31) is stable. For any $M > 0$, the energy equality holds:

$$\begin{aligned} \frac{1}{2} \int_{\Omega} |u^M|^2 dx + \sum_{n=0}^{M-1} \int_{\Omega} \left(\frac{1}{2} |u^{n+1} - u^n|^2 + k\nu |\nabla u^{n+1}|^2 + \frac{k}{\epsilon_{n+1}} |\nabla \cdot u^{n+1}|^2 \right) dx \\ = \frac{1}{2} \int_{\Omega} |u^0|^2 dx + \sum_{n=0}^{M-1} k \int_{\Omega} u^{n+1} \cdot f^{n+1} dx, \end{aligned}$$

and the stability bound holds:

$$\begin{aligned} \frac{1}{2} \int_{\Omega} |u^M|^2 dx + \sum_{n=0}^{M-1} \int_{\Omega} \left(\frac{1}{2} |u^{n+1} - u^n|^2 + \frac{k\nu}{2} |\nabla u^{n+1}|^2 + \frac{k}{\epsilon_{n+1}} |\nabla \cdot u^{n+1}|^2 \right) dx \\ \leq \frac{1}{2} \int_{\Omega} |u^0|^2 dx + \sum_{n=0}^{M-1} \frac{k}{2\nu} \|f^{n+1}\|_{-1}^2. \end{aligned}$$

Proof. Consider (32) the constant time-step first-order method, let T denote the final time, set $M = T/k$. Take the L^2 inner product of (32) with u^{n+1} . We obtain

$$\frac{1}{k} (\|u^{n+1}\|^2 - (u^n, u^{n+1})) + \nu \|\nabla u^{n+1}\|^2 + \frac{1}{\epsilon_{n+1}} \|\nabla \cdot u^{n+1}\|^2 = (f^{n+1}, u^{n+1}).$$

Apply the polarization identity (17) to the term (u^n, u^{n+1})

$$\frac{1}{2k} (\|u^{n+1}\|^2 - \|u^n\|^2 + \|u^{n+1} - u^n\|^2) + \nu \|\nabla u^{n+1}\|^2 + \frac{1}{\epsilon_{n+1}} \|\nabla \cdot u^{n+1}\|^2 = (f^{n+1}, u^{n+1}).$$

Sum from $n = 0, \dots, M-1$ and multiply by k , we will have the energy equality. By the definition of the dual norm and Young's inequality,

$$\frac{1}{2k} (\|u^{n+1}\|^2 - \|u^n\|^2 + \|u^{n+1} - u^n\|^2) + \nu \|\nabla u^{n+1}\|^2 + \frac{1}{\epsilon_{n+1}} \|\nabla \cdot u^{n+1}\|^2 \leq \frac{1}{2\nu} \|f^{n+1}\|_{-1}^2 + \frac{\nu}{2} \|\nabla u^{n+1}\|^2.$$

Sum from $n = 0, \dots, M-1$

$$\frac{1}{2k} \|u^M\|^2 + \sum_{n=0}^{M-1} \left(\frac{1}{2k} \|u^{n+1} - u^n\|^2 + \frac{\nu}{2} \|\nabla u^{n+1}\|^2 + \frac{1}{\epsilon_{n+1}} \|\nabla \cdot u^{n+1}\|^2 \right) \leq \frac{1}{2k} \|u^0\|^2 + \sum_{n=0}^{M-1} \frac{1}{2\nu} \|f^{n+1}\|_{-1}^2.$$

Multiply by $2k$ and drop positive terms on the left hand side

$$\|u^M\|^2 \leq \|u^0\|^2 + 2k \sum_{n=0}^{M-1} \frac{1}{2\nu} \|f^{n+1}\|_{-1}^2.$$

□

2.2.2 Stability of $\|u_t\|$ for the linear Stokes problem

As $\nabla \cdot u = -\epsilon p$, in order to ensure $\nabla \cdot u \rightarrow 0$ as $\epsilon \rightarrow 0$, we need to bound $\|p_\epsilon\|$ following the idea in Fiordilino [21]. By using the *LBB* inf-sup condition (20):

$$\begin{aligned} \beta \|p\| &\leq \sup_{v \in X} \frac{(p, \nabla \cdot v)}{\|\nabla v\|} = \sup_{v \in X} \frac{-(f, v) + (u_t, v) + (u \cdot \nabla u, v) + \nu(\nabla u, \nabla v)}{\|\nabla v\|} \\ &\leq \|f\|_{-1} + \|u_t\|_{-1} + C\|\nabla u\|^2 + \nu\|\nabla u\|, \end{aligned}$$

this implies we must begin with a bound of $\|u_t\|_{-1}$.

Remark 2.2.2. *The linear Stokes problem is NSE without the nonlinear term $u \cdot \nabla u$. The stability conditions on ϵ that are derived from the linear Stokes problem are essential for the case of nonlinear NSE. The stability analysis of the nonlinear term of NSE will be more involved but not alter the fundamental approach of this proof. Hence, this case shall be omitted.*

Consider the first-order method with penalty:

$$\frac{u^{n+1} - u^n}{k} - \nu \Delta u^{n+1} - \nabla \left(\frac{1}{\epsilon_{n+1}} \nabla \cdot u^{n+1} \right) = f^{n+1}. \quad (33)$$

Theorem 2.2.3. *(0-stability of linear Stokes) For any $0 \leq n \leq M - 1$, if there is some constant α such that $0 \leq \alpha k < 1$ and $(1 - k\alpha)\epsilon_n \leq \epsilon_{n+1}$ holds, then the following stability bound holds*

$$\begin{aligned} &\sum_{n=0}^{M-1} \left(\frac{k}{2} \left\| \frac{u^{n+1} - u^n}{k} \right\|^2 + \frac{\nu}{2} \|\nabla(u^{n+1} - u^n)\|^2 + \frac{1}{2\epsilon_{n+1}} \|\nabla \cdot (u^{n+1} - u^n)\|^2 \right) \\ &\quad + \frac{\nu}{2} \|\nabla u^M\|^2 + \frac{1}{2\epsilon_M} \|\nabla \cdot u^M\|^2 \\ &\leq \exp(\alpha T) \left\{ \frac{\nu}{2} \|\nabla u^0\|^2 + \frac{1}{2\epsilon_0} \|\nabla \cdot u^0\|^2 + \sum_{n=0}^{M-1} \frac{k}{2} \|f^{n+1}\|^2 \right\}. \end{aligned}$$

Remark 2.2.4. *If $\alpha = 0$ in (34), i.e., if $\epsilon_{n+1} \geq \epsilon_n$ for all n , then we have unconditional stability.*

Proof. Take the L^2 inner product of (33) with $u^{n+1} - u^n$,

$$\frac{1}{k} \|u^{n+1} - u^n\|^2 + \nu (\nabla u^{n+1}, \nabla(u^{n+1} - u^n)) + \frac{1}{\epsilon_{n+1}} (\nabla \cdot u^{n+1}, \nabla \cdot (u^{n+1} - u^n)) = (f^{n+1}, u^{n+1} - u^n).$$

We will address terms successively. Denote $\gamma_{n+1} = 1/\epsilon_{n+1}$ and apply the polarization identity (17) to the second and the third terms on the left,

$$\begin{aligned} \nu (\nabla u^{n+1}, \nabla(u^{n+1} - u^n)) &= \frac{\nu}{2} (\|\nabla u^{n+1}\|^2 - \|\nabla u^n\|^2 + \|\nabla(u^{n+1} - u^n)\|^2), \\ \frac{1}{\epsilon_{n+1}} (\nabla \cdot u^{n+1}, \nabla \cdot (u^{n+1} - u^n)) &= \frac{\gamma_{n+1}}{2} (\|\nabla \cdot u^{n+1}\|^2 - \|\nabla \cdot u^n\|^2 + \|\nabla \cdot (u^{n+1} - u^n)\|^2). \end{aligned}$$

By adding and subtracting $\gamma_n \|\nabla \cdot u^n\|^2/2$, we have

$$\begin{aligned} &\frac{\gamma_{n+1}}{2} (\|\nabla \cdot u^{n+1}\|^2 - \|\nabla \cdot u^n\|^2 + \|\nabla \cdot (u^{n+1} - u^n)\|^2) \\ &= \frac{\gamma_{n+1}}{2} \|\nabla \cdot u^{n+1}\|^2 - \frac{\gamma_n}{2} \|\nabla \cdot u^n\|^2 + \frac{\gamma_{n+1}}{2} \|\nabla \cdot (u^{n+1} - u^n)\|^2 + \frac{\gamma_n - \gamma_{n+1}}{2} \|\nabla \cdot u^n\|^2. \end{aligned}$$

By Cauchy-Schwarz and Young's inequalities (15)

$$(f^{n+1}, u^{n+1} - u^n) \leq \frac{k}{2} \|f^{n+1}\|^2 + \frac{1}{2k} \|u^{n+1} - u^n\|^2.$$

By combining similar terms, we have

$$\begin{aligned} &\frac{1}{2k} \|u^{n+1} - u^n\|^2 + \left[\left(\frac{\nu}{2} \|\nabla u^{n+1}\|^2 + \frac{\gamma_{n+1}}{2} \|\nabla \cdot u^{n+1}\|^2 \right) - \left(\frac{\nu}{2} \|\nabla u^n\|^2 + \frac{\gamma_n}{2} \|\nabla \cdot u^n\|^2 \right) \right] \\ &\quad + \frac{\nu}{2} \|\nabla(u^{n+1} - u^n)\|^2 + \frac{\gamma_{n+1}}{2} \|\nabla \cdot (u^{n+1} - u^n)\|^2 + \frac{\gamma_n - \gamma_{n+1}}{2} \|\nabla \cdot u^n\|^2 \leq \frac{k}{2} \|f^{n+1}\|^2. \end{aligned}$$

Moving $(\gamma_n - \gamma_{n+1})/2 \|\nabla \cdot u^n\|^2$ to the right. We obtain

$$\begin{aligned} &\frac{1}{2k} \|u^{n+1} - u^n\|^2 + \left[\left(\frac{\nu}{2} \|\nabla u^{n+1}\|^2 + \frac{\gamma_{n+1}}{2} \|\nabla \cdot u^{n+1}\|^2 \right) - \left(\frac{\nu}{2} \|\nabla u^n\|^2 + \frac{\gamma_n}{2} \|\nabla \cdot u^n\|^2 \right) \right] \\ &\quad + \frac{\nu}{2} \|\nabla(u^{n+1} - u^n)\|^2 + \frac{\gamma_{n+1}}{2} \|\nabla \cdot (u^{n+1} - u^n)\|^2 \leq \frac{k}{2} \|f^{n+1}\|^2 + \frac{\gamma_{n+1} - \gamma_n}{2} \|\nabla \cdot u^n\|^2, \\ &= \frac{k}{2} \|f^{n+1}\|^2 + k \left(\frac{\gamma_{n+1} - \gamma_n}{k\gamma_n} \right) \left(\frac{\gamma_n}{2} \|\nabla \cdot u^n\|^2 \right). \end{aligned}$$

For each fixed constant $\alpha \geq 0$, we need $(\gamma_{n+1} - \gamma_n)/k\gamma_n \leq \alpha$ to avoid catastrophic growth.

This leads to

$$\begin{aligned} \gamma_{n+1} - \gamma_n &\leq k\alpha\gamma_n, & \left(\frac{1}{\epsilon_{n+1}} - \frac{1}{\epsilon_n}\right) \epsilon_n \epsilon_{n+1} &\leq k\alpha \frac{1}{\epsilon_n} \epsilon_n \epsilon_{n+1}, \\ \epsilon_n &\leq (1 + k\alpha)\epsilon_{n+1}, & \frac{1}{1 + k\alpha} \epsilon_n &\leq \epsilon_{n+1}. \end{aligned}$$

If $k\alpha < 1$, we approximate with the first two terms of the Taylor expansion

$$\frac{1}{1 + k\alpha} \geq 1 - k\alpha.$$

Thus we have the stability condition on ϵ

$$(1 - k\alpha)\epsilon_n \leq \epsilon_{n+1}. \quad (34)$$

Under condition (34)

$$\begin{aligned} \frac{1}{2k} \|u^{n+1} - u^n\|^2 + \left[\left(\frac{\nu}{2} \|\nabla u^{n+1}\|^2 + \frac{1}{2\epsilon_{n+1}} \|\nabla \cdot u^{n+1}\|^2 \right) - \left(\frac{\nu}{2} \|\nabla u^n\|^2 + \frac{1}{2\epsilon_n} \|\nabla \cdot u^n\|^2 \right) \right] \\ + \frac{\nu}{2} \|\nabla(u^{n+1} - u^n)\|^2 + \frac{1}{2\epsilon_{n+1}} \|\nabla \cdot (u^{n+1} - u^n)\|^2 \leq \frac{k}{2} \|f^{n+1}\|^2 + k\alpha \left(\frac{1}{2\epsilon_n} \|\nabla \cdot u^n\|^2 \right). \end{aligned} \quad (35)$$

Sum from $n = 0, 1, \dots, M-1$

$$\begin{aligned} \sum_{n=0}^{M-1} \left(\frac{1}{2k} \|u^{n+1} - u^n\|^2 + \frac{\nu}{2} \|\nabla(u^{n+1} - u^n)\|^2 + \frac{1}{2\epsilon_{n+1}} \|\nabla \cdot (u^{n+1} - u^n)\|^2 \right) \\ + \frac{\nu}{2} \|\nabla u^M\|^2 + \frac{1}{2\epsilon_M} \|\nabla \cdot u^M\|^2 \\ \leq \frac{\nu}{2} \|\nabla u^0\|^2 + \frac{1}{2\epsilon_0} \|\nabla \cdot u^0\|^2 + \sum_{n=0}^{M-1} \frac{k}{2} \|f^{n+1}\|^2 + k \sum_{n=0}^{M-1} \alpha \left(\frac{1}{2\epsilon_n} \|\nabla \cdot u^n\|^2 \right). \end{aligned}$$

Apply the Gronwall inequality (1.3.9)

$$\begin{aligned} \sum_{n=0}^{M-1} \left(\frac{1}{2k} \|u^{n+1} - u^n\|^2 + \frac{\nu}{2} \|\nabla(u^{n+1} - u^n)\|^2 + \frac{1}{2\epsilon_{n+1}} \|\nabla \cdot (u^{n+1} - u^n)\|^2 \right) \\ + \frac{\nu}{2} \|\nabla u^M\|^2 + \frac{1}{2\epsilon_M} \|\nabla \cdot u^M\|^2 \\ \leq \exp\left(k \sum_{n=0}^{M-1} \alpha\right) \left\{ \frac{\nu}{2} \|\nabla u^0\|^2 + \frac{1}{2\epsilon_0} \|\nabla \cdot u^0\|^2 + \sum_{n=0}^{M-1} \frac{k}{2} \|f^{n+1}\|^2 \right\}, \\ = \exp(\alpha T) \left\{ \frac{\nu}{2} \|\nabla u^0\|^2 + \frac{1}{2\epsilon_0} \|\nabla \cdot u^0\|^2 + \sum_{n=0}^{M-1} \frac{k}{2} \|f^{n+1}\|^2 \right\}. \end{aligned}$$

Thus we proved that, if $(1 - k\alpha)\epsilon_n \leq \epsilon_{n+1}$ for some $\alpha \geq 0$ and $\alpha k < 1$, stability of discrete u_t holds. □

Remark 2.2.5. When ϵ decreases, (34) is needed to ensure the boundedness of discrete $\|u_t\|$; If (34) does not hold, $\|u_t\|$ may have catastrophic growth see Figure 13.

Theorem 2.2.6. Let u be the solution to penalized NSE (26)-(27), then $u_t \in L^{4/3}(0, T; H^{-1})$, equivalently

$$\int_0^T \|u_t\|_{-1}^{4/3} dt < C(u^0, f, k, \nu, T, \min_{t^* \in [0, T]} \epsilon(t^*)).$$

Proof. Recall

$$\|u_t\|_{-1} = \sup_{v \in X} \frac{(u_t, v)}{\|\nabla v\|}.$$

By skew-symmetry

$$\begin{aligned} (u_t, v) &= - \int_{\Omega} b^*(u, u, v) dx - \nu(\nabla u, \nabla v) - \frac{1}{\epsilon(t)}(\nabla \cdot u, \nabla \cdot v) + (f, v), \\ &\leq C(\|u\|^{1/2} \|\nabla u\|^{1/2}) \|\nabla v\| \|\nabla u\| + \nu \|\nabla u\| \|\nabla v\| + \frac{1}{\epsilon(t)} \|\nabla \cdot u\| \|\nabla v\| + \|f\|_{-1} \|\nabla v\|. \end{aligned}$$

Thus,

$$\frac{(u_t, v)}{\|\nabla v\|} \leq C\|u\|^{1/2} \|\nabla u\|^{3/2} + \nu \|\nabla u\| + \frac{1}{\epsilon(t)} \|\nabla \cdot u\| + \|f\|_{-1}.$$

$\|u\|$ is bounded by the problem data and initial condition from the stability of the velocity Theorem 3.1.

$$\|u_t\|_{-1} \leq C(u^0, f, k, \nu) \|\nabla u\|^{3/2} + \nu \|\nabla u\| + \frac{1}{\epsilon(t)} \|\nabla \cdot u\| + \|f\|_{-1}.$$

Then

$$\begin{aligned} \int_0^T \|u_t\|_{-1}^{4/3} dt &\leq C(u^0, f, k, \nu) \int_0^T \|\nabla u\|^2 dt + C(\nu) \int_0^T \|\nabla u\|^{4/3} dt \\ &\quad + C \int_0^T \left(\frac{1}{\epsilon(t)} \|\nabla \cdot u\| \right)^{4/3} dt + C \int_0^T \|f\|_{-1}^{4/3} dt. \end{aligned}$$

From Theorem 2.2.1 the stability bound

$$\int_0^T \|\nabla u\|^2 dt < C(u^0, f, k, \nu), \quad \text{and} \quad \int_0^T \frac{1}{\epsilon(t)} \|\nabla \cdot u\|^2 dt < C(u^0, f, k, \nu).$$

By Hölder's inequality (15)

$$\begin{aligned} \int_0^T \|\nabla u\|^{4/3} dt &\leq \left(\int_0^T 1^3 dt \right)^{1/3} \left(\int_0^T (\|\nabla u\|^{4/3})^{3/2} dt \right)^{2/3} = C(T) \left(\int_0^T \|\nabla u\|^2 dt \right)^{2/3}, \\ \int_0^T \left(\frac{1}{\epsilon(t)} \|\nabla \cdot u\| \right)^{4/3} dt &\leq \max_{t^* \in [0, T]} \left(\frac{1}{\epsilon(t^*)} \right)^{2/3} \left(\int_0^T 1^3 dt \right)^{1/3} \left(\int_0^T \left(\frac{1}{\epsilon(t)^{2/3}} \|\nabla \cdot u\|^{4/3} \right)^{3/2} dt \right)^{2/3}, \\ &= C(T, \min_{t^* \in [0, T]} \epsilon(t^*)) \left(\int_0^T \frac{1}{\epsilon(t)} \|\nabla \cdot u\|^2 dt \right)^{2/3}. \end{aligned}$$

Then the result follows. \square

2.3 Error Analysis

Next, we will prove an error estimate for the semi-discrete, variable- ϵ penalty method.

Find $(u_\epsilon^h, p_\epsilon^h) \in (X^h, Q^h)$ such that

$$(u_{\epsilon,t}^h, v^h) + b^*(u_\epsilon^h, u_\epsilon^h, v^h) + \nu(\nabla u_\epsilon^h, \nabla v^h) - (p_\epsilon^h, \nabla \cdot v^h) + (q^h, \nabla \cdot u_\epsilon^h) + \epsilon(t)(p_\epsilon^h, q^h) = (f, v^h), \quad (36)$$

for all $(v^h, q^h) \in (X^h, Q^h)$.

Definition 2.3.1. (*Stokes Projection [45]*) The Stokes projection operator

$P_S : (X, Q) \rightarrow (X^h, Q^h)$, $P_S(u, p) = (\tilde{u}, \tilde{p})$, satisfies

$$\begin{aligned} \nu(\nabla(u - \tilde{u}), \nabla v^h) - (p - \tilde{p}, \nabla \cdot v^h) &= 0, \\ (\nabla \cdot (u - \tilde{u}), q^h) &= 0, \end{aligned} \quad (37)$$

for any $v^h \in X^h, q^h \in Q^h$.

Proposition 2.3.2. (*Error estimate for the Stokes Projection*) Suppose the discrete inf-sup condition (11) holds. Let C_1 be a constant independent of h and ν and $C_2 = C(\nu, \Omega)$. If Ω is a convex polygonal/polyhedral domain, then the error in the Stokes Projection (37) satisfies

$$\begin{aligned} \|p - \tilde{p}\| &\leq \inf_{q^h \in Q^h} \left(1 + \frac{1}{\beta^h}\right) \|p - q^h\| + \frac{\nu}{\beta^h} \|\nabla(u - \tilde{u})\|, \\ \nu \|\nabla(u - \tilde{u})\|^2 &\leq C_1 [\nu \inf_{v^h \in X^h} \|\nabla(u - v^h)\|^2 + \nu^{-1} \inf_{q^h \in Q^h} \|p - q^h\|^2], \\ \text{and } \|u - \tilde{u}\| &\leq C_2 h \left(\inf_{v^h \in X^h} \|\nabla(u - v^h)\| + \inf_{q^h \in Q^h} \|p - q^h\| \right). \end{aligned}$$

Proof. From the first equation of (37),

$$(p - \tilde{p}, \nabla \cdot v^h) = \nu(\nabla(u - \tilde{u}), \nabla v^h).$$

Let $q^h \in Q^h$, by the discrete inf-sup condition (11),

$$\begin{aligned} \beta^h \|q^h - \tilde{p}\| &\leq \sup_{v^h \in X^h} \frac{(q^h - \tilde{p}, \nabla \cdot v^h)}{\|\nabla v^h\|} = \sup_{v^h \in X^h} \frac{(q^h - p, \nabla \cdot v^h) + (p - \tilde{p}), \nabla \cdot v^h)}{\|\nabla v^h\|}, \\ &= \sup_{v^h \in X^h} \frac{(q^h - p, \nabla \cdot v^h) + \nu(\nabla(u - \tilde{u}), \nabla v^h)}{\|\nabla v^h\|}, \\ &\leq \sup_{v^h \in X^h} \frac{\|q^h - p\| \|\nabla v^h\| + \nu \|\nabla(u - \tilde{u})\| \|\nabla v^h\|}{\|\nabla v^h\|}, \\ &= \|p - q^h\| + \nu \|\nabla(u - \tilde{u})\|. \end{aligned}$$

Then,

$$\|p - \tilde{p}\| \leq \inf_{q^h \in Q^h} (\|p - q^h\| + \|q^h - \tilde{p}\|) \leq \inf_{q^h \in Q^h} (1 + \frac{1}{\beta^h}) \|p - q^h\| + \frac{\nu}{\beta^h} \|\nabla(u - \tilde{u})\|.$$

For detailed proof of the last two inequalities, see Proposition 2.2 and Remark 2.2 of [45]. \square

We also need an estimator for $\|\nabla(u - \tilde{u})_t\|$. Take the partial derivative with respect to time t of (37) to yield

$$\begin{aligned} \nu(\nabla(u - \tilde{u})_t, \nabla v^h) - ((p - \tilde{p})_t, \nabla \cdot v^h) &= 0, \\ (\nabla \cdot (u - \tilde{u})_t, q^h) &= 0, \end{aligned}$$

for all $v^h \in X^h, q^h \in Q^h$.

Let $v^h = \phi_t^h, q^h = (\tilde{p} - I(p))_t$, by a similar argument as in Proposition 2.3.2, we have

$$\nu \|\nabla(u - \tilde{u})_t\|^2 \leq C[\nu \inf_{v^h \in X^h} \|\nabla(u - v^h)_t\|^2 + \nu^{-1} \inf_{q^h \in Q^h} \|(p - q^h)_t\|^2], \quad (38)$$

where C is a constant independent of h and ν .

Theorem 2.3.3. (*Error Analysis of semi-discrete variable ϵ penalty method*) Let (X^h, Q^h) be the finite element spaces satisfying (10) and (11). Let u_ϵ be a solution of (26). Suppose the interpolation estimate (12) in $H^{-1}(\Omega)$ holds and $\|\nabla u_\epsilon\| \in L^4(0, T)$, then we have the following error estimate:

$$\begin{aligned} & \sup_{0 \leq t \leq T} \|(u_\epsilon - u_\epsilon^h)(t)\|^2 + \int_0^T \frac{\nu}{4} \|\nabla(u_\epsilon - u_\epsilon^h)\|^2 dt \leq \\ & e^{\int_0^T a(t) dt} \left\{ \|(u_\epsilon - u_\epsilon^h)(0)\|^2 + \inf_{v^h(t) \in X^h} \max_{0 \leq t \leq T} \|(u_\epsilon - v^h)(t)\|^2 \right. \\ & \left. + \int_0^T C(\nu, \beta^h) \epsilon(t) h^{2m} \left(\|u_\epsilon\|_{H^{m+1}(\Omega)}^2 + \|p_\epsilon\|_{H^m(\Omega)}^2 \right) dt \right\} \\ & + C(\nu, \Omega) \left[(h^{-d/3} + h^{2-d/3} + h^{2-d/2}) h^{2m} \left(\|u_\epsilon\|_{L^2(0, T; H^{m+1}(\Omega))}^2 + \|p_\epsilon\|_{L^2(0, T; H^m(\Omega))}^2 \right) \right. \\ & \left. + h^{2m+2} \left(\|u_{\epsilon, t}\|_{L^2(0, T; H^{m+1}(\Omega))}^2 + \|p_{\epsilon, t}\|_{L^2(0, T; H^m(\Omega))}^2 \right) \right] \Big\}, \\ & \text{where } a(t) = C(\nu) \|\nabla u_\epsilon\|^4 + \frac{1}{4}. \end{aligned}$$

Proof. We denote (u_ϵ, p_ϵ) as penalty solutions to (26).

Multiplying first equation of (26) by $v^h \in X^h$ and second equation of (26) by $q^h \in Q^h$ gives

$$(u_{\epsilon, t}, v^h) + b^*(u_\epsilon, u_\epsilon, v^h) + \nu(\nabla u_\epsilon, \nabla v^h) - (p_\epsilon, \nabla \cdot v^h) + (q^h, \nabla \cdot u_\epsilon) + \epsilon(t)(p_\epsilon, q^h) = (f, v^h). \quad (39)$$

Subtract (36) from (39) and denote $e = u_\epsilon - u_\epsilon^h$,

$$\begin{aligned} & (e_t, v^h) + b^*(u_\epsilon, u_\epsilon, v^h) - b^*(u_\epsilon^h, u_\epsilon^h, v^h) + \nu(\nabla e, \nabla v^h) \\ & - (p_\epsilon - p_\epsilon^h, \nabla \cdot v^h) + (q^h, \nabla \cdot e) + \epsilon(t)(p_\epsilon - p_\epsilon^h, q^h) = 0. \end{aligned}$$

Denote $\eta = u_\epsilon - \tilde{u}$, $\phi^h = u_\epsilon^h - \tilde{u}$, $e = \eta - \phi^h$ and $\tilde{u} \in X^h, \lambda^h \in Q^h$,

$$\begin{aligned} & (\phi_t^h, v^h) + \nu(\nabla \phi^h, \nabla v^h) - (p_\epsilon^h - \lambda^h, \nabla \cdot v^h) + (q^h, \nabla \cdot \phi^h) + \epsilon(t)(p_\epsilon^h - \lambda^h, q^h) \\ & = (\eta_t, v^h) + \nu(\nabla \eta, \nabla v^h) - (p_\epsilon - \lambda^h, \nabla \cdot v^h) + (q^h, \nabla \cdot \eta) + \epsilon(t)(p_\epsilon - \lambda^h, q^h) \\ & \quad + b^*(u_\epsilon, u_\epsilon, v^h) - b^*(u_\epsilon^h, u_\epsilon^h, v^h). \end{aligned}$$

Pick $\tilde{u} \in X^h, \lambda^h \in Q^h$ to be the Stokes Projection (37) of (u_ϵ, p_ϵ) such that

$$\begin{aligned} \nu(\nabla(u_\epsilon - \tilde{u}), \nabla v^h) - (p_\epsilon - \lambda^h, \nabla \cdot v^h) &= 0 \text{ for all } v^h \in X^h, \\ (\nabla \cdot (u_\epsilon - \tilde{u}), q^h) &= 0 \text{ for all } q^h \in Q^h. \end{aligned}$$

Set $v^h = \phi^h, q^h = p_\epsilon^h - \lambda^h$. We obtain,

$$\begin{aligned} \frac{1}{2} \frac{d}{dt} \|\phi^h\|^2 + \nu \|\nabla \phi^h\|^2 + \epsilon(t) \|p_\epsilon^h - \lambda^h\|^2 &= (\eta_t, \phi^h) + b^*(u_\epsilon, u_\epsilon, \phi^h) - b^*(u_\epsilon^h, u_\epsilon^h, \phi^h) \\ &\quad + \epsilon(t) (p_\epsilon - \lambda^h, p_\epsilon^h - \lambda^h). \end{aligned}$$

Consider the nonlinear terms

$$\begin{aligned} b^*(u_\epsilon, u_\epsilon, \phi^h) - b^*(u_\epsilon^h, u_\epsilon^h, \phi^h) &= b^*(u_\epsilon, u_\epsilon, \phi^h) - b^*(u_\epsilon^h, u_\epsilon, \phi^h) + b^*(u_\epsilon^h, u_\epsilon, \phi^h) - b^*(u_\epsilon^h, u_\epsilon^h, \phi^h) \\ &= b^*(e, u_\epsilon, \phi^h) + b^*(u_\epsilon^h, e, \phi^h) = b^*(\eta, u_\epsilon, \phi^h) - b^*(\phi^h, u_\epsilon, \phi^h) + b^*(u_\epsilon^h, \eta, \phi^h). \end{aligned}$$

Thus we have

$$\begin{aligned} \frac{1}{2} \frac{d}{dt} \|\phi^h\|^2 + \nu \|\nabla \phi^h\|^2 + \epsilon(t) \|p_\epsilon^h - \lambda^h\|^2 &= (\eta_t, \phi^h) + b^*(\eta, u_\epsilon, \phi^h) - b^*(\phi^h, u_\epsilon, \phi^h) + b^*(u_\epsilon^h, \eta, \phi^h) \\ &\quad + \epsilon(t) (p_\epsilon - \lambda^h, p_\epsilon^h - \lambda^h). \end{aligned}$$

Consider the right hand side terms of the equation

$$\begin{aligned} |(\eta_t, \phi^h)| &\leq \frac{1}{2\nu} \|\eta_t\|_{-1}^2 + \frac{\nu}{2} \|\nabla \phi^h\|^2, \\ |\epsilon(t) (p_\epsilon - \lambda^h, p_\epsilon^h - \lambda^h)| &\leq \frac{\epsilon(t)}{2} \|p_\epsilon - \lambda^h\|^2 + \frac{\epsilon(t)}{2} \|p_\epsilon^h - \lambda^h\|. \end{aligned}$$

Apply the trilinear inequality (16) to the first nonlinear term $b^*(\eta, u_\epsilon, \phi^h)$ to obtain

$$|b^*(\eta, u_\epsilon, \phi^h)| = \frac{1}{2} |(\eta \cdot \nabla u_\epsilon, \phi^h) - (\eta \cdot \nabla \phi^h, u_\epsilon)| \leq \frac{1}{2} [\|\eta\|_{L_4} \|\nabla u_\epsilon\| \|\phi^h\|_{L_4} + \|\eta\|_{L_4} \|\nabla \phi^h\| \|u_\epsilon\|_{L_4}].$$

Using the Sobolev inequality (14), we have $\|\phi^h\|_{L_4} \leq C \|\nabla \phi^h\|$ and $\|u_\epsilon\|_{L_4} \leq C \|\nabla u_\epsilon\|$,

$$|b^*(\eta, u_\epsilon, \phi^h)| \leq C \|\eta\|_{L_4} \|\nabla u_\epsilon\| \|\nabla \phi^h\| \leq \frac{\nu}{4} \|\nabla \phi^h\|^2 + C(\nu) \|\nabla u_\epsilon\|^2 \|\eta\|_{L_4}^2.$$

Apply Lemma 1.3.2 to the term $|b^*(\phi^h, u_\epsilon, \phi^h)|$,

$$|b^*(\phi^h, u_\epsilon, \phi^h)| \leq C(\Omega) \|\phi^h\|^{1/2} \|\nabla \phi^h\|^{3/2} \|\nabla u_\epsilon\|.$$

Using Hölder's and Young's inequality (15) with $p = 4/3, q = 4$,

$$|b^*(\phi^h, u_\epsilon, \phi^h)| \leq \frac{\nu}{16} \|\nabla \phi\|^2 + C(\nu) \|\phi^h\|^2 \|\nabla u_\epsilon\|^4.$$

Next, we bound the nonlinear term $b^*(u_\epsilon^h, \eta, \phi^h)$ and use the trilinear inequality (16)

$$\begin{aligned} |b^*(u_\epsilon^h, \eta, \phi^h)| &= \frac{1}{2} |(u_\epsilon^h \cdot \nabla \eta, \phi^h) - (u_\epsilon^h \cdot \nabla \phi^h, \eta)| \\ &\leq \frac{1}{2} [\|u_\epsilon^h\|_{L_6} \|\nabla \eta\|_{L_3} \|\phi^h\| + \|u_\epsilon^h\|_{L_6} \|\nabla \phi^h\| \|\eta\|_{L_3}] \\ &\leq \frac{1}{4} \|\phi^h\|^2 + \frac{1}{4} \|u_\epsilon^h\|_{L_6}^2 \|\nabla \eta\|_{L_3}^2 + \frac{\nu}{16} \|\nabla \phi^h\|^2 + C(\nu) \|u_\epsilon^h\|_{L_6}^2 \|\eta\|_{L_3}^2. \end{aligned}$$

Collect all the terms, combine similar terms and multiply through by 2, we have

$$\begin{aligned} \frac{d}{dt} \|\phi^h\|^2 + \frac{\nu}{4} \|\nabla \phi^h\|^2 + \epsilon(t) \|p_\epsilon^h - \lambda^h\|^2 &\leq (C(\nu) \|\nabla u_\epsilon\|^4 + \frac{1}{2}) \|\phi^h\|^2 \\ + C(\nu) [\|\eta_t\|_{-1}^2 + \|\nabla u_\epsilon\|^2 \|\eta\|_{L_4}^2 + \|u_\epsilon^h\|_{L_6}^2 \|\eta\|_{L_3}^2] &+ \frac{1}{2} \|u_\epsilon^h\|_{L_6}^2 \|\nabla \eta\|_{L_3}^2 + \epsilon(t) \|p_\epsilon - \lambda^h\|^2. \end{aligned}$$

Denote $a(t) = C(\nu) \|\nabla u_\epsilon\|^4 + \frac{1}{2}$ and its antiderivative

$$A(T) := \int_0^T a(t) dt < \infty \text{ for } \|\nabla u_\epsilon\| \in L^4(0, T).$$

Multiply through by the integrating factor $e^{-A(t)}$

$$\begin{aligned} \frac{d}{dt} [e^{-A(T)} \|\phi^h\|^2] + e^{-A(T)} \left[\frac{\nu}{4} \|\nabla \phi^h\|^2 + \epsilon(t) \|p^h - \lambda^h\|^2 \right] &\leq \\ e^{-A(T)} \left\{ C(\nu) [\|\eta_t\|_{-1}^2 + \|\nabla u_\epsilon\|^2 \|\eta\|_{L_4}^2 + \|u_\epsilon^h\|_{L_6}^2 \|\eta\|_{L_3}^2] + \frac{1}{2} \|u_\epsilon^h\|_{L_6}^2 \|\nabla \eta\|_{L_3}^2 + \epsilon(t) \|p_\epsilon - \lambda^h\|^2 \right\}. \end{aligned}$$

Integrate over $[0, T]$ and multiply through by $e^{A(T)}$ gives

$$\begin{aligned} \|\phi^h(T)\|^2 + \int_0^T \frac{\nu}{4} \|\nabla \phi^h\|^2 + \epsilon(t) \|p^h - \lambda^h\|^2 dt &\leq e^{A(T)} \left\{ \|\phi^h(0)\|^2 \right. \\ + \int_0^T C(\nu) [\|\eta_t\|_{-1}^2 + \|\nabla u_\epsilon\|^2 \|\eta\|_{L_4}^2 + \|u_\epsilon^h\|_{L_6}^2 \|\eta\|_{L_3}^2] &+ \frac{1}{2} \|u_\epsilon^h\|_{L_6}^2 \|\nabla \eta\|_{L_3}^2 + \epsilon(t) \|p_\epsilon - \lambda^h\|^2 dt \left. \right\}. \end{aligned}$$

Applying Hölder's inequality (15) gives

$$\begin{aligned} \int_0^T \|u_\epsilon^h\|_{L_6}^2 \|\eta\|_{L_3}^2 dt &\leq \|u_\epsilon^h\|_{L^6(0, T; L^6)}^2 \|\eta\|_{L^3(0, T; L^3)}^2, \\ \int_0^T \|\nabla u_\epsilon\|^2 \|\eta\|_{L_4}^2 dt &\leq \|\nabla u_\epsilon\|_{L^4(0, T; L^2)}^2 \|\eta\|_{L^4(0, T; L^4)}^2, \\ \int_0^T \|u_\epsilon^h\|_{L_6}^2 \|\nabla \eta\|_{L_3}^2 dt &\leq \|u_\epsilon^h\|_{L^6(0, T; L^6)}^2 \|\nabla \eta\|_{L^3(0, T; L^3)}^2. \end{aligned}$$

$\|u_\epsilon^h\|_{L^6(0,T;L^6)}$ and $\|\nabla u_\epsilon\|_{L^4(0,T;L^2)}$ are bounded by problem data by the stability bound. Using the Sobolev inequality (18), $L^p - L^2$ type inverse inequality (19), the interpolation estimate (12) and the Poincaré-Friedrichs' inequality (13)

$$\begin{aligned}\|\eta\|_{L^3} &\leq C\|\eta\|^{1-d/6}\|\nabla\eta\|^{d/6}, & \|\eta\|_{L^4} &\leq C\|\eta\|^{1-d/4}\|\nabla\eta\|^{d/4}, \\ \|\nabla\eta\|_{L^3} &\leq Ch^{-d/6}\|\nabla\eta\|, & \|\eta_t\|_{-1} &\leq Ch\|\eta_t\| \leq Ch\|\nabla\eta_t\|.\end{aligned}$$

By Proposition 2.3.2 and (38)

$$\begin{aligned}\|\nabla(u_\epsilon - \tilde{u})\|^2 &\leq C(\nu)\left[\inf_{v^h \in X^h} \|\nabla(u_\epsilon - v^h)\|^2 + \inf_{q^h \in Q^h} \|p_\epsilon - q^h\|^2\right], \\ \|u_\epsilon - \tilde{u}\|^2 &\leq C(\nu, \Omega)h^2\left[\inf_{v^h \in X^h} \|\nabla(u_\epsilon - v^h)\|^2 + \inf_{q^h \in Q^h} \|p_\epsilon - q^h\|^2\right], \\ \|\nabla(u_\epsilon - \tilde{u})_t\|^2 &\leq C(\nu)\left[\inf_{v^h \in X^h} \|\nabla(u_\epsilon - v^h)_t\|^2 + \inf_{q^h \in Q^h} \|(p_\epsilon - q^h)_t\|^2\right], \\ \|p_\epsilon - \lambda^h\|^2 &\leq C(\nu, \beta^h)\left[\inf_{v^h \in X^h} \|\nabla(u_\epsilon - v^h)\|^2 + \inf_{q^h \in Q^h} \|p_\epsilon - q^h\|^2\right].\end{aligned}$$

Thus,

$$\begin{aligned}&\|\phi^h(T)\|^2 + \int_0^T \frac{\nu}{4} \|\nabla\phi^h\|^2 + \epsilon(t)\|p^h - \lambda^h\|^2 dt \leq \\ &e^{A(T)}\left\{\|\phi^h(0)\|^2 + \int_0^T C(\nu, \beta^h)\epsilon(t)\left(\inf_{v^h \in X^h} \|\nabla(u_\epsilon - v^h)\|^2 + \inf_{q^h \in Q^h} \|p_\epsilon - q^h\|^2\right) dt\right. \\ &+ C(\nu, \Omega)\left[(h^{-d/3} + h^{2-d/3} + h^{2-d/2})\left(\inf_{v^h \in X^h} \|\nabla(u_\epsilon - v^h)\|_{L^2(0,T;L^2)}^2 + \inf_{q^h \in Q^h} \|p_\epsilon - q^h\|_{L^2(0,T;L^2)}^2\right)\right. \\ &\left. + h^2\left(\inf_{v^h \in X^h} \|\nabla(u_\epsilon - v^h)_t\|_{L^2(0,T;L^2)}^2 + \inf_{q^h \in Q^h} \|(p_\epsilon - q^h)_t\|_{L^2(0,T;L^2)}^2\right)\right]\left.\right\}.\end{aligned}$$

Using the approximation properties (10) of the spaces (X^h, Q^h)

$$\begin{aligned}&\|\phi^h(T)\|^2 + \int_0^T \frac{\nu}{4} \|\nabla\phi^h\|^2 + \epsilon(t)\|p^h - \lambda^h\|^2 dt \leq \\ &e^{A(T)}\left\{\|\phi^h(0)\|^2 + \int_0^T C(\nu, \beta^h)\epsilon(t)h^{2m}\left(\|u_\epsilon\|_{H^{m+1}(\Omega)}^2 + \|p_\epsilon\|_{H^m(\Omega)}^2\right) dt\right. \\ &+ C(\nu, \Omega)\left[(h^{-d/3} + h^{2-d/3} + h^{2-d/2})h^{2m}\left(\|u_\epsilon\|_{L^2(0,T;H^{m+1}(\Omega))}^2 + \|p_\epsilon\|_{L^2(0,T;H^m(\Omega))}^2\right)\right. \\ &\left. + h^{2m+2}\left(\|u_{\epsilon,t}\|_{L^2(0,T;H^{m+1}(\Omega))}^2 + \|p_{\epsilon,t}\|_{L^2(0,T;H^m(\Omega))}^2\right)\right]\left.\right\}.\end{aligned}$$

Drop the pressure term on the left-hand side and apply triangle inequality, then we have the error estimate. \square

2.4 Algorithms

The backward Euler method was chosen as our method of time discretization. A time filter to increase the accuracy from first to second order was added [26], and later used to implement time adaptivity easily.

We use the time discretization in [26]: for $y' = f(t, y)$, select $\tau = k_{n+1}/k_n$, $\alpha = \tau(1 + \tau)/(1 + 2\tau)$, then

$$\begin{aligned} \frac{y_{n+1}^1 - y_n}{k_{n+1}} &= f(t_{n+1}, y_{n+1}), \\ y_{n+1} &= y_{n+1}^1 - \frac{\alpha}{2} \left(\frac{2k_n}{k_n + k_{n+1}} y_{n+1} - 2y_n + \frac{2k_{n+1}}{k_n + k_{n+1}} y_{n-1} \right), \\ EST &= |y_{n+1} - y_{n+1}^1|. \end{aligned} \tag{40}$$

This step uses the information of the previous two time-steps.

This above algorithm is second-order accurate for $\alpha = 2/3$ with constant time-step $\tau = 1$. Apply this time filter to our adaptive penalty method; we get the following variable ϵ , constant time-step Algorithm 1.

Next, we extend the algorithm to variable time-step methods based on the previous work by Guzel and Layton [26] and Layton and McLaughlin [48]. We summarize as follows. In the variable time-step, the first-order and second-order method, the next time-step is adapted based on the following:

$$\begin{aligned} \text{first-order prediction } k_{new} &= k_{old} \left(\frac{tTOL}{tEST_1} \right)^{1/2}, \\ \text{second-order prediction } k_{new} &= k_{old} \left(\frac{tTOL}{tEST_2} \right)^{1/3}. \end{aligned}$$

Let D_2 denote the difference

$$D_2(n+1) = \frac{2k_n}{k_n + k_{n+1}} u_{n+1}^1 - 2u_n + \frac{2k_{n+1}}{k_n + k_{n+1}} u_{n-1}.$$

Algorithm 1: Variable ϵ , constant time-step, second-order penalty method

Given $u_n, u_{n-1}, \epsilon_n, \epsilon_{n+1}$, tolerance TOL, lower tolerance minTOL, $\epsilon_{min}, \epsilon_{max}$, and α .

Set $u^* = 2u_n - u_{n-1}$ Solve for u_{n+1}^1

$$\frac{u_{n+1}^1 - u_n}{k} + u^* \cdot \nabla u_{n+1}^1 + \frac{1}{2}(\nabla \cdot u^*)u_{n+1}^1 - \nabla \left(\frac{1}{\epsilon_{n+1}} \nabla \cdot u_{n+1}^1 \right) - \nu \Delta u_{n+1}^1 = f_{n+1}.$$

Apply time filter, Compute estimator EST

$$u_{n+1} = u_{n+1}^1 - \frac{1}{3}\{u_{n+1}^1 - 2u_n + u_{n-1}\},$$
$$EST_{n+1} = \|\nabla \cdot u_{n+1}\| / \|\nabla u_{n+1}\|.$$

Adapt ϵ using the standard decision tree:

if $EST_{n+1} \geq TOL$ **then**

if $\epsilon_{n+1} = \epsilon_{min}$ **then**

 | CONTINUE

end

else

 | $\epsilon_{n+1} \leftarrow \max\{(1 - \alpha k)\epsilon_{n+1}, 0.5\epsilon_{n+1}, \epsilon_{min}\}$;

 | REPEAT step

end

end

if $EST_{n+1} \leq minTOL$ **then**

 | $\epsilon_{n+2} \leftarrow \min\{2\epsilon_{n+1}, \epsilon_{max}\}$;

 | CONTINUE ;

end

Recover pressure p_{n+1} if needed by: $p_{n+1} = -\frac{1}{\epsilon_{n+1}} \nabla \cdot u_{n+1}$.

A simple estimate of the local truncation error in the first-order estimation is taken to be

the difference between u_{n+1} and u_{n+1}^1

$$\alpha_1 = \frac{\tau(1 + \tau)}{1 + 2\tau},$$

$$tEST_1 = \|u_{n+1} - u_{n+1}^1\| = \frac{\alpha_1}{2} \|D_2(n + 1)\|.$$

And the local truncation error of the second-order method is given by

$$\alpha_2 = \frac{\tau_n(\tau_{n+1}\tau_n + \tau_n + 1)(4\tau_{n+1}^3 + 5\tau_{n+1}^2 + \tau_{n+1})}{3(\tau_n\tau_{n+1}^2 + 4\tau_n\tau_{n+1} + 2\tau_{n+1} + \tau_n + 1)},$$

$$tEST_2 = \frac{\alpha_2}{6} \left\| \frac{3k_{n-1}}{k_{n+1} + k_n + k_{n-1}} D_2(n + 1) - \frac{3k_{n+1}}{k_{n+1} + k_n + k_{n-1}} D_2(n) \right\|.$$

For both first-order and second-order variable time-step methods, ϵ is still adapted independently using the same decision tree as in Algorithm 1.

Remark 2.4.1. *The estimator $\|\nabla \cdot u_{n+1}\|/\|\nabla u_{n+1}\|$ is chosen over $\|\nabla \cdot u_{n+1}\|$ as it is dimension free and removes dependence on the size of u .*

Next, we consider the variable time-step variable order method. This algorithm computes two velocity approximations. u^1 is first-order, and u is second-order by applying the time filter. The first-order variable time-step method is unconditionally stable, while the second-order variable time-step method is A-stable, which would require a time-step condition for stability. Combining both first and second-order methods increases accuracy and efficiency by adapting the method order .

The following Algorithm 4 gives the variable ϵ , variable time-step variable order (VSVO) penalty method. First (n=1) and second (n=2) order variable time-step method can be also obtained from this following algorithm by using corresponding time-step estimator $tEST_n$ and time-step $STEPn$. In order to use first-order method, u_{n+1}^1 is used and for second-order method, u_{n+1} is used instead. For detailed variable ϵ , variable time-step, first and second-order algorithms, see Algorithm 2 and Algorithm 3.

Algorithm 2: Variable ϵ , variable time-step, first-order penalty method

Given $u_n, u_{n-1}, \epsilon_{n+1}, \epsilon_n$, tolerance for ϵ : $TOL=10^{-6}$ and lower tolerance

$minTOL=TOL/10$, lower and upper bound of

$\epsilon : \epsilon_{min} = 10^{-8}, \epsilon_{max} = 10^{-5}, \alpha = 2$, tolerance for Δt : $tTOL=10^{-5}$ and lower

tolerance $mintTOL=tTOL/10$

Compute $\tau = \frac{k_{n+1}}{k_n}$ and $\alpha_1 = \frac{\tau(1+\tau)}{1+2\tau}$

Solve for u_{n+1}^1

Set $u^* = (1 + \tau)u_n - \tau u_{n-1}$

$$\frac{u_{n+1}^1 - u_n}{k_{n+1}} + u^* \cdot \nabla u_{n+1}^1 + \frac{1}{2}(\nabla \cdot u^*)u_{n+1}^1 - \nabla \left(\frac{1}{\epsilon_{n+1}} \nabla \cdot u_{n+1}^1 \right) - \nu \Delta u_{n+1}^1 = f_{n+1}.$$

Compute estimator EST and difference D_2

$$D_2(n+1) = \frac{2k_n}{k_n + k_{n+1}} u_{n+1}^1 - 2u_n + \frac{2k_{n+1}}{k_n + k_{n+1}} u_{n-1},$$

$$EST_e(n+1) = \|\nabla \cdot u_{n+1}\| / \|\nabla u_{n+1}\|,$$

$$tEST_1(n+1) = \frac{\alpha_1}{2} \|D_2(n+1)\|.$$

Adapt ϵ and k using the standard decision tree:

if $EST_e(n+1) > TOL$ or $tEST_1(n+1) > tTOL$ **then**

$\epsilon_{n+1} \leftarrow \max\{(1 - \alpha k_{n+1})\epsilon_{n+1}, 0.5\epsilon_{n+1}, \epsilon_{min}\};$
 $k_{n+1} \leftarrow \max\left\{0.9k_n \left(\frac{tTOL}{tEST_1(n+1)}\right)^{1/2}, 0.5k_{n+1}\right\};$
REPEAT step

else

if $EST_{n+1} < minTOL$ or $tEST_{n+1} < mintTOL$ **then**

$\epsilon_{n+2} \leftarrow \min\{2\epsilon_{n+1}, \epsilon_{max}\};$
 $k_{n+2} \leftarrow \max\left\{\min\left\{0.9k_{n+1} \left(\frac{tTOL}{tEST_1(n+1)}\right)^{1/2}, 2k_{n+1}\right\}, 0.5k_{n+1}\right\};$
CONTINUE;

end

end

Recover pressure p_{n+1} if needed by: $p_{n+1} = -\frac{1}{\epsilon_{n+1}} \nabla \cdot u_{n+1}$.

Algorithm 3: Variable ϵ , variable time-step, second-order penalty method

Given $u_n, u_{n-1}, \epsilon_{n+1}, \epsilon_n$, tolerance for ϵ TOL= 10^{-6} and lower tolerance

minTOL=TOL/10, lower and upper bound of

$\epsilon : \epsilon_{min} = 10^{-8}, \epsilon_{max} = 10^{-5}, \alpha = 2$, tolerance for Δt : tTOL= 10^{-5} and lower

tolerance mintTOL=tTOL/10

Compute $\tau = \frac{k_{n+1}}{k_n}$ and $\alpha_1 = \frac{\tau(1+\tau)}{1+2\tau}, \alpha_2 = \frac{\tau_n(\tau_{n+1}\tau_n+\tau_{n+1})(4\tau_{n+1}^3+5\tau_{n+1}^2+\tau_{n+1})}{3(\tau_n\tau_{n+1}^2+4\tau_n\tau_{n+1}+2\tau_{n+1}+\tau_n)}$

Set $u^* = (1 + \tau)u_n - \tau u_{n-1}$

Solve for u_{n+1}^1

$$\frac{u_{n+1}^1 - u_n}{k_{n+1}} + u^* \cdot \nabla u_{n+1}^1 + \frac{1}{2}(\nabla \cdot u^*)u_{n+1}^1 - \nabla \left(\frac{1}{\epsilon_{n+1}} \nabla \cdot u_{n+1}^1 \right) - \nu \Delta u_{n+1}^1 = f_{n+1}.$$

Compute estimator EST and difference D_2 and apply time filter

$$D_2(n+1) = \frac{2k_n}{k_n + k_{n+1}}u_{n+1}^1 - 2u_n + \frac{2k_{k+1}}{k_n + k_{n+1}}u_{n-1},$$

$$u_{n+1} = u_{n+1}^1 - \frac{\alpha_1}{2}D_2(n+1),$$

$$EST_e(n+1) = \|\nabla \cdot u_{n+1}\| / \|\nabla u_{n+1}\|,$$

$$tEST_2(n+1) = \frac{\alpha_2}{6} \left\| \frac{3k_{n-1}}{k_{n+1} + k_n + k_{n-1}}D_2(n+1) - \frac{3k_{n+1}}{k_{n+1} + k_n + k_{n-1}}D_2(n) \right\|.$$

if $EST_e(n+1) > TOL$ or $tEST_2(n+1) > tTOL$ **then**

$\epsilon_{n+1} \leftarrow \max\{(1 - \alpha k_{n+1})\epsilon_{n+1}, 0.5\epsilon_{n+1}, \epsilon_{min}\};$
 $k_{n+1} \leftarrow \max\left\{0.9k_n \left(\frac{tTOL}{tEST_1(n+1)}\right)^{1/3}, 0.5k_{n+1}\right\};$
REPEAT step

else

if $EST_{n+1} < minTOL$ or $tEST_{n+1} < mintTOL$ **then**

$\epsilon_{n+2} \leftarrow \min\{2\epsilon_{n+1}, \epsilon_{max}\};$
 $k_{n+2} \leftarrow \max\left\{\min\left\{0.9k_{n+1} \left(\frac{tTOL}{tEST_1(n+1)}\right)^{1/3}, 2k_{n+1}\right\}, 0.5k_{n+1}\right\};$
CONTINUE;

end

end

Recover pressure p_{n+1} by: $p_{n+1} = -\frac{1}{\epsilon_{n+1}}\nabla \cdot u_{n+1}$.

Algorithm 4: Variable ϵ , variable time-step, variable order penalty method

Given $u_n, u_{n-1}, \epsilon_{n+1}, \epsilon_n$, tolerance for ϵ : TOL= 10^{-6} and lower tolerance

minTOL=TOL/10, lower and upper bound of ϵ : $\epsilon_{min} = 10^{-8}, \epsilon_{max} = 10^{-5}, \alpha = 2$,

tolerance for Δt : tTOL= 10^{-5} and lower tolerance mintTOL=tTOL/10

Compute $\tau = \frac{k_{n+1}}{k_n}$ and $\alpha_1 = \frac{\tau(1+\tau)}{1+2\tau}, \alpha_2 = \frac{\tau_n(\tau_{n+1}\tau_n+\tau_n+1)(4\tau_{n+1}^3+5\tau_{n+1}^2+\tau_{n+1})}{3(\tau_n\tau_{n+1}^2+4\tau_n\tau_{n+1}+2\tau_{n+1}+\tau_n+1)}$

Set $u^* = (1 + \tau)u_n - \tau u_{n-1}$

Solve for u_{n+1}^1 ,

$$\frac{u_{n+1}^1 - u_n}{k_{n+1}} + u^* \cdot \nabla u_{n+1}^1 + \frac{1}{2}(\nabla \cdot u^*)u_{n+1}^1 - \nabla \left(\frac{1}{\epsilon_{n+1}} \nabla \cdot u_{n+1}^1 \right) - \nu \Delta u_{n+1}^1 = f_{n+1}.$$

Compute estimators for Δt and ϵ and difference D_2 and apply time filter

$$D_2(n+1) = \frac{2k_n}{k_n + k_{n+1}}u_{n+1}^1 - 2u_n + \frac{2k_{k+1}}{k_n + k_{n+1}}u_{n-1}, u_{n+1} = u_{n+1}^1 - \frac{\alpha_1}{2}D_2(n+1),$$

$$EST_e(n+1) = \|\nabla \cdot u_{n+1}\|/\|\nabla u_{n+1}\|, tEST_1(n+1) = \frac{\alpha_1}{2}\|D_2(n+1)\|,$$

$$tEST_2(n+1) = \frac{\alpha_2}{6} \left\| \frac{3k_{n-1}}{k_{n+1} + k_n + k_{n-1}}D_2(n+1) - \frac{3k_{n+1}}{k_{n+1} + k_n + k_{n-1}}D_2(n) \right\|.$$

Adapt ϵ and k using the standard decision tree:

(continue in next page)

(Algorithm 4 continued)

if $EST_e(n+1) > TOL$ or $\min\{tEST_1(n+1), tEST_2(n+1)\} > tTOL$ **then**

$\epsilon_{n+1} \leftarrow \max\{(1 - \alpha k_{n+1})\epsilon_{n+1}, 0.5\epsilon_{n+1}, \epsilon_{min}\};$
 $STEP1 = \max\left\{0.9k_n \left(\frac{tTOL}{tEST_1(n+1)}\right)^{1/2}, 0.5k_{n+1}\right\};$
 $STEP2 = \max\left\{0.9k_n \left(\frac{tTOL}{tEST_2(n+1)}\right)^{1/3}, 0.5k_{n+1}\right\};$
 $k_{n+1} \leftarrow \max\{STEP1, STEP2\};$
 REPEAT step

else

if $EST_{n+1} < minTOL$ or $\min\{tEST_1(n+1), tEST_2(n+1)\} < mintTOL$ **then**
 $\epsilon_{n+2} \leftarrow \min\{2\epsilon_{n+1}, \epsilon_{max}\};$
 $STEP1 \leftarrow \max\left\{\min\left\{0.9k_{n+1} \left(\frac{tTOL}{tEST_1(n+1)}\right)^{1/2}, 2k_{n+1}\right\}, 0.5k_{n+1}\right\};$
 $STEP2 \leftarrow \max\left\{\min\left\{0.9k_{n+1} \left(\frac{tTOL}{tEST_2(n+1)}\right)^{1/3}, 2k_{n+1}\right\}, 0.5k_{n+1}\right\};$
 $k_{n+2} \leftarrow \max\{STEP1, STEP2\};$
 CONTINUE

end

end

Pick method with larger time-step for next step:

if $STEP1 > STEP2$ **then**

| $u_{n+1} = u_{n+1}^1$

end

Recover pressure p_{n+1} if needed by: $p_{n+1} = -\frac{1}{\epsilon_{n+1}} \nabla \cdot u_{n+1}$.

Remark 2.4.2. *In this algorithm, 0.9 is used as a standard safety factor [48].*

2.5 Numerical Experiments

2.5.1 Modified Taylor-Green vortex, taken from [18]

First we verify the adaptive ϵ penalty method does better than normal constant ϵ penalty method by comparing the adaptive ϵ tests (Algorithm 1) with two different constant ϵ options: 1) constant $\epsilon = 10^{-8}\nu$ and 2) constant $\epsilon = k$. Here option 1) is usually the approach used by engineering people, and option 2) is derived from a previous penalty paper by Shen [59].

2.5.1.1 Modified test 1

This test is a modified version of the historically used problem Taylor-Green vortex. The exact solution is given by

$$\begin{aligned} u(x, y, t) &= F(t)(\cos x \sin y, -\sin x \cos y), \\ p(x, y, t) &= -\frac{1}{4}F(t)^2(\cos 2x + \cos 2y). \end{aligned}$$

Here $F(t)$ can be any differentiable function of t . With velocity and pressure defined as above, the body force is therefore

$$f(x, y, t) = (2\nu F(t) + F'(t))(\cos x \sin y, -\cos y \sin x).$$

To construct $F(t)$, first we construct a sharp transition function between 0 and 1 as follows

$$g(t) = \begin{cases} 0 & \text{if } t \leq 0, \\ \exp(-\frac{1}{(10t)^{10}}) & \text{if } t > 0. \end{cases}$$

A differentiable function $F(t)$ therefore can be constructed with shifts and reflections of this function $g(t)$. The plot of $F(t)$ are shown as follows in Figure 1. This is a periodic function with sharp increase and decrease. The test was done with 100 nodes per side of the square $[0, 2\pi] \times [0, 2\pi]$ using P_2 elements, and with final time of $T = 25$.

The result shown in Figure 2 is done with 100 mesh points on each side and $\Delta t = 0.005$. The three different methods are: 1) constant epsilon penalty method with $\epsilon = 10^{-8}\nu$, 2) constant epsilon penalty method with $\epsilon = k$ and 3) variable penalty method (Algorithm 1).

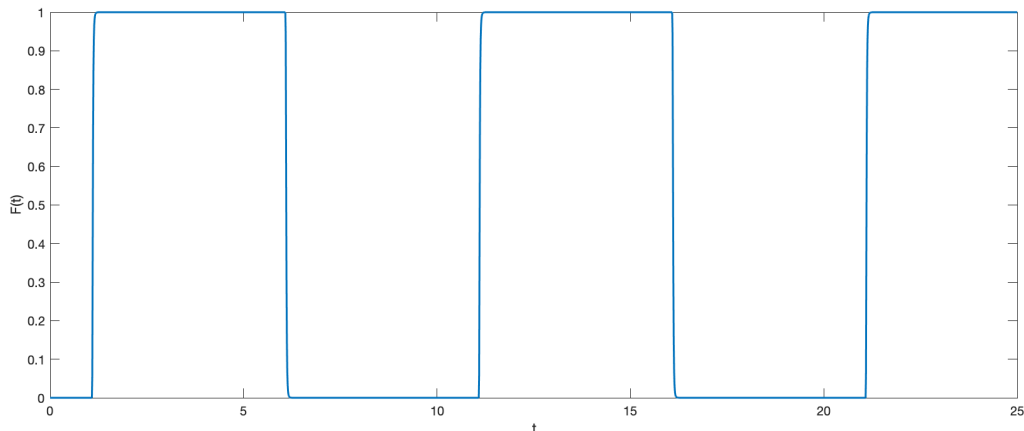


Figure 1: plot of the differentiable function $F(t)$ over time interval $[0, 25]$

All three methods are accomplished with a time-filter. The result shown in Figure 2 are plots of $\|\nabla \cdot u\|$, discrete $\|u_t\|$, evolution of ϵ , velocity error $\|u - u^h\|$ and pressure error $\|p - p^h\|$. In the fourth plot of velocity error $\|u - u^h\|$, the adaptive ϵ penalty method has a smaller error. In the third plot of ϵ , ϵ of the adaptive penalty method does change periodically, and these changes correspond to the sharp change of $F(t)$ in Figure 1. When there is a sharp decrease of ϵ in the third plot, there is a sharp increase in $\|u_t\|$ in the second plot. Moreover, this verifies the necessity of epsilon restriction condition (34).

There are some spikes of pressure error of scale $\mathcal{O}(10^2)$ for all three different penalty methods from the last plot of Figure 2. To further see difference of the pressure error, we zoomed in and get Figure 3. The pressure error are all of scale $\mathcal{O}(10^{-2})$ except for those spikes. And among the three penalty methods, adaptive ϵ has comparable smaller pressure error and constant $\epsilon = 10^{-8}\nu$ has bigger pressure error.

Next, we check the time accumulated velocity error over the time interval $[0, 25]$. The velocity error $\|u - u^h\|_{L_2, L_2}$ is shown in Table 1. The error of adaptive penalty is $\mathcal{O}(10^{-2})$ while for the other two constant penalty methods errors are $\mathcal{O}(10^{-1})$. Thus, we see there is an advantage in applying the adaptive penalty method.

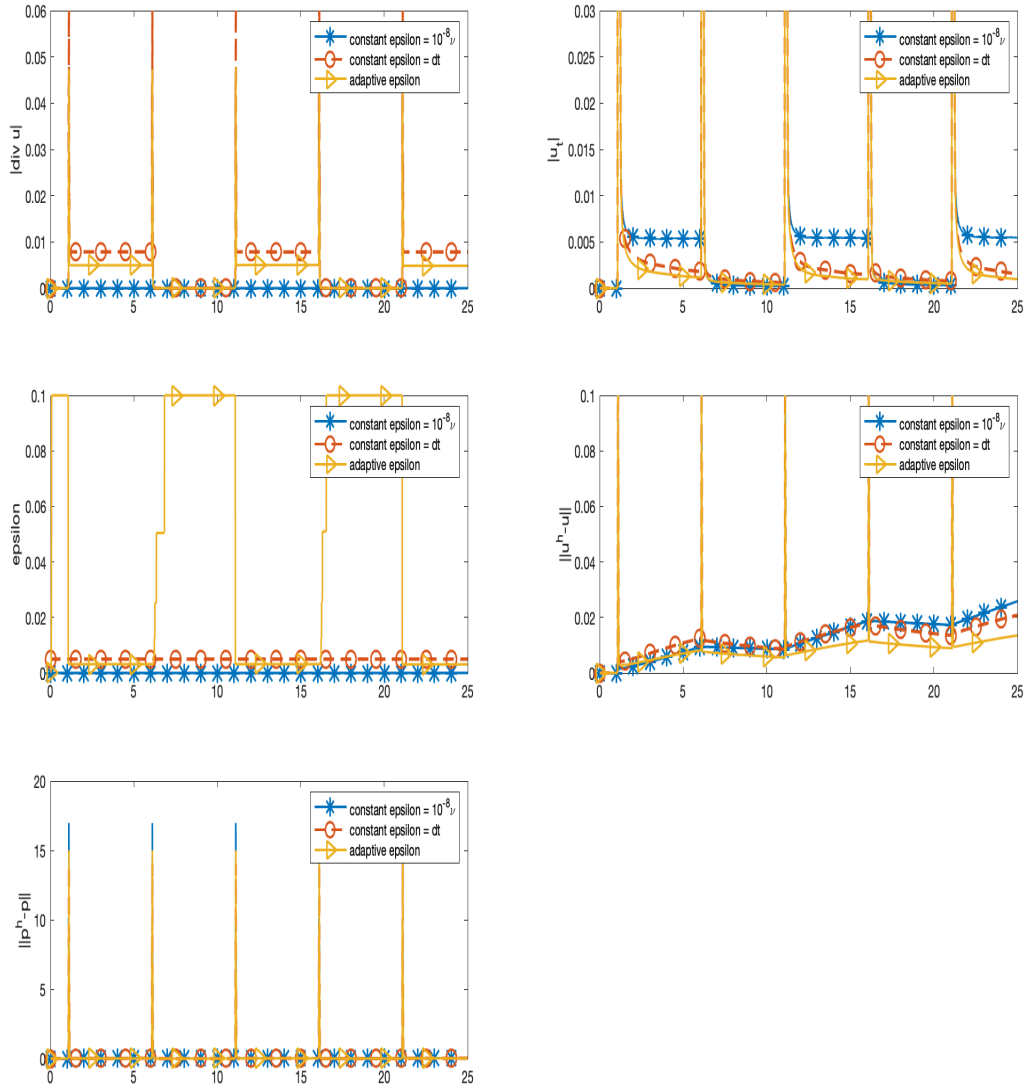


Figure 2: Test1: Comparison between adaptive penalty (Algorithm 1) and two constant penalty methods, tests are done with 100 mesh points per side and $\Delta t = 0.005$.

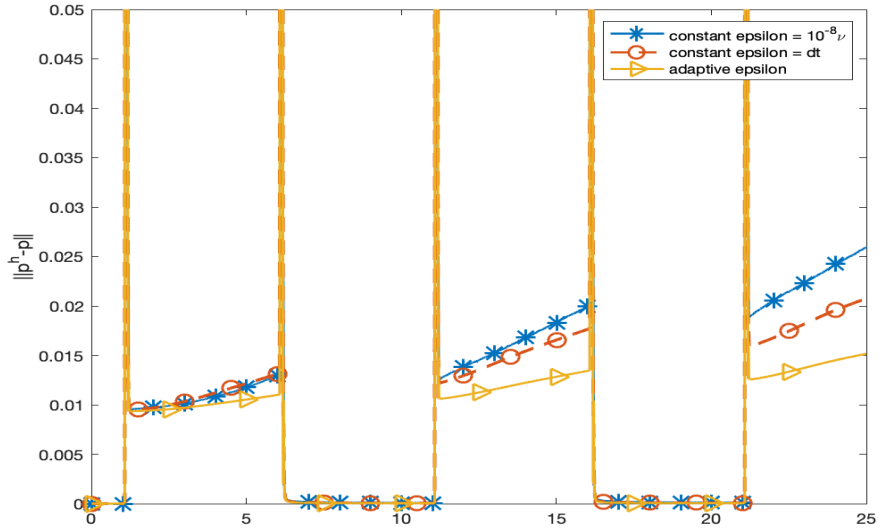


Figure 3: Test1: Pressure error comparison between adaptive penalty (Algorithm 1) and two constant penalty methods, tests are done with 100 mesh points per side and $\Delta t = 0.005$.

k	constant $\epsilon = 10^{-8}\nu$	constant $\epsilon = k$	variable ϵ
0.005	0.246098	0.255838	0.0570719

Table 1: Comparison of velocity error $\| \|u - u^h\| \|_{L_2 L_2}$

2.5.1.2 Modified test 2

This test is also a modified version of Taylor-Green vortex and the exact solution is given by

$$\begin{aligned}
 u(x, y, t) &= e^{-2\nu t} (\cos x \sin y, -\sin x \cos y), \\
 p(x, y, t) &= -\frac{1}{4} e^{-4\nu t} (\cos 2x + \cos 2y) + x(\sin 2t + \cos 3t) + y(\sin 3t + \cos 2t).
 \end{aligned}$$

This is inserted into the NSE and the body force $f(x, y, t)$ calculated.

The test was done using uniform meshes with 100 nodes per side of the square $[0, 2\pi] \times [0, 2\pi]$. We solve using P_2 elements and calculate up to time $T = 25$. Here we still compare three different methods: 1) constant epsilon penalty method with $\epsilon = 10^{-8}\nu$, 2) constant epsilon penalty method with $\epsilon = k$ and 3) variable penalty method (Algorithm 1). All three methods are calculated with $\Delta t = 0.005$ with time-filter. The results are shown in Figure 4, Figure 5, Figure 7 and Figure 8.

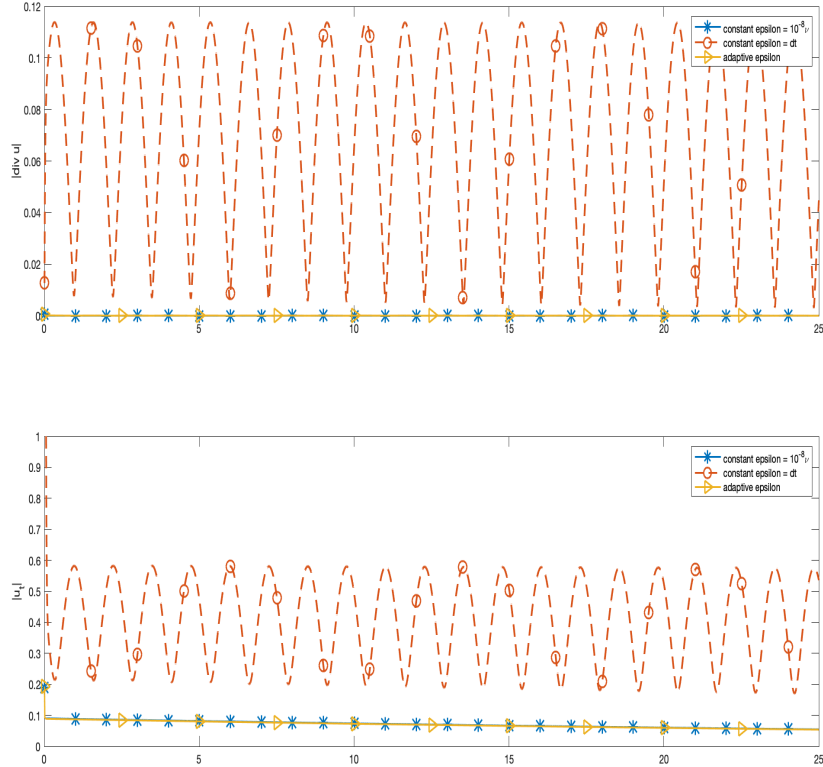


Figure 4: Test2: Comparison of $\|\nabla \cdot u\|$ and discrete $\|u_t\|$ between adaptive penalty (Algorithm 1) and two constant penalty methods, tests are done with 100 mesh points per side and $\Delta t = 0.005$.

Figure 4 shows the evolution of $\|\nabla \cdot u\|$ and discrete $\|u_t\|$. Constant penalty $\epsilon = k$ has much more larger $\|\nabla \cdot u\|$ and $\|u_t\|$ than both constant penalty $\epsilon = 10^{-8}\nu$ and adaptive penalty methods. The results of constant $\epsilon = k$ is inaccurate as $\|\nabla \cdot u\| = \mathcal{O}(10^{-1})$.

To further see the difference between constant penalty $\epsilon = 10^{-8}\nu$ and adaptive penalty. We zoomed in to get Figure 5 and further zoomed in to get a plot of $\|\nabla \cdot u\|$ of constant $\epsilon = 10^{-8}\nu$ only see Figure 6. Constant $\epsilon = 10^{-8}\nu$ and adaptive penalty has comparable $\|u_t\|$ values, both of order $\mathcal{O}(10^{-2})$. But adaptive penalty has larger $\|\nabla \cdot u\|$ values than constant penalty $\epsilon = 10^{-8}\nu$. $\|\nabla \cdot u\|$ of adaptive penalty is $\mathcal{O}(10^{-5})$ from Figure 5 and $\|\nabla \cdot u\|$ of constant penalty $\epsilon = 10^{-8}\nu$ is $\mathcal{O}(10^{-9})$ from Figure 6.

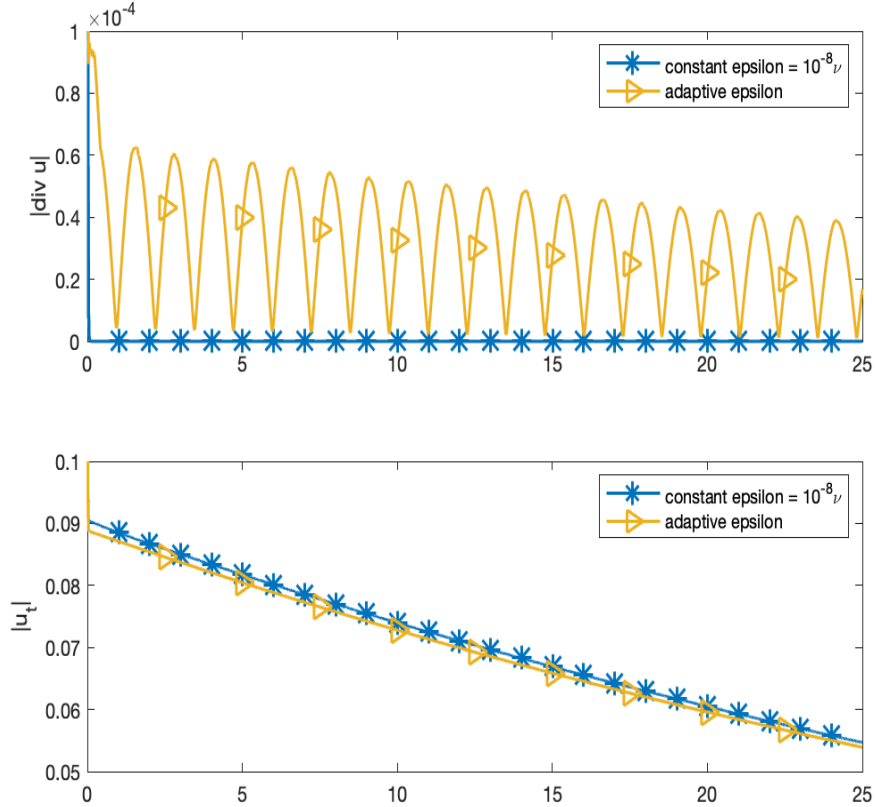


Figure 5: Test2: Zoomed in comparison of $\|\nabla \cdot u\|$ and discrete $\|u_t\|$ between adaptive penalty (Algorithm 1) and constant penalty $\epsilon = 10^{-8}\nu$, tests are done with 100 mesh points per side and $\Delta t = 0.005$.

The second plot of Figure 7 is the velocity error $\|u - u^b\|$, adaptive ϵ has a much smaller error compared to the other two constant penalty methods. The first plot of Figure 7 is the evolution of ϵ of 1) constant $\epsilon = 10^{-8}\nu$ and 3) adaptive penalty. The evolution of ϵ of 2)

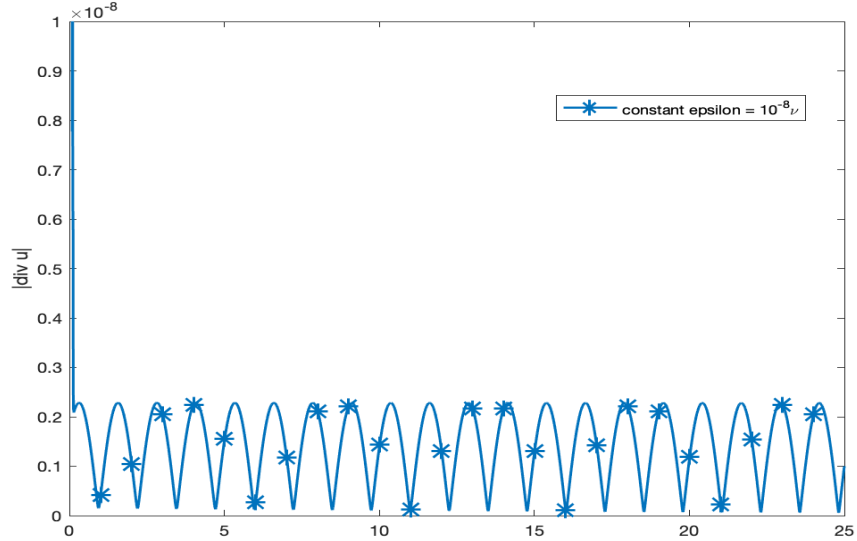


Figure 6: Test2: Evolution of $\|\nabla \cdot u\|$ of constant penalty $\epsilon = 10^{-8}\nu$, tests are done with 100 mesh points per side and $\Delta t = 0.005$.

constant $\epsilon = k$ is not shown in this plot due to the limitation of y -axis. ϵ of 3) adaptive penalty changes with time and gradually becomes stable over time. This shows that the adaptive penalty method does pick a good ϵ automatically. Because the penalty method is very sensitive to the choice of ϵ as we see in Figure 9, a good choice of ϵ is not easy at the beginning. Furthermore, by using the adaptive penalty method, we could eventually find that good ϵ with a little more calculation.

The behavior of pressure is not good as seen in Figure 8. Both pressure and pressure error fluctuate. Accurate pressure recovery remains an open question.

As a conclusion, there are three main advantages of the adaptive penalty method over the usual constant penalty method:

1. The errors of adaptive ϵ and constant ϵ are comparable. Finding a good, constant ϵ value can require an exhaustive search.
2. Constant $\epsilon = 10^{-8}\nu$ behaves better than constant $\epsilon = k$ in our tests. But as in the previous two tests, with $\nu = 0.01$, $\epsilon = 10^{-8}\nu = 10^{-10}$ leads to an extremely ill conditioned

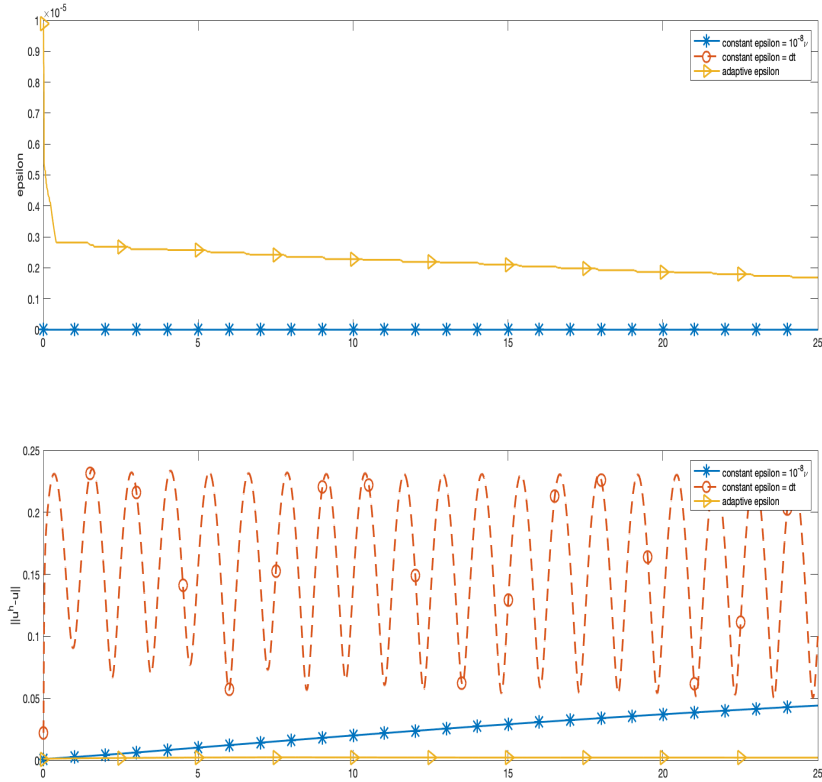


Figure 7: Test2: Evolution of ϵ and $\|u - u^h\|$ between adaptive penalty (Algorithm 1) and two constant penalty methods, tests are done with 100 mesh points per side and $\Delta t = 0.005$.

linear system. While adaptive ϵ levels out with $\epsilon \approx 10^{-5}$ and gives $\|\nabla \cdot u\| = \mathcal{O}(10^{-5})$. Adaptive ϵ controls $\|\nabla \cdot u\|$ better than $\epsilon = k$ and controls $\|\nabla \cdot u\|$ almost as well as $\epsilon = 10^{-8}\nu$ but leads to a much better conditioned system. Further, adaptive ϵ has smaller velocity error than $\epsilon = 10^{-8}\nu$. Overall, adaptive ϵ performed better.

3. The only way to find the best ϵ is by exhaustive search for problems with an already known solution. This is not possible for new problems but is not needed with the adaptive penalty.

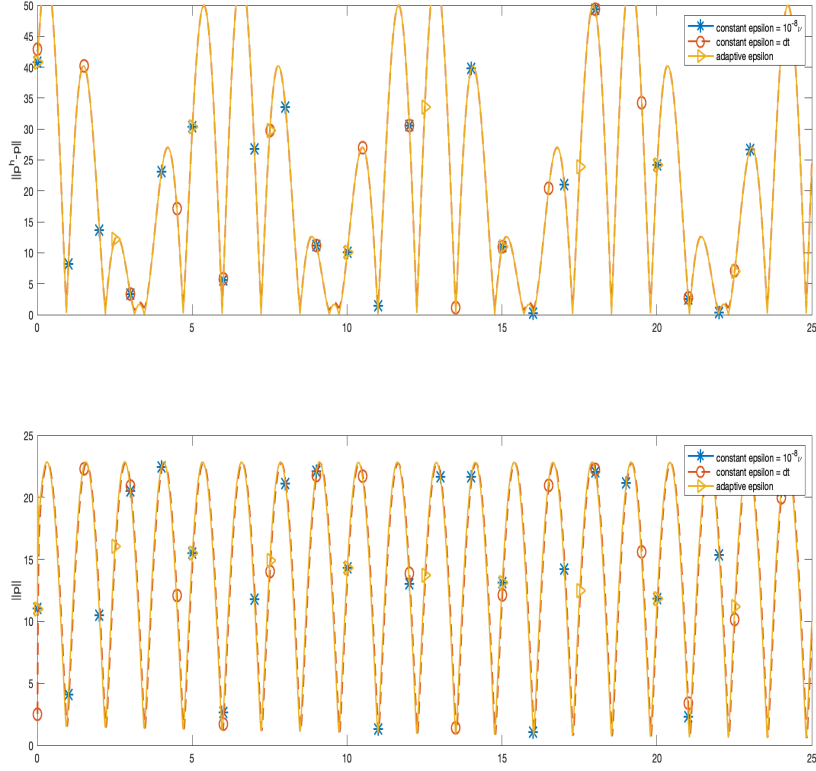


Figure 8: Test2: Comparison of $\|p - p^h\|$ and discrete $\|p^h\|$ between adaptive penalty (Algorithm 1) and two constant penalty methods, tests are done with 100 mesh points per side and $\Delta t = 0.005$.

2.5.2 A test with exact solution, taken from [17]

This exact solution experiment tests the accuracy of the adaptive penalty algorithm. The following test has the exact solution for the 2D Navier-Stokes problem ($\nu = 1$).

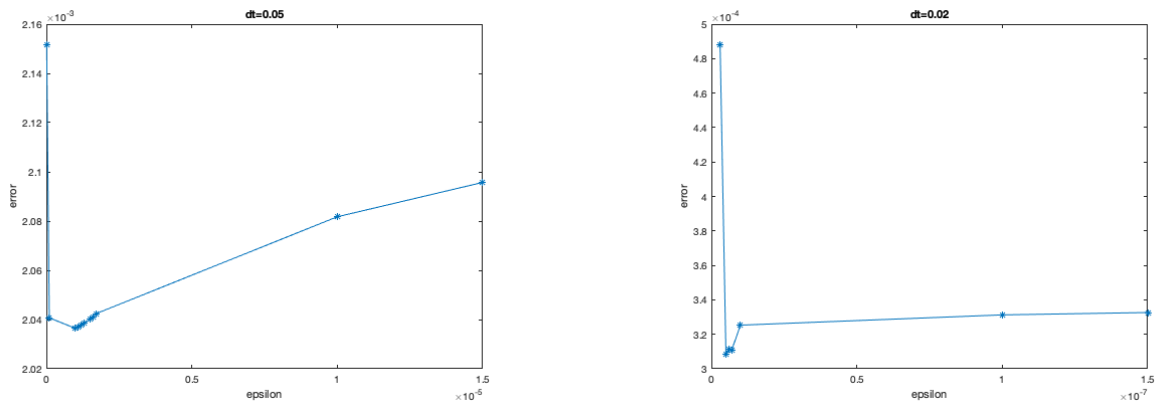
Let the domain $\Omega = (-1, 1) \times (-1, 1)$. The exact solution is as follows:

$$u(x, y, t) = \pi \sin t (\sin 2\pi y \sin^2 \pi x, -\sin 2\pi x \sin^2 \pi y)$$

$$p(x, y, t) = \sin t \cos \pi x \sin \pi y$$

This is inserted into the NSE and the body force $f(x, t)$ calculated.

Uniform meshes were used with 270 nodes per side on the boundary. The mesh is fine enough that the error resulting from the meshsize is relatively smaller than that from the step-size. Taylor-Hood elements (P2-P1) were used in this test. We ran the test up to $T = 10$.



(a) $\Delta t = 0.05$, minimum error occurs at $\epsilon = 10^{-6}$

(b) $\Delta t = 0.02$, minimum error occurs at $\epsilon = 5 * 10^{-9}$

Figure 9: $\|(u - u^h)(10)\|$ with constant time-step and different values of penalty parameter ϵ

Figure 9 indicates that velocity error is very sensitive to the choice of ϵ . This sensitivity is a known effect, motivating the ϵ -adaptive algorithm of the penalized NSE (28). It also suggests that ϵ too large is safer than ϵ too small.

2.5.2.1 Constant time-step, variable ϵ test

First, we tested the constant time-step, variable ϵ test based on Algorithm 1. The error at final time $T=10$ is in Table 2. We observe that the velocity error is good, but the pressure approximation is poor. The recovery of pressure still remains a big problem. Also, when Δt gets smaller, the velocity error reached a plateau.

dt	# steps	$\ (u - u^h)(10)\ $	rate	$\ (u - u^h)(10)\ _{L^\infty}$	rate	$\ (p - p^h)(10)\ _{L^\infty}$	rate
0.1	100	0.00965699	-	0.00869	-	0.268895	-
0.05	200	0.00203366	2.2475	0.002075	2.0662	0.229891	0.2261
0.02	500	0.000332169	1.9775	0.0004969	1.5599	0.222597	0.0352
0.01	1000	0.000324625	0.0331	0.00043955	0.1769	0.196683	0.1786

Table 2: Constant time-step variable ϵ error comparison

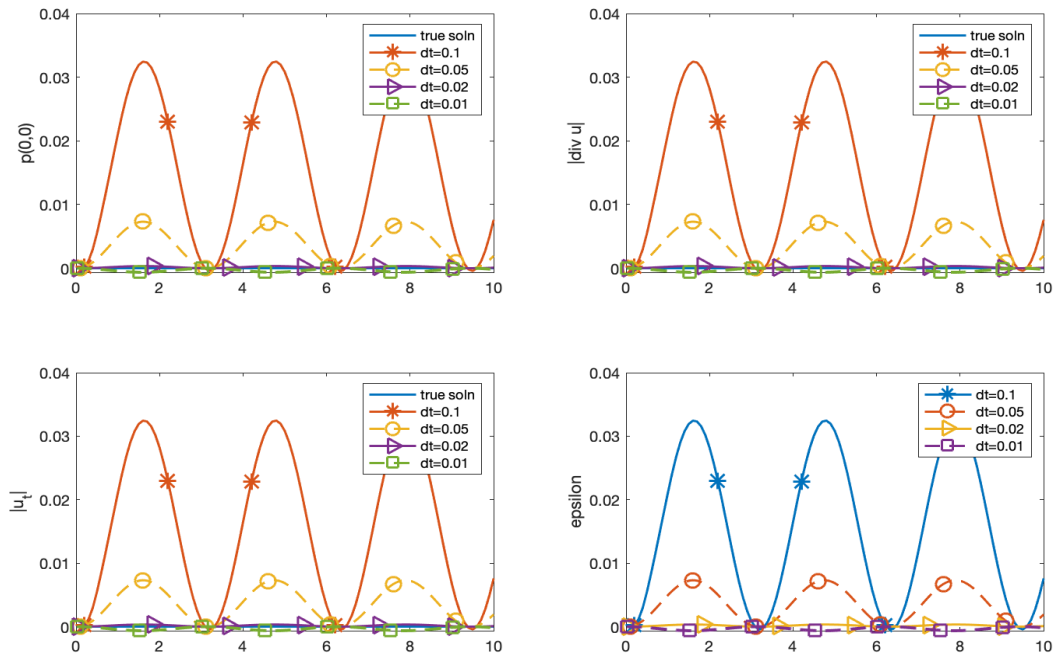


Figure 10: Comparison of results with different Δt of variable ϵ , constant time-step method (Algorithm 1)

$\|\nabla \cdot u\|$ in Figure 10 is well controlled for all three different time-steps. $\|u_t\|$ in Figure 10 is very close to the true value of problem. Decreasing the time-step improves accuracy of the pressure at origin $(0, 0)$. The oscillations in the errors of $p(0, 0)$ and $\|\nabla \cdot u\|$ arise from

the multiplier $\sin(t)$ in the exact solution.

This test has a smooth solution, $\|\nabla u\|$ does not vary too much in the whole test. And this result in the estimator $EST = \|\nabla \cdot u\|/\|\nabla u\|$ is also very smooth. So ϵ does not vary too much in this test. Both $\|u_t\|$ and $\|\nabla \cdot u\|$ are well controlled. The values of $\|u_t\|$ are very close to the true value. The values of $\|\nabla \cdot u\|$ are very close to 0 (up to 10^{-4}) which is the incompressibility condition. One surprising effect we see from the plot of $\|\nabla \cdot u\|$ is that smaller Δt leads to larger $\|\nabla \cdot u\|$, which contradicts expectations from theory. This is due to for smaller Δt , this adaptive ϵ algorithm suggests larger ϵ . $\nabla \cdot u$ and p need to satisfy the relation $\nabla \cdot u + \epsilon p = 0$ and this implies $\|\nabla \cdot u\| = \epsilon\|p\|$.

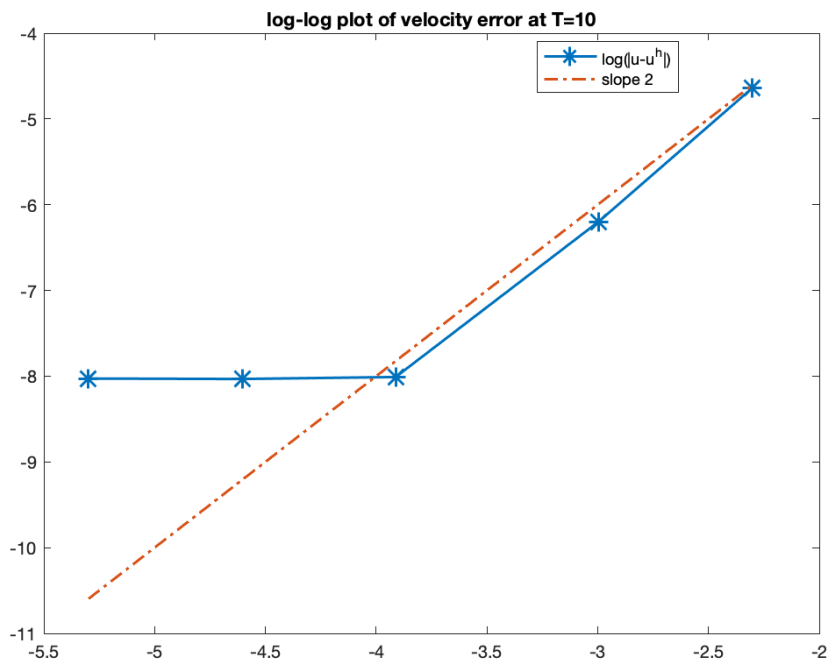


Figure 11: log-log plot, log of velocity error at final step $T=10$ $\|(u - u^h)(10)\|$ v.s. $\log \Delta t$ using variable ϵ constant time-step method (Algorithm 1). Slope of plot $\|(u - u^h)(10)\|$ is close to 2.

Figure 11 is the log-log plot of velocity error at final time $T=10$ versus the time-step k . We see the curve of $\log(\|(u - u^h)(10)\|) - \log(k)$ has slope close to 2. This constant time-step, variable ϵ , backward Euler algorithm with time filter (Algorithm 1) is second-order accurate.

The error does not change too much when the time-step gets too small. This is due to the choice of tolerance, TOL , for algorithm here is 10^{-6} and at this time-step reached the error plateau.

2.5.2.2 Double Adaptive

Next, we test the same problem using the variable time-step algorithm (Algorithm 2, Algorithm 3 and Algorithm 4). The errors of variable time-step, variable ϵ method are presented at Table 3. From the table, the variable order method gives slightly better results than the first-order and second-order methods. The velocity error is of order 10^{-3} using VSVO and is of order 10^{-2} for both first and second-order algorithms. The pressure error of VSVO is approximately 50% smaller than first and second-order algorithms.

method	# steps	$\ (u - u^h)(10)\ $	$\ (u - u^h)(10)\ _{L^\infty}$	$\ (p - p^h)(10)\ _{L^\infty}$
first	3450	0.0609278	0.0512269	0.348461
second	447	0.0567343	0.0476828	0.344317
vsvo	566	0.00364638	0.00314834	0.190205

Table 3: Variable time-step error comparison

For the variable time-step methods, in Figure 12 we track the evolution of ϵ and Δt , the pressure at the origin, $\|\nabla \cdot u\|$ and $\|u_t\|$. The last plot of Figure 12 shows that the second-order method consistently chooses a larger time-step than the first-order method. In the beginning, VSVO picks the second-order method, and after some time, VSVO picks the first-order method. The VSVO algorithm takes larger time-steps than both the first and second-order methods.

From Figure 13, the plot of $\|u_t\|$, we see some spikes. The time where we see spikes is exactly ϵ is decreased a lot (see Figure 12.) From the analysis of stability of $\|u_t\|$, when we decrease ϵ , (34) must be satisfied to avoid catastrophic growth of $\|u_t\|$. When adapting ϵ and k to ensure $EST < TOL$, we may reject due to EST exceeding TOL and redo the step several times. This may result in the sudden decrease of ϵ , as in Figure 12. This kind of

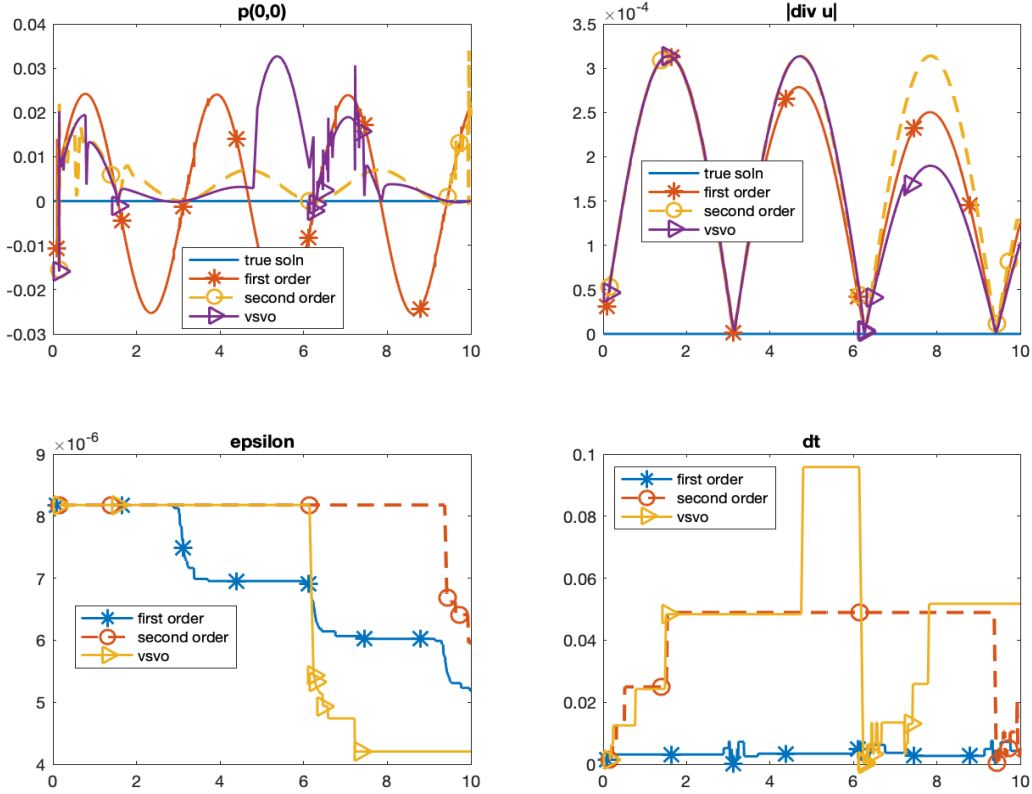


Figure 12: Comparison of variable time-step, variable ϵ method (Algorithm 2,3,4)

sudden decrease of ϵ violates (34) and results in the spikes as in Figure 13. This illustrates the necessity of controlling the change in ϵ using the method we derived from stability analysis and decreasing ϵ using (34): $(1 - k\alpha)\epsilon_n \leq \epsilon_{n+1}$.

2.5.3 Flow Between Offset Circles, taken from [48]

The domain is a disk with a smaller off center obstacle inside. Let $r_1 = 1, r_2 = 0.1, c = (c_1, c_2) = (1/2, 0)$, then the domain is given by

$$\Omega = \{(x, y) : x^2 + y^2 < r_1^2 \text{ and } (x - c_1)^2 + (y - c_2)^2 > r_2^2\}.$$

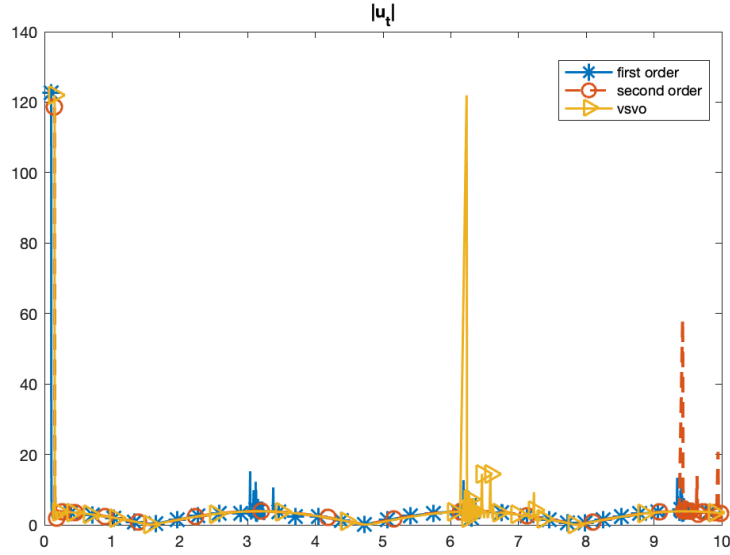


Figure 13: $\|u_t\|$ plot of variable time-step, variable ϵ method (Algorithm 2,3,4) The spikes show at the time when ϵ decrease too fast (violation of (34))

The flow is driven by a counterclockwise rotational body force

$$f(x, y, t) = \min\{t, 1\}(-4y * (1 - x^2 - y^2), 4x * (1 - x^2 - y^2))^T, \quad \text{for } 0 \leq t \leq 10,$$

with no-slip boundary conditions on both circles. We discretize in space using $P^2 - P^1$ Taylor-Hood elements. There are 200 mesh points around the outer circle and 50 mesh points around the inner circle. The finite element discretization has a maximal mesh width of $h_{max} = 0.048686$. The flow is driven by a counterclockwise force ($f=0$ on the outer circle). The flow rotates about the origin and interacts with the immersed circle.

To better compare the results, tests is also done using the following algorithm:

Backward Euler with grad-div stabilization parameter $\gamma = 1$ see Jenkins, John, Linke and Rebholz [34]

$$\begin{aligned} \frac{u^{n+1} - u^n}{k} + u^n \cdot \nabla u^{n+1} + \frac{1}{2}(\nabla \cdot u^n)u^{n+1} + \nabla p^{n+1} - \nu \Delta u^{n+1} - \gamma \nabla \nabla \cdot u^{n+1} &= f_{n+1}, \\ \nabla \cdot u^{n+1} &= 0. \end{aligned} \quad (41)$$

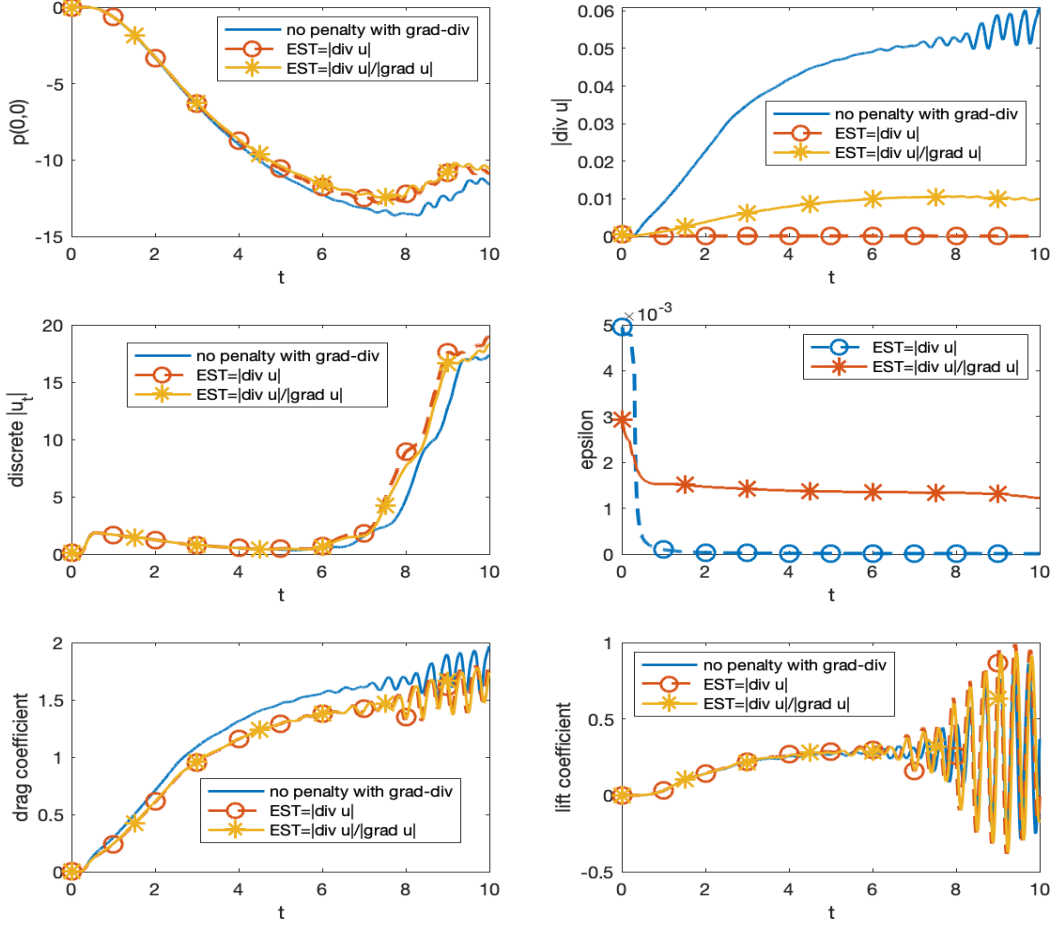


Figure 14: Comparison between different estimators $\|\nabla \cdot u\|$ and $\|\nabla \cdot u\|/\|\nabla u\|$, $Re = 100$, $\Delta t = 0.005$ with Algorithm 1 (constant time-step, variable ϵ). No penalty uses Backward Euler with grad-div stabilization (41) with $\Delta t = 0.001$. Tests without penalty use 320 mesh points around the outer circle and 80 mesh points around the inner circle. The finite element discretization has a maximal mesh width of $h_{max} = 0.0347224$.

For both estimators $EST = \|\nabla \cdot u\|$ and $EST = \|\nabla \cdot u\|/\|\nabla u\|$, we use constant time-step variable ϵ (Algorithm 1) with the same tolerance TOL and lower tolerance $minTOL$. We track the evolution of ϵ , the pressure at the origin, the evolution of $\|\nabla \cdot u\|$, $\|u_t\|$ and the

lift, drag coefficients. These are all shown in Figure 14.

The fourth plot in Figure 14 shows that with $EST = \|\nabla \cdot u\|/\|\nabla u\|$ chooses larger ϵ values than with estimator $EST = \|\nabla \cdot u\|$. The evolution of pressure, lift and drag coefficients behave similarly for both estimators. $\|\nabla \cdot u\|$ is smaller using adaptive ϵ penalty algorithm (Algorithm 1) than using Backward Euler with grad-div stabilization (41). $\|\nabla \cdot u\|$ from the penalty method is at least 5 times smaller $\|\nabla \cdot u\|$ from coupled Backward Euler with grad-div stabilization (41). The adaptive penalty method has better control of $\|\nabla \cdot u\|$ than the coupled Backward algorithm with grad-div stabilization term (41). Lift coefficient calculated from adaptive ϵ penalty method looks good.

3.0 Adapting ϵ in space

We propose, analyze and test a new adaptive penalty scheme that picks the penalty parameter ϵ element by element small where $\nabla \cdot u^h$ is large. We start by analyzing and testing the new scheme on the most simple but interesting setting, the Stokes problem. Finally, we extend and test the algorithm on the incompressible Navier-Stokes equation on complex flow problems. Tests indicate that the new adaptive- ϵ penalty method algorithm predicts flow behavior accurately. The scheme is developed in the penalty method but also can be used to pick a grad-div stabilization parameter.

3.1 Introduction

Consider the incompressible Navier-Stokes equations (NSE) with no-slip boundary condition:

$$\begin{aligned} u_t + u \cdot \nabla u + \nabla p - \nu \Delta u &= f, \text{ and } \nabla \cdot u = 0, \text{ in } \Omega \times [0, T], \\ u &= 0, \text{ on } \partial\Omega \times [0, T], \text{ and } u(x, 0) = u_0(x), \text{ in } \Omega. \end{aligned} \quad (42)$$

Here u is the velocity, f is the known body force, p is the pressure, and ν is the viscosity. The penalty approximation to the Navier-Stokes equations replaces $\nabla \cdot u = 0$ by $\nabla \cdot u + \epsilon p = 0$ and eliminates the pressure. This uncouples velocity and pressure, and the resulting system is much easier to solve:

$$\begin{aligned} u_{\epsilon,t} + u_{\epsilon} \cdot \nabla u_{\epsilon} + \frac{1}{2}(\nabla \cdot u_{\epsilon})u_{\epsilon} - \nu \Delta u_{\epsilon} - \nabla \left(\frac{1}{\epsilon} \nabla \cdot u_{\epsilon} \right) &= f \text{ in } \Omega \times [0, T], \\ u_{\epsilon} &= 0, \text{ on } \partial\Omega \times [0, T], \text{ and } u_{\epsilon}(x, 0) = u_0(x), \text{ in } \Omega. \end{aligned} \quad (43)$$

Here $u_{\epsilon} \cdot \nabla u_{\epsilon} + \frac{1}{2}(\nabla \cdot u_{\epsilon})u_{\epsilon}$ is the modified bilinear term introduced by Temam [61]. This bilinear term ensures the dissipativity of the system (43). Supposing the spatial discretization, a simple penalty method is given as follows. Given $u^n \approx u(x, t_n)$, $k_n = t^{n+1} - t^n$ the

n^{th} time step

$$\begin{aligned} \frac{u_\epsilon^{n+1} - u_\epsilon^n}{k_n} + u_\epsilon^n \cdot \nabla u_\epsilon^{n+1} + \frac{1}{2}(\nabla \cdot u_\epsilon^n)u_\epsilon^{n+1} - \nu \Delta u_\epsilon^{n+1} - \nabla \left(\frac{1}{\epsilon_{n+1}} \nabla \cdot u_\epsilon^{n+1} \right) &= f(t^{n+1}), \text{ in } \Omega, \\ u_\epsilon^{n+1} &= 0, \text{ on } \partial\Omega \text{ and } u_\epsilon^0 = u_\epsilon(x, 0) = u_0(x), \text{ in } \Omega. \end{aligned} \tag{44}$$

The term $-\nabla(\epsilon^{-1}\nabla \cdot u)$ also arises in artificial compression [48, 17] method and with grad-div stabilization [34, 54, 13]. Penalty methods require less computing time and reduced storage but still face two unsolved problems:

1. How to recover the pressure accurately, and
2. How to pick an effective value of the grad-div coefficient ϵ .

Herein we present a self-adaptive algorithm answering question 2.

Many papers are devoted to the parameter choice of grad-div term for both grad-div stabilization and penalty problems. Jenkins, John, Linke, and Rebholz [34] found that the grad-div parameter for Stokes problem depends on the used norm, the solution, the finite element space, and the type of mesh used. Ainsworth, Allendes, Barrenechea and Rankin [1] introduced an approach to select stabilization parameters for the Stokes problem.

The velocity error of penalty methods is also sensitive to the choice of ϵ , see Bercovier and Engelman [4]. Care must be taken when choosing ϵ . If ϵ is too large, it will poorly model incompressible flow. Choosing ϵ too small will cause numerical conditioning problems, see Hughes, Liu and Brooks [32]. In [32], the authors introduced a theory for determining the penalty parameter, which depends on Reynolds number Re and viscosity μ . The optimal choice of the penalty parameter also varies according to the time discretization schemes and space discretization schemes used, see Shen [59]. With so many dependencies, an automatic choice of ϵ naturally becomes a problem to consider.

In Layton and McLaughlin [48] self-adaptive ϵ selection in time (but not in space) algorithms were developed, analyzed and tested. The basic idea in [48] is to monitor $\|\nabla \cdot u^n\|$ and pick $\epsilon = \epsilon(t_n)$ to make $\|\nabla \cdot u^n\| < \text{Tolerance}$ in (44) in the computation of u^{n+1} .

The natural question we answer herein is: can we let $\epsilon = \epsilon(x, t)$ and pick $\epsilon(x, t_n)$ pointwise or element by element small where $\nabla \cdot u^h$ is large to enforce in a realizable sense

$$\int_{\Omega} |\nabla \cdot u^h|^2 dx < \text{Tolerance}^2. \quad (45)$$

This means ϵ is chosen small where $\nabla \cdot u^h$ is large (and large where small). As a result, the term $(\epsilon^{-1} \nabla \cdot u^h, \nabla \cdot u^h)$ becomes nonlinear. To our knowledge, this natural idea has not been considered. Picking ϵ pointwise and elementwise are two related ideas, but the resulting two algorithms are different; see (50) and (52) below.

The idea we use is the path of many adaptive methods: monitor the residual (the left-hand side of (45)), localize the global tolerance (45) and where the local residual $\int_{\Delta} |\nabla \cdot u^h|^2 dx$ is large, pick ϵ_{Δ} small (and visa versa). Picking ϵ locally in space leads to a nonlinear grad-div term in (44) quite amenable to numerical analysis. In the next sections, we start the detailed analysis and test of this idea using the simplest setting, the Stokes problem.

3.1.1 Previous Work

Bernardi, Girault and Hecht [5, 6] derived posterior error estimates for the Stokes problem with penalty. They performed the tests on adaptive meshes and tested using local penalty parameters. Falk [20] derived a new finite element method that uses the trial function, which is not div-free. By eliminating the constraint, one can use simple finite elements, which inspired the proof in Section 3.2.2. Heavner and Rebholz [29] considered a local choice of grad-div stabilization parameter. Moreover, in numerical tests, they showed that local choice of stabilization parameter provides more accurate solutions.

3.1.2 Formulation

We begin the analysis and testing of this idea for the simplest interesting setting, the Stokes problem

$$-\nu \Delta u + \nabla p = f(x), \quad \nabla \cdot u = 0. \quad (46)$$

On a bounded, open polyhedral domain Ω subject to no-slip boundary conditions $u = 0$ on $\partial\Omega$. Let d denote the dimension of Ω , $d = \dim(\Omega) = 2$ or 3 .

The penalty method replaces $\nabla \cdot u = 0$ by $\nabla \cdot u_\epsilon + \epsilon p = 0$ and eliminate pressure using $p = -\epsilon^{-1} \nabla \cdot u_\epsilon$:

$$-\nu \Delta u_\epsilon - \nabla \left(\frac{1}{\epsilon} \nabla \cdot u_\epsilon \right) = f(x) \text{ in } \Omega. \quad (47)$$

Let $X^h \subset X := (H^{0,1}(\Omega))^d$, $d = 2$ or 3 denote a finite element space for the fluid velocity. (\cdot, \cdot) is the L^2 inner product with norm $\|\cdot\|$ and Δ denotes a mesh element (so that $\int_\Omega \phi \, dx = \sum_\Delta \int_\Delta \phi \, dx$). The area/volume of a region D is denoted $|D|$. The $L^2(\Delta)$ norm on a mesh element $(\int_\Delta \phi^2 \, dx)^{1/2}$ is denoted as $\|\phi\|_\Delta$.

The penalty approximation we consider to (46) is: find $u^h \in X^h$ such that

$$\nu(\nabla u_\epsilon^h, \nabla v^h) + \sum_\Delta \int_\Delta \epsilon_\Delta^{-1} \nabla \cdot u_\epsilon^h \nabla \cdot v^h \, dx = (f, v^h), \quad \forall v^h \in V^h. \quad (48)$$

The idea is the same as behind most adaptive algorithms: Monitor the residual to control the error; localize a global residual tolerance; where the local residual $\|\nabla \cdot u^h\|_\Delta^2$ is large pick ϵ_Δ small.

To develop this, we begin with the basic stability estimate. Setting $v^h = u^h$ in (48) we find

$$\begin{aligned} \nu \|\nabla u_\epsilon^h\|^2 + \sum_\Delta \int_\Delta \epsilon_\Delta^{-1} |\nabla \cdot u_\epsilon^h|^2 \, dx &= (f, u_\epsilon^h) = (f, u) + o(1), \\ \text{thus } \sum_\Delta \int_\Delta \epsilon_\Delta^{-1} |\nabla \cdot u_\epsilon^h|^2 \, dx &= \mathcal{O}(1). \end{aligned}$$

This suggests that globally halving (doubling) ϵ halves (doubles) $\|\nabla \cdot u_\epsilon^h\|^2$.

Next, we localize the global tolerance TOL for $\|\nabla \cdot u_\epsilon^h\|$ as follows:

We seek $\|\nabla \cdot u_\epsilon^h\|^2 \approx \frac{1}{2} \text{TOL}^2$ or

$$\|\nabla \cdot u_\epsilon^h\|^2 = \sum_\Delta \int_\Delta |\nabla \cdot u_\epsilon^h|^2 \, dx \approx \frac{1}{2} \text{TOL}^2 = \frac{1}{2} \sum_\Delta \frac{\text{TOL}^2}{|\Omega|} |\Delta|.$$

Thus we define the local tolerance

$$\text{LocTol}_\Delta := \frac{1}{2} \frac{\text{TOL}^2}{|\Omega|} |\Delta|,$$

and seek to enforce

$$\|\nabla \cdot u_\epsilon^h\|_\Delta^2 \approx \text{LocTol}_\Delta.$$

If this local tolerance is satisfied, the global tolerance is satisfied:

$$\|\nabla \cdot u_\epsilon^h\|^2 = \sum_{\Delta} \int_{\Delta} |\nabla \cdot u_\epsilon^h|^2 dx \approx \sum_{\Delta} LocTol_{\Delta} = \frac{1}{2}TOL^2.$$

The usual procedure would be to select (on each triangle Δ) ϵ_{old} , solve for u_ϵ^h , compute the ratio

$$r = \frac{LocTol_{\Delta}}{\|\nabla \cdot u_\epsilon^h\|_{\Delta}^2},$$

then adjust ϵ by $\epsilon_{new} = r \times \epsilon_{old}$ and resolve. The first step is therefore (starting with $\epsilon_{\Delta} \equiv 1$)

$$\epsilon_{\Delta} = \|\nabla \cdot u_\epsilon^h\|_{\Delta}^{-2} \times LocTol_{\Delta},$$

There are two options. Both result in a nonlinear discretization.

Option 1. Elementwise Penalty (EP)

$$\epsilon_{\Delta} := \frac{LocTol_{\Delta}}{\|\nabla \cdot u_\epsilon^h\|_{\Delta}^2},$$

so that

$$\sum_{\Delta} \int_{\Delta} \epsilon_{\Delta}^{-1} \nabla \cdot u_\epsilon^h \nabla \cdot v^h dx = \sum_{\Delta} LocTol_{\Delta}^{-1} \|\nabla \cdot u_\epsilon^h\|_{\Delta}^2 \int_{\Delta} \nabla \cdot u_\epsilon^h \nabla \cdot v^h dx. \quad (49)$$

Then (48) becomes: find $u_\epsilon^h \in X^h$ such that

$$\int_{\Omega} \nu \nabla u_\epsilon^h : \nabla v^h dx + \sum_{\Delta} \frac{1}{LocTol_{\Delta}} \|\nabla \cdot u_\epsilon^h\|_{\Delta}^2 \int_{\Delta} \nabla \cdot u_\epsilon^h \nabla \cdot v^h dx = \int_{\Omega} f \cdot v^h dx. \quad (50)$$

Option 2. Pointwise Penalty (PP)

$$\epsilon_{\Delta}(x) := \frac{LocTol_{\Delta}}{|\nabla \cdot u_\epsilon^h(x)|^2},$$

so that

$$\sum_{\Delta} \int_{\Delta} \epsilon_{\Delta}^{-1} \nabla \cdot u_\epsilon^h \nabla \cdot v^h dx = \sum_{\Delta} LocTol_{\Delta}^{-1} \int_{\Delta} |\nabla \cdot u_\epsilon^h|^2 \nabla \cdot u_\epsilon^h \nabla \cdot v^h dx. \quad (51)$$

Then (48) becomes: find $u_\epsilon^h \in X^h$ such that

$$\int_{\Omega} \nu \nabla u_\epsilon^h : \nabla v^h dx + \sum_{\Delta} \frac{1}{LocTol_{\Delta}} \int_{\Delta} |\nabla \cdot u_\epsilon^h|^2 \nabla \cdot u_\epsilon^h \nabla \cdot v^h dx = \int_{\Omega} f \cdot v^h dx. \quad (52)$$

We focus herein on the analysis of option 2 (PP) and the numerical result of option 1 (EP). In option 2 (PP), the resulting nonlinearity is both strongly monotone and locally Lipschitz continuous, sharing structures with the p-Laplacian. Then, there is a well-trodden analytical path to be adapted here. Before proceeding, we address two points:

1. Imposing the global condition locally suggests but does not imply the local condition is satisfied. This will be tested in our experiments Section 3.4.1. We adapt based on the local condition but aim for global TOL to be satisfied.
2. No analysis herein addresses how to pick TOL. TOL is user supplied.

Section 3.2 analyzes the stability and error for the Stokes problem of the new pointwise penalty (PP) method. In Section 3.3, algorithmic aspects are discussed for the Stokes problem and the Navier-Stokes problem using the elementwise penalty (EP) method. In Section 3.4, we present three numerical tests using the elementwise penalty (EP). The first two are for the Stokes problem, and the third one is an extension to the Navier-Stokes equations.

3.2 Analysis

In this section, we derived stability bounds for both new penalty methods (PP (52) and EP (50)) and error estimates for the pointwise penalty (PP) method (52).

3.2.1 Stability

First, we consider the elementwise penalty (EP) method (50). Recall that $LocTol_{\Delta} = \frac{1}{2}TOL^2 \frac{|\Delta|}{|\Omega|}$.

Theorem 3.2.1. *Suppose \mathcal{T}^h be a mesh of Ω and Δ denote a mesh element in \mathcal{T}^h , the solution to (50) is stable, and the following stability bound holds*

$$\frac{\nu}{2} \|\nabla u_{\epsilon}^h\|^2 + \sum_{\Delta} \frac{1}{LocTol_{\Delta}} \|\nabla \cdot u_{\epsilon}^h\|_{\Delta}^4 \leq \frac{1}{2\nu} \|f\|_{-1}^2.$$

Proof. Take $v^h = u_{\epsilon}^h$ in (50):

$$\nu \|\nabla u_{\epsilon}^h\|^2 + \sum_{\Delta} \frac{1}{LocTol_{\Delta}} \|\nabla \cdot u_{\epsilon}^h\|_{\Delta}^2 \|\nabla \cdot u_{\epsilon}^h\|_{\Delta}^2 = \int_{\Omega} f \cdot u_{\epsilon}^h \, dx,$$

As $(f, u_{\epsilon}^h) \leq \|f\|_{-1} \|\nabla u_{\epsilon}^h\|$ and apply Hölder's and Young's inequalities (15):

$$\nu \|\nabla u_{\epsilon}^h\|^2 + \sum_{\Delta} \frac{1}{LocTol_{\Delta}} \|\nabla \cdot u_{\epsilon}^h\|_{\Delta}^4 \leq \frac{1}{2\nu} \|f\|_{-1}^2 + \frac{\nu}{2} \|\nabla u_{\epsilon}^h\|^2.$$

Combine similar terms and the claimed stability bound then follows. □

From Theorem 3.2.1, we have the following proposition.

Proposition 3.2.2. *Let N denote the number of elements Δ in mesh \mathcal{T}^h and TOL denote the global tolerance, then the solution u_ϵ^h to (50) satisfy*

$$\|\nabla \cdot u_\epsilon^h\|^4 \leq \left(\frac{N \cdot \max |\Delta|}{4\nu|\Omega|} \right) TOL^2 \|f\|_{-1}^2.$$

Proof. From Theorem 3.2.1, we have

$$\sum_{\Delta} \frac{1}{LocTol_{\Delta}} \|\nabla \cdot u_\epsilon^h\|_{\Delta}^4 \leq \frac{1}{2\nu} \|f\|_{-1}^2.$$

Recall $LocTol_{\Delta} = \frac{1}{2} TOL^2 \frac{|\Delta|}{|\Omega|}$,

$$\begin{aligned} \sum_{\Delta} \frac{2}{TOL^2} \frac{|\Omega|}{|\Delta|} \|\nabla \cdot u_\epsilon^h\|_{\Delta}^4 &\leq \frac{1}{2\nu} \|f\|_{-1}^2, \\ \sum_{\Delta} \frac{1}{|\Delta|} \|\nabla \cdot u_\epsilon^h\|_{\Delta}^4 &\leq \frac{TOL^2}{4\nu|\Omega|} \|f\|_{-1}^2, \\ \frac{1}{\max |\Delta|} \sum_{\Delta} \left(\int_{\Delta} |\nabla \cdot u_\epsilon^h|^2 dx \right)^2 &\leq \frac{TOL^2}{4\nu|\Omega|} \|f\|_{-1}^2, \\ \sum_{\Delta} \left(\int_{\Delta} |\nabla \cdot u_\epsilon^h|^2 dx \right)^2 &\leq \frac{\max |\Delta|}{|\Omega|} \frac{TOL^2}{4\nu} \|f\|_{-1}^2. \end{aligned}$$

Using the Cauchy Schwartz inequality:

$$\frac{1}{N} \left(\sum_{\Delta} \int_{\Delta} |\nabla \cdot u_\epsilon^h|^2 dx \right)^2 \leq \sum_{\Delta} \left(\int_{\Delta} |\nabla \cdot u_\epsilon^h|^2 dx \right)^2 \leq \frac{\max |\Delta|}{|\Omega|} \frac{TOL^2}{4\nu} \|f\|_{-1}^2.$$

Then the result follows. □

Next, we consider the pointwise penalty (PP) method (52). Recall that $LocTol_{\Delta} = \frac{1}{2} TOL^2 \frac{|\Delta|}{|\Omega|}$.

Theorem 3.2.3. *Suppose \mathcal{T}^h be a mesh of Ω and Δ denote the mesh element in \mathcal{T}^h , the solution to (52) is stable, and the following stability bound holds*

$$\frac{\nu}{2} \|\nabla u_\epsilon^h\|^2 + \sum_{\Delta} \frac{1}{LocTol_{\Delta}} \|\nabla \cdot u_\epsilon^h\|_{L^4(\Delta)}^4 \leq \frac{1}{2\nu} \|f\|_{-1}^2.$$

Proof. Take $v^h = u_\epsilon^h$ in (52):

$$\nu \|\nabla u_\epsilon^h\|^2 + \sum_{\Delta} \frac{1}{LocTol_{\Delta}} \int_{\Delta} |\nabla \cdot u_\epsilon^h|^4 dx = \int_{\Omega} f \cdot u_\epsilon^h dx,$$

As $(f, u_\epsilon^h) \leq \|f\|_{-1} \|\nabla u_\epsilon^h\|$ and apply Hölder's and Young's inequalities (15):

$$\nu \|\nabla u_\epsilon^h\|^2 + \sum_{\Delta} \frac{1}{LocTol_{\Delta}} \|\nabla \cdot u_\epsilon^h\|_{L^4(\Delta)}^4 \leq \frac{1}{2\nu} \|f\|_{-1}^2 + \frac{\nu}{2} \|\nabla u_\epsilon^h\|^2.$$

Combine similar terms and the claimed stability bound then follows. \square

Directly from the result of Theorem 3.2.3, we have the following proposition.

Proposition 3.2.4. *Let TOL denote the global tolerance, then the solution u_ϵ^h to (52) satisfy*

$$\|\nabla \cdot u_\epsilon^h\|_{L^4}^4 \leq \left(\frac{\max |\Delta|}{4\nu|\Omega|} \right) TOL^2 \|f\|_{-1}^2.$$

Proof. From Theorem 3.2.3, there holds

$$\sum_{\Delta} \frac{1}{LocTol_{\Delta}} \|\nabla \cdot u_\epsilon^h\|_{L^4(\Delta)}^4 \leq \frac{1}{2\nu} \|f\|_{-1}^2.$$

Recall $LocTol_{\Delta} = \frac{1}{2} TOL^2 \frac{|\Delta|}{|\Omega|}$,

$$\begin{aligned} \sum_{\Delta} \frac{2}{TOL^2} \frac{|\Omega|}{|\Delta|} \|\nabla \cdot u_\epsilon^h\|_{L^4(\Delta)}^4 &\leq \frac{1}{2\nu} \|f\|_{-1}^2, \\ \sum_{\Delta} \frac{1}{|\Delta|} \|\nabla \cdot u_\epsilon^h\|_{L^4(\Delta)}^4 &\leq \frac{TOL^2}{4\nu|\Omega|} \|f\|_{-1}^2, \\ \frac{1}{\max |\Delta|} \sum_{\Delta} \left(\int_{\Delta} |\nabla \cdot u_\epsilon^h|^4 dx \right)^1 &\leq \frac{TOL^2}{4\nu|\Omega|} \|f\|_{-1}^2. \end{aligned}$$

Then the result follows. \square

3.2.2 Error analysis

We consider the error between continuous Stokes problem (46) and discretized pointwise penalized (PP) Stokes problem (52). Recall $Q := \{q \in L^2(\Omega) : \int_{\Omega} q \, dx = 0\}$. The variational form of the Stokes problem (46) is:

Find $(u, p) \in (X, Q)$ such that

$$\begin{aligned} \int_{\Omega} \nu \nabla u : \nabla v \, dx - \int_{\Omega} p(\nabla \cdot v) \, dx &= \int_{\Omega} f \cdot v \, dx \quad \text{for all } v \in X, \\ \text{and } \int_{\Omega} (\nabla \cdot u)q \, dx &= 0 \quad \text{for all } q \in Q. \end{aligned} \tag{53}$$

Theorem 3.2.5. *Let (u, p) be a solution to the Stokes problem (53) and u_{ϵ}^h be the solution of the penalty approximation (52). Let d denote the dimension of Ω and C_1, C_2 be two constants defined as in (21) and (22). TOL denote the global tolerance and $LocTol_{\Delta}$ be the local tolerance for each element Δ in mesh \mathcal{T}^h . Then it follows that*

$$\begin{aligned} &\nu \|\nabla(u - u_{\epsilon}^h)\|^2 + C_1 \sum_{\Delta} LocTol_{\Delta}^{-1} \|\nabla \cdot (u - u_{\epsilon}^h)\|_{L^4(\Delta)}^4 \\ &\leq \inf_{v^h \in X^h} C(C_1, C_2) \sum_{\Delta} LocTol_{\Delta}^{-1} \|\nabla \cdot (u - v^h)\|_{L^4(\Delta)}^4 \\ &+ C(\nu) h^{2m-2} \|u\|_{H^{m+1}(\Omega)}^2 + h^2 \|p\|^2 + C\nu^{-1/4} \|f\|_{-1}^{1/2} TOL^{1/2} (\max |\Delta|)^{1/4} \|p\|^2. \end{aligned}$$

Remark 3.2.6. *If X^h has a divergence free subspace with good approximation properties, the first term of the RHS of the estimate in Theorem 3.2.5 vanishes.*

Proof. As $a(u, u, v^h) = \sum_{\Delta} LocTol_{\Delta}^{-1} \int_{\Delta} |\nabla \cdot u|^2 \nabla \cdot u \nabla \cdot v^h \, dx$ and $\nabla \cdot u = 0$, so $a(u, u, v^h) = 0$.

From (53), adding $a(u, u, v)$ to the left-hand-side :

$$\nu(\nabla u, \nabla v) - (p, \nabla \cdot v) + a(u, u, v) = (f, v), \quad \forall v \in X.$$

Subtract (52) and let $v = v^h$:

$$\nu(\nabla(u - u_{\epsilon}^h), \nabla v^h) + a(u, u, v^h) - a(u_{\epsilon}^h, u_{\epsilon}^h, v^h) = (p, \nabla \cdot v^h).$$

Denote $e = u - u_\epsilon^h$, let $\forall \tilde{u} \in X^h, \eta = u - \tilde{u}$ and $\phi^h = u_\epsilon^h - \tilde{u}$, then $e = \eta - \phi^h$, the error equation becomes:

$$\begin{aligned} & \nu(\nabla\eta, \nabla v^h) + a(u, u, v^h) - a(\tilde{u}, \tilde{u}, v^h) \\ &= \nu(\nabla\phi^h, \nabla v^h) + a(u_\epsilon^h, u_\epsilon^h, v^h) - a(\tilde{u}, \tilde{u}, v^h) + (p, \nabla \cdot v^h), \end{aligned}$$

Letting $v^h = \phi^h$, the error equation becomes:

$$\nu(\nabla\phi^h, \nabla\phi^h) + a(u_\epsilon^h, u_\epsilon^h, \phi^h) - a(\tilde{u}, \tilde{u}, \phi^h) = \nu(\nabla\eta, \nabla\phi^h) + a(u, u, \phi^h) - a(\tilde{u}, \tilde{u}, \phi^h) - (p, \nabla \cdot \phi^h).$$

Apply Strong Monotonicity (21) to $a(u_\epsilon^h, u_\epsilon^h, \phi^h) - a(\tilde{u}, \tilde{u}, \phi^h)$:

$$\begin{aligned} & a(u_\epsilon^h, u_\epsilon^h, \phi^h) - a(\tilde{u}, \tilde{u}, \phi^h) \\ &= \sum_{\Delta} \frac{1}{LocTol_{\Delta}} \int_{\Delta} (|\nabla \cdot u_\epsilon^h|^2 \nabla \cdot u_\epsilon^h - |\nabla \cdot \tilde{u}|^2 \nabla \cdot \tilde{u}) \nabla \cdot (u_\epsilon^h - \tilde{u}) \, dx \\ &\geq \sum_{\Delta} \frac{1}{LocTol_{\Delta}} C_1 \int_{\Delta} |\nabla \cdot (u_\epsilon^h - \tilde{u})|^4 \, dx. \end{aligned}$$

Apply Local Lipschitz continuity (22) to $a(u, u, \phi^h) - a(\tilde{u}, \tilde{u}, \phi^h)$:

$$\begin{aligned} & a(u, u, \phi^h) - a(\tilde{u}, \tilde{u}, \phi^h) \\ &= \sum_{\Delta} \frac{1}{LocTol_{\Delta}} \int_{\Delta} (|\nabla \cdot u|^2 \nabla \cdot u - |\nabla \cdot \tilde{u}|^2 \nabla \cdot \tilde{u}) \nabla \cdot \phi^h \, dx \\ &\leq \sum_{\Delta} \frac{1}{LocTol_{\Delta}} C_2 r_{\Delta}^2 \left(\int_{\Delta} |\nabla \cdot (u - \tilde{u})|^4 \, dx \right)^{1/4} \left(\int_{\Delta} |\nabla \cdot \phi^h|^4 \right)^{1/4} \end{aligned}$$

$$\text{where } r_{\Delta} = \max\{\|\nabla \cdot u\|_{L^4(\Delta)}, \|\nabla \cdot \tilde{u}\|_{L^4(\Delta)}\} = \|\nabla \cdot \tilde{u}\|_{L^4(\Delta)}.$$

Then the error equation becomes

$$\begin{aligned} & \nu \|\nabla\phi^h\|^2 + \sum_{\Delta} \frac{C_1}{LocTol_{\Delta}} \|\nabla \cdot \phi^h\|_{L^4(\Delta)}^4 \leq \nu(\nabla\eta, \nabla\phi^h) \\ &+ \sum_{\Delta} \frac{C_2 r_{\Delta}^2}{LocTol_{\Delta}} \|\nabla \cdot \eta\|_{L^4(\Delta)} \|\nabla \cdot \phi^h\|_{L^4(\Delta)} - (p, \nabla \cdot \phi^h). \end{aligned}$$

Apply Hölder's and Young's inequality (15) with $p = 4, q = 4/3$:

$$\begin{aligned}
& \nu \|\nabla \phi^h\|^2 + \sum_{\Delta} \frac{C_1}{LocTol_{\Delta}} \|\nabla \cdot \phi^h\|_{L^4(\Delta)}^4 \\
& \leq \frac{\nu}{2} \|\nabla \eta\|^2 + \frac{\nu}{2} \|\nabla \phi^h\|^2 - (p, \nabla \cdot \phi^h) \\
& + \sum_{\Delta} \left(\frac{C_1^{1/4}}{LocTol_{\Delta}^{1/4}} \|\nabla \cdot \phi^h\|_{L^4(\Delta)} \right) \left(\frac{C_2 r_{\Delta}^2}{C_1^{1/4} LocTol_{\Delta}^{3/4}} \|\nabla \cdot \eta\|_{L^4(\Delta)} \right) \\
& \leq \frac{\nu}{2} \|\nabla \eta\|^2 + \frac{\nu}{2} \|\nabla \phi^h\|^2 - (p, \nabla \cdot \phi^h) \\
& + \left(\sum_{\Delta} \frac{C_1}{LocTol_{\Delta}} \|\nabla \cdot \phi^h\|_{L^4(\Delta)}^4 \right)^{1/4} \left(\sum_{\Delta} \frac{C_2^{4/3} r_{\Delta}^{8/3}}{C_1^{1/3} LocTol_{\Delta}} \|\nabla \cdot \eta\|_{L^4(\Delta)}^{4/3} \right)^{3/4} \\
& \leq \frac{\nu}{2} \|\nabla \eta\|^2 + \frac{\nu}{2} \|\nabla \phi^h\|^2 - (p, \nabla \cdot \phi^h) \\
& + \frac{\delta}{4} \left(\sum_{\Delta} \frac{C_1}{LocTol_{\Delta}} \|\nabla \cdot \phi^h\|_{L^4(\Delta)}^4 \right)^1 + \frac{\delta^{-1/3}}{4/3} \left(\sum_{\Delta} \frac{C_2^{4/3} r_{\Delta}^{8/3}}{C_1^{1/3} LocTol_{\Delta}} \|\nabla \cdot \eta\|_{L^4(\Delta)}^{4/3} \right)^1.
\end{aligned}$$

Letting $\delta = 2$ and combining similar terms gives

$$\begin{aligned}
& \frac{\nu}{2} \|\nabla \phi^h\|^2 + \frac{1}{2} \sum_{\Delta} \frac{C_1}{LocTol_{\Delta}} \|\nabla \cdot \phi^h\|_{L^4(\Delta)}^4 \\
& \leq \frac{\nu}{2} \|\nabla \eta\|^2 + \frac{3}{4\sqrt[3]{2}} \sum_{\Delta} \frac{C_2^{4/3} r_{\Delta}^{8/3}}{C_1^{1/3} LocTol_{\Delta}} \|\nabla \cdot \eta\|_{L^4(\Delta)}^{4/3} - (p, \nabla \cdot \phi^h).
\end{aligned}$$

Consider the last term of the error equation inspired by the proof of Falk [20]:

$$\begin{aligned}
(p, \nabla \cdot \phi^h) & = (p, \nabla \cdot (u_{\epsilon}^h - \tilde{u})) \\
& = (p, \nabla \cdot u_{\epsilon}^h) + (p, \nabla \cdot (u - \tilde{u})) \\
& \leq \sum_{\Delta} \int_{\Delta} p \nabla \cdot u_{\epsilon}^h \, dx + \frac{h^2}{2} \|p\|^2 + \frac{1}{2h^2} \|\nabla \cdot \eta\|^2 \\
& \leq \sum_{\Delta} \int_{\Delta} \frac{1}{LocTol_{\Delta}^{1/4}} |\nabla \cdot u_{\epsilon}^h| LocTol_{\Delta}^{1/4} |p| \, dx + \frac{h^2}{2} \|p\|^2 + \frac{1}{2h^2} \|\nabla \cdot \eta\|^2 \\
& \leq \sum_{\Delta} \left(\int_{\Delta} \frac{1}{LocTol_{\Delta}} |\nabla \cdot u_{\epsilon}^h|^4 \, dx \right)^{1/4} \left(\int_{\Delta} LocTol_{\Delta}^{1/3} |p|^{4/3} \, dx \right)^{3/4} \\
& + \frac{h^2}{2} \|p\|^2 + \frac{1}{2h^2} \|\nabla \cdot \eta\|^2
\end{aligned}$$

$$\begin{aligned}
&\leq \left(\sum_{\Delta} \int_{\Delta} \frac{1}{LocTol_{\Delta}} |\nabla \cdot u_{\epsilon}^h|^4 dx \right)^{1/4} \left(\sum_{\Delta} \int_{\Delta} LocTol_{\Delta}^{1/3} |p|^{4/3} dx \right)^{3/4} \\
&+ \frac{h^2}{2} \|p\|^2 + \frac{1}{2h^2} \|\nabla \cdot \eta\|^2 \\
&\leq \left(\sum_{\Delta} \frac{1}{LocTol_{\Delta}} \|\nabla \cdot u_{\epsilon}^h\|_{L^4(\Delta)}^4 \right)^{1/4} \left(\sum_{\Delta} \left(\int_{\Delta} LocTol_{\Delta} \right)^{1/3} \left(\int_{\Delta} |p|^2 \right)^{2/3} \right)^{3/4} \\
&+ \frac{h^2}{2} \|p\|^2 + \frac{1}{2h^2} \|\nabla \cdot \eta\|^2 \\
&\leq \left(\sum_{\Delta} \frac{1}{LocTol_{\Delta}} \|\nabla \cdot u_{\epsilon}^h\|_{L^4(\Delta)}^4 \right)^{1/4} \left(\left(\sum_{\Delta} \int_{\Delta} LocTol_{\Delta} \right)^{1/3} \left(\sum_{\Delta} \int_{\Delta} |p|^2 \right)^{2/3} \right)^{3/4} \\
&+ \frac{h^2}{2} \|p\|^2 + \frac{1}{2h^2} \|\nabla \cdot \eta\|^2 \\
&= \left(\sum_{\Delta} \frac{1}{LocTol_{\Delta}} \|\nabla \cdot u_{\epsilon}^h\|_{L^4(\Delta)}^4 \right)^{1/4} \left(\sum_{\Delta} |\Delta| LocTol_{\Delta} \right)^{1/4} \|p\| + \frac{h^2}{2} \|p\|^2 + \frac{1}{2h^2} \|\nabla \cdot \eta\|^2.
\end{aligned}$$

By the stability bound,

$$\frac{\nu}{2} \|\nabla u_{\epsilon}^h\|^2 + \sum_{\Delta} \frac{1}{LocTol_{\Delta}} \|\nabla \cdot u_{\epsilon}^h\|_{L^4(\Delta)}^4 \leq \frac{1}{2\nu} \|f\|_{-1}^2.$$

Thus,

$$(p, \nabla \cdot \phi^h) \leq C\nu^{-1/4} \|f\|_{-1}^{1/2} \left(\sum_{\Delta} |\Delta| LocTol_{\Delta} \right)^{1/4} \|p\| + \frac{h^2}{2} \|p\|^2 + \frac{1}{2h^2} \|\nabla \cdot \eta\|^2.$$

Plug back to the error equation:

$$\begin{aligned}
\frac{\nu}{2} \|\nabla \phi^h\|^2 + \sum_{\Delta} \frac{C_1}{2LocTol_{\Delta}} \|\nabla \cdot \phi^h\|_{L^4(\Delta)}^4 &\leq \frac{\nu}{2} \|\nabla \eta\|^2 + \sum_{\Delta} \frac{3C_2^{4/3} r_{\Delta}^{8/3}}{4\sqrt[3]{2} C_1^{1/3} LocTol_{\Delta}} \|\nabla \cdot \eta\|_{L^4(\Delta)}^{4/3} \\
&+ C\nu^{-1/4} \|f\|_{-1}^{1/2} \left(\sum_{\Delta} |\Delta| LocTol_{\Delta} \right)^{1/4} \|p\| + \frac{h^2}{2} \|p\|^2 + \frac{1}{2h^2} \|\nabla \cdot \eta\|^2,
\end{aligned}$$

where

$$\begin{aligned}
\left(\sum_{\Delta} |\Delta| LocTol_{\Delta} \right)^{1/4} &:= \left(\sum_{\Delta} |\Delta| \frac{1}{2} \frac{TOL^2}{|\Omega|} |\Delta| \right)^{1/4} = \left(\frac{TOL^2}{2|\Omega|} \sum_{\Delta} |\Delta|^2 \right)^{1/4} \\
&\leq \frac{TOL^{1/2}}{2^{1/4}} \left(\frac{1}{|\Omega|} \max |\Delta| \sum_{\Delta} |\Delta| \right)^{1/4} = TOL^{1/2} \left(\frac{\max |\Delta|}{2} \right)^{1/4}.
\end{aligned}$$

Apply triangle inequality: $\|e\| \leq \|\eta\| + \|\phi^h\|$

$$\begin{aligned} \nu \|\nabla e\|^2 + \sum_{\Delta} \frac{C_1}{LocTol_{\Delta}} \|\nabla \cdot e\|_{L^4(\Delta)}^4 &\leq \inf_{v^h \in X^h} \left\{ \nu \|\nabla(u - v^h)\|^2 + h^{-2} \|\nabla \cdot (u - v^h)\|^2 \right. \\ &\quad \left. + C(C_1, C_2) \sum_{\Delta} LocTol_{\Delta}^{-1} \left(r_{\Delta}^{8/3} \|\nabla \cdot (u - v^h)\|_{L^4(\Delta)}^{4/3} + \|\nabla \cdot (u - v^h)\|_{L^4(\Delta)}^4 \right) \right\} \\ &\quad + h^2 \|p\|^2 + C\nu^{-1/4} \|f\|_{-1}^{1/2} Tol^{1/2} (\max |\Delta|)^{1/4} \|p\|^2, \end{aligned}$$

where

$$\begin{aligned} \sum_{\Delta} LocTol_{\Delta}^{-1} r_{\Delta}^{8/3} \|\nabla \cdot (u - v^h)\|_{L^4(\Delta)}^{4/3} &= \sum_{\Delta} LocTol_{\Delta}^{-1} \|\nabla \cdot v^h\|_{L^4(\Delta)}^{8/3} \|\nabla \cdot (u - v^h)\|_{L^4(\Delta)}^{4/3} \\ &= \sum_{\Delta} LocTol_{\Delta}^{-1} \|\nabla \cdot (u - v^h)\|_{L^4(\Delta)}^4. \end{aligned}$$

The error satisfies

$$\begin{aligned} \nu \|\nabla e\|^2 + \sum_{\Delta} \frac{C_1}{LocTol_{\Delta}} \|\nabla \cdot e\|_{L^4(\Delta)}^4 &\leq \inf_{v^h \in X^h} \left\{ \nu \|\nabla(u - v^h)\|^2 + h^{-2} \|\nabla \cdot (u - v^h)\|^2 \right. \\ &\quad \left. + C(C_1, C_2) \sum_{\Delta} LocTol_{\Delta}^{-1} \|\nabla \cdot (u - v^h)\|_{L^4(\Delta)}^4 \right\} + h^2 \|p\|^2 + C\nu^{-1/4} \|f\|_{-1}^{1/2} Tol^{1/2} (\max |\Delta|)^{1/4} \|p\|^2. \end{aligned}$$

As $\|\nabla \cdot (u - v^h)\| \leq \|\nabla(u - v^h)\|$,

$$\begin{aligned} \nu \|\nabla e\|^2 + \sum_{\Delta} \frac{C_1}{LocTol_{\Delta}} \|\nabla \cdot e\|_{L^4(\Delta)}^4 &\leq \inf_{v^h \in X^h} \left\{ C(\nu)(1 + h^{-2}) \|\nabla(u - v^h)\|^2 \right. \\ &\quad \left. + C(C_1, C_2) \sum_{\Delta} LocTol_{\Delta}^{-1} \|\nabla \cdot (u - v^h)\|_{L^4(\Delta)}^4 \right\} + h^2 \|p\|^2 + C\nu^{-1/4} \|f\|_{-1}^{1/2} Tol^{1/2} (\max |\Delta|)^{1/4} \|p\|^2. \end{aligned}$$

Using the approximation properties (10) of the spaces X^h

$$\begin{aligned} \nu \|\nabla e\|^2 + \sum_{\Delta} \frac{C_1}{LocTol_{\Delta}} \|\nabla \cdot e\|_{L^4(\Delta)}^4 &\leq \inf_{v^h \in X^h} C(C_1, C_2) \sum_{\Delta} LocTol_{\Delta}^{-1} \|\nabla \cdot (u - v^h)\|_{L^4(\Delta)}^4 \\ &\quad + C(\nu) h^{2m-2} \|u\|_{H^{m+1}(\Omega)}^2 + h^2 \|p\|^2 + C\nu^{-1/4} \|f\|_{-1}^{1/2} Tol^{1/2} (\max |\Delta|)^{1/4} \|p\|^2. \end{aligned}$$

□

3.3 Algorithm

This section presents the algorithms to implement the elementwise variable ϵ elementwise penalty (EP) method (50) introduced in Section 3.1.2. The following Algorithm 5 is for Stokes problem.

Algorithm 5: Elementwise variable ϵ penalty (EP) method for Stokes

Given tolerance TOL, epsilon lower bound LowerEps and mesh \mathcal{T} , MaxIter=10

Compute on each element triangle $LocTol_{\Delta} = \frac{1}{2} \frac{TOL^2}{|\Omega|} |\Delta|$

Set $\epsilon_{\Delta} = 1$

Solve for u^h using penalty method: find $u^h \in X^h$ such that

$$\nu(\nabla u_{\epsilon}^h, \nabla v^h) + \sum_{\Delta} \int_{\Delta} \epsilon_{\Delta}^{-1} \nabla \cdot u_{\epsilon}^h \nabla \cdot v^h dx = (f, v^h) \quad \forall v^h \in X^h$$

while *iteration* \leq *MaxIter* and *retry=true* **do**

 Loop over all triangle elements $\Delta \in \mathcal{T}$

 Compute estimator for each triangle

$$est_{\Delta} = \int_{\Delta} |\nabla \cdot u_{\epsilon}^h|^2 dx$$

if $est_{\Delta} > LocTol_{\Delta}$ **then**

$$r = \frac{LocTol_{\Delta}}{est_{\Delta}};$$

$$\epsilon_{\Delta} \leftarrow \max(LowerEps, r \times \epsilon_{\Delta});$$

retry=true;

end

 REPEAT step;

end

Recover pressure p if needed

$$p_{\Delta} = -\frac{1}{\epsilon_{\Delta}} \nabla \cdot u_{\epsilon}^h$$

Remark 3.3.1. We need to set a maximum number of iterations *MaxIter* in the loop to avoid the program running infinitely. However, this may lead to the situation that $est_{\Delta} \geq$

LocTol $_{\Delta}$ local tolerance is not satisfied. However, our ultimate goal is $\|\nabla \cdot u^h\| < TOL$ no matter whether local tolerance is satisfied or not.

We also want to test the elementwise variable ϵ penalty method on the unsteady Navier-Stokes equation. For time-dependent problem (44), there are two options:

1. use $\|\nabla \cdot u_{\epsilon}^h\|_{\Delta}$ from the previous time step, adjust ϵ and do not repeat the current time-step,
2. for each time-step, repeat using ϵ_{new} and loop until tolerance or maximum iteration is reached.

Since this is a new algorithm, we do not know which is better. We still need to do further research, and Algorithm 6 follows.

Algorithm 6: Elementwise variable ϵ penalty (EP) method for Navier-Stokes

Given tolerance TOL, epsilon lower bound LowerEps and mesh \mathcal{T}^h , final time T_{final} ,

time-step Δt , initial condition $u_0(x)$

Compute on each element triangle $\text{LocTol}_\Delta = \frac{1}{2} \frac{\text{TOL}^2}{|\Omega|} |\Delta|$

Set $\epsilon_{\Delta,1} = 1, t_0 = 0$;

while $t < T_{final}$ **do**

 Update $t_{n+1} = t_n + \Delta t$;

 Given $u_{\epsilon,n}^h$, solve for $u_{\epsilon,n+1}^h$ using penalty method: find $u_{\epsilon,n+1}^h \in X^h$ such that

$$\begin{aligned} & \left(\frac{u_{\epsilon,n+1}^h - u_{\epsilon,n}^h}{\Delta t}, v^h \right) + (u_{\epsilon,n}^h \cdot \nabla u_{\epsilon,n+1}^h, v^h) + \frac{1}{2} \left((\nabla \cdot u_{\epsilon,n}^h) u_{\epsilon,n+1}^h, v^h \right) + \nu (\nabla u_{\epsilon,n+1}^h, \nabla v^h) \\ & + \sum_{\Delta} \int_{\Delta} \epsilon_{\Delta,n+1}^{-1} \nabla \cdot u_{\epsilon,n+1}^h \nabla \cdot v^h \, dx = (f^{n+1}, v^h) \quad \forall v^h \in X^h \end{aligned}$$

 Loop over all triangle elements $\Delta \in \mathcal{T}^h$

 Compute estimator for each triangle

$$est_{\Delta} = \int_{\Delta} |\nabla \cdot u_{\epsilon,n+1}^h|^2 \, dx$$

 Update ϵ_{Δ} :

$$r = \frac{\text{LocTol}_{\Delta}}{est_{\Delta}},$$

$$\epsilon_{\Delta,n+2} \leftarrow \max(\text{LowerEps}, r \times \epsilon_{\Delta,n+1}),$$

 retry = false;

 Recover pressure p if needed

$$p_{\Delta,n+1} = -\frac{1}{\epsilon_{\Delta,n+1}} \nabla \cdot u_{\epsilon,n+1}^h.$$

end

3.4 Numerical Tests

In the following numerical tests Section 3.4.1 and Section 3.4.2, the problems are tested using both elementwise penalty algorithm (Algorithm 5) and also this following coupled system: find $u^h \in X^h, p^h \in Q^h$ such that

$$\begin{aligned} \nu(\nabla u^h, \nabla v^h) - (p^h, \nabla \cdot v^h) &= (f, v^h) \quad \forall v^h \in X^h, \\ (\nabla \cdot u^h, q^h) &= 0 \quad \forall q^h \in Q^h. \end{aligned} \tag{54}$$

3.4.1 Test 1: An exact solution problem, taken from Burman and Hansbo [12]

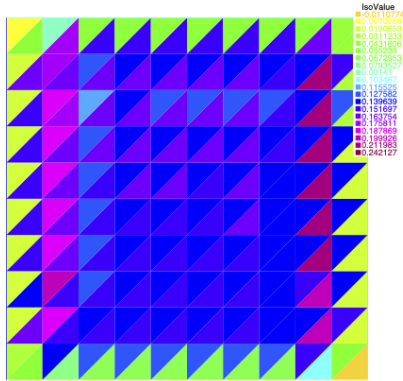
This model problem is constructed to test the convergence rate. The analytic solution is given below

$$u(x, y) = 20xy^3, \quad v(x, y) = 5x^4 - 5y^4, \quad p(x, y) = 60x^2y - 20y^3 - 5. \tag{55}$$

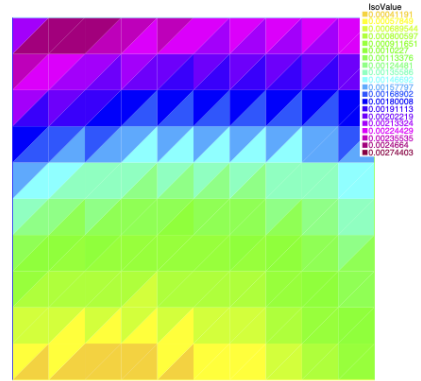
on $\Omega = (0, 1) \times (0, 1)$. Inserting (55) into Stokes equations (46) with $Re = 100$ recovers the body force f .

In this test, take ϵ lower bound $LowerEps = 10^{-8}$, global tolerance $TOL = 10^{-5}$ and $LocTol_{\Delta} = \frac{1}{2} \frac{TOL^2}{|\Omega|} |\Delta| \approx 1.5625 \times 10^{-11}$ for the case of 40 mesh points on each side. From Table 7 with 40 mesh points per side: $\|\nabla \cdot u^h\|^2 = 5.49293 \times 10^{-6} < TOL$, the global tolerance condition satisfied using elementwise penalty. However from Figure 17(b): $\max \|\nabla \cdot u^h\|_{\Delta}^2 \approx 1.15 \times 10^{-5} |\Delta| \approx 3.59 \times 10^{-9} > LocTol$, the local condition does not satisfy but is very close to the local tolerance.

Table 4, Table 5 and Table 6 present the numerical errors of Test 1 of comparison between coupled system (54) and elementwise penalty method (Algorithm 5). The convergence rate of the elementwise penalty is also presented in the fourth column.

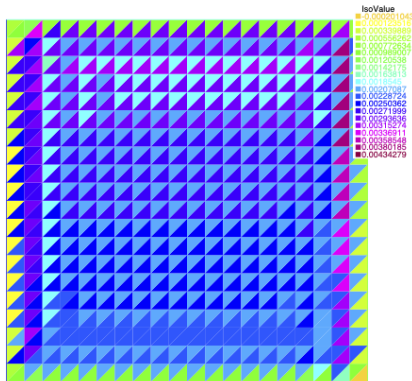


(a) Coupled Stokes problem, the scale is about 10^{-1}

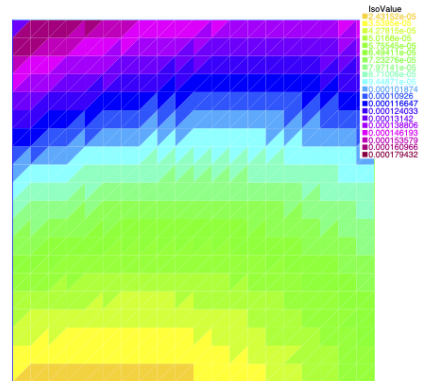


(b) Elementwise penalty method (Algorithm1) for Stokes problem, the scale is about 10^{-3}

Figure 15: $|\nabla \cdot u^h|_{\Delta}^2 / |\Delta|$ with 10 mesh points on each side

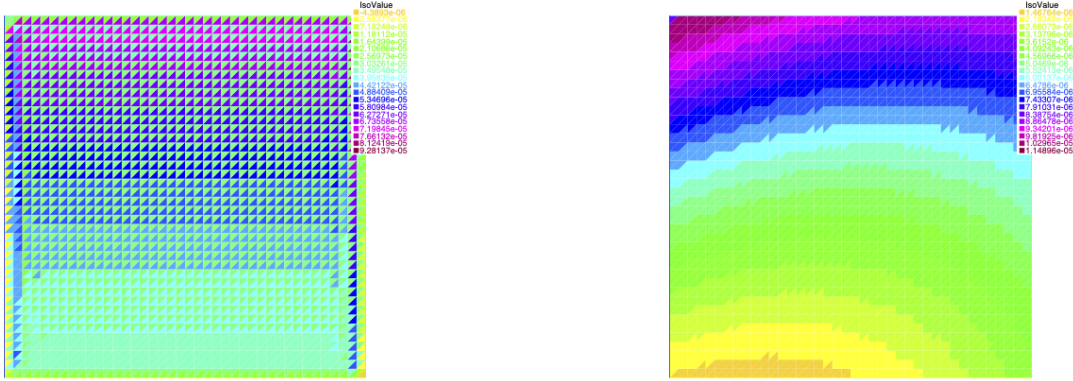


(a) Coupled Stokes problem, the scale is about 10^{-3}



(b) Elementwise penalty method (Algorithm1) for Stokes problem, the scale is about 10^{-4}

Figure 16: $|\nabla \cdot u^h|_{\Delta}^2 / |\Delta|$ with 20 mesh points on each side



(a) Coupled Stokes problem, the scale is about 10^{-5}

(b) Elementwise penalty method (Algorithm1) for Stokes problem, the scale is about 10^{-6}

Figure 17: $|\nabla \cdot u^h|_{\Delta}^2/|\Delta|$ with 40 mesh points on each side

# mesh points on each side	coupled $\ u - u^h\ _{L^2}$	penalty $\ u - u^h\ _{L^2}$	rate
10	0.00520688	0.00528456	-
20	0.000327941	0.00132306	1.99790
40	2.05561e-05	0.000340571	1.95785

Table 4: numerical error $\|u - u^h\|_{L^2}$ and convergence rate of elementwise penalty (compared with coupled system (54))

3.4.2 Test 2: Flow between offset cylinders, taken from Layton and McLaughlin [48]

This test is to test Algorithm 5 on a more complex flow problem and also a comparison between the coupled system and elementwise penalty scheme.

The domain is a disk with a smaller off-center disk inside. Let $r_1 = 1, r_2 = 0.1, c_1 = 0.5$

# mesh points on each side	coupled $\ \nabla(u - u^h)\ _{L^2}$	penalty $\ \nabla(u - u^h)\ _{L^2}$	rate
10	0.384253	0.433158	-
20	0.0494622	0.21608	1.00333
40	0.0062691	0.107975	1.00087

Table 5: numerical error $\|\nabla(u - u^h)\|_{L^2}$ and convergence rate of elementwise penalty (compared with coupled system (54))

# mesh points on each side	coupled $\ \nabla \cdot (u - u^h)\ _{L^4}^2$	penalty $\ \nabla \cdot (u - u^h)\ _{L^4}^2$	rate
10	0.186365	0.00049467	-
20	0.00302458	3.12998e-05	3.98224
40	4.81016e-05	1.96239e-06	3.99547

Table 6: numerical error $\|\nabla \cdot (u - u^h)\|_{L^4}^2$ and convergence rate of elementwise penalty (compared with coupled system (54))

# mesh points on each side	coupled $\ \nabla \cdot u^h\ ^2$	penalty $\ \nabla \cdot u^h\ ^2$
10	0.135344	0.00140525
20	0.002331	8.78752e-05
40	4.23739e-05	5.49293e-06

Table 7: $\|\nabla \cdot u^h\|^2$ numerical result of Test 1

and $c_2 = 0$, the domain is given by

$$\Omega = \{(x, y) : x^2 + y^2 \leq r_1^2 \text{ and } (x - c_1)^2 + (y - c_2)^2 \geq r_2^2\}.$$

We take $\text{Re}=100$ and the body force is given by

$$f(x, y) = (-4y(1 - x^2 - y^2), 4x(1 - x^2 - y^2)).$$

In this test, ϵ lower bound $LowerEps = 10^{-10}$ and global tolerance $TOL = 10^{-6}$. There are 60 mesh points on the outer circle and 30 mesh points on the inner circle. The mesh is denser near the inner circle. And for this mesh the shortest edge of all triangles is $min_e h_e = 0.0220132$ and the longest edge $max_e h_e = 0.141732$. The smallest area of element triangle $min_{\Delta} |\Delta| = 0.000166354$ and the largest area of triangle $max_{\Delta} |\Delta| = 0.00528893$. The local tolerance $LocTol_{\Delta} = \frac{1}{2} \frac{TOL^2}{|\Omega|} |\Delta|$ ranges from 10^{-16} to 10^{-17} .

In this test, from Table 8: $\|\nabla \cdot u^h\|^2 = 1.01872 \times 10^{-19} < TOL^2$ and from Figure 18(b): $\max \|\nabla \cdot u^h\|_{\Delta}^2 \approx 8.59 \times 10^{-17} |\Delta| \approx 10^{-20} < LocTol_{\Delta}$. Here local condition and global condition are both satisfied.

method	$\ \nabla \cdot u^h\ ^2$
coupled	0.255675
elementwise penalty	1.01872e-19

Table 8: numerical result $\|\nabla \cdot u^h\|^2$ of Test 2 Stokes problem

In the test using elementwise penalty (Algorithm 5) at final iteration, $\epsilon_{max} = 2.92232 * 10^{-8}$ and $\epsilon_{min} = 10^{-10}$.

From Figure 18, the incompressibility condition is satisfied for the penalty method. For the coupled system $\max \|\nabla \cdot u^h\|_{\Delta}^2 / |\Delta| \approx 30.08$ which does not satisfy the incompressibility condition.

From the velocity plot Figure 19, the coupled system and elementwise penalty system have similar results. But the elementwise penalty method has far smaller $\|\nabla \cdot u^h\|^2$ values.

3.4.3 Test3. Comparison test between constant penalty and elementwise penalty see Layton and Xu [52]

In this test, we verify the adaptive elementwise penalty method (Algorithm 5) does better than normal constant penalty method by comparison Algorithm 1 with constant $\epsilon = 10^{-8}\nu$ for all elements. Here constant $\epsilon = 10^{-8}\nu$ is usually the approach used by engineering papers.

This comparison test problem is solved by using $P1$, conforming linear elements. Let the

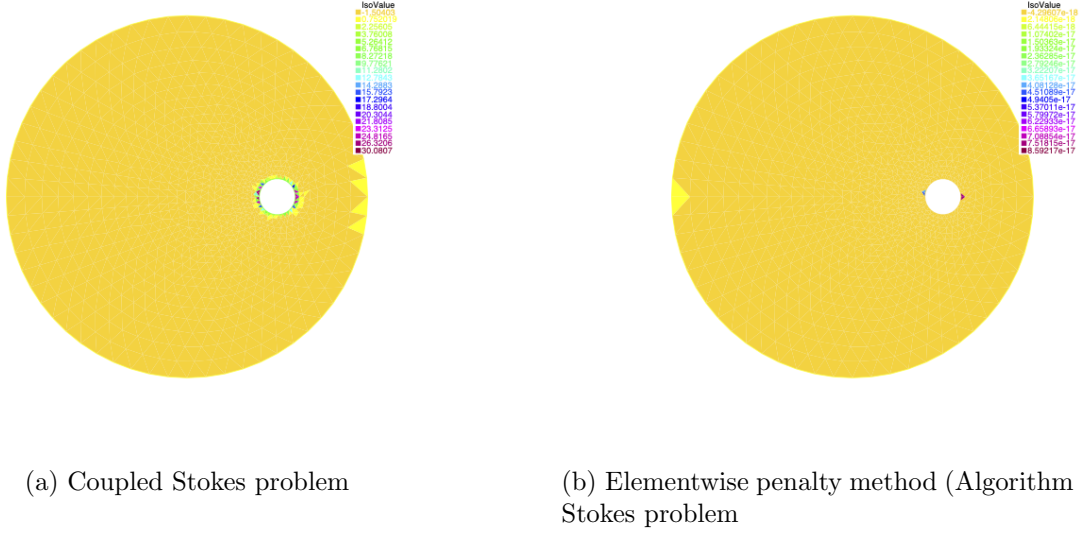


Figure 18: $\|\nabla \cdot u^h\|_{\Delta}^2 / |\Delta|$ of Test 2, comparison between coupled (54) and elementwise penalty system (Algorithm 5) (Note the scale in two plots are different. Coupled Stokes problem $\max_{\Delta} \|\nabla \cdot u^h\|_{\Delta}^2 = \mathcal{O}(10^2)$, elementwise penalty method $\max_{\Delta} \|\nabla \cdot u^h\|_{\Delta}^2 = \mathcal{O}(10^{-17})$)

body force,

$$f(x, y) = (\sin(x + y), \cos(x + y))^T,$$

on $\Omega = (0, 1) \times (0, 1)$. In this test, $Re = 1$, global tolerance $TOL = 10^{-6}$ and there are 40 mesh points on each side. The test results are shown in Table 9.

From Table 9, constant penalty $\epsilon = 10^{-8}$ is a ill conditioned linear system while elementwise penalty with average $\epsilon = 6.3 \times 10^{-4}$ leads to a much better conditioned system. And $\|\nabla \cdot u^h\|_{\Delta}^2$ of adaptive elementwise penalty is smaller than constant penalty, thus adaptive elementwise penalty controls $\|\nabla \cdot u\|$ better than constant penalty method.

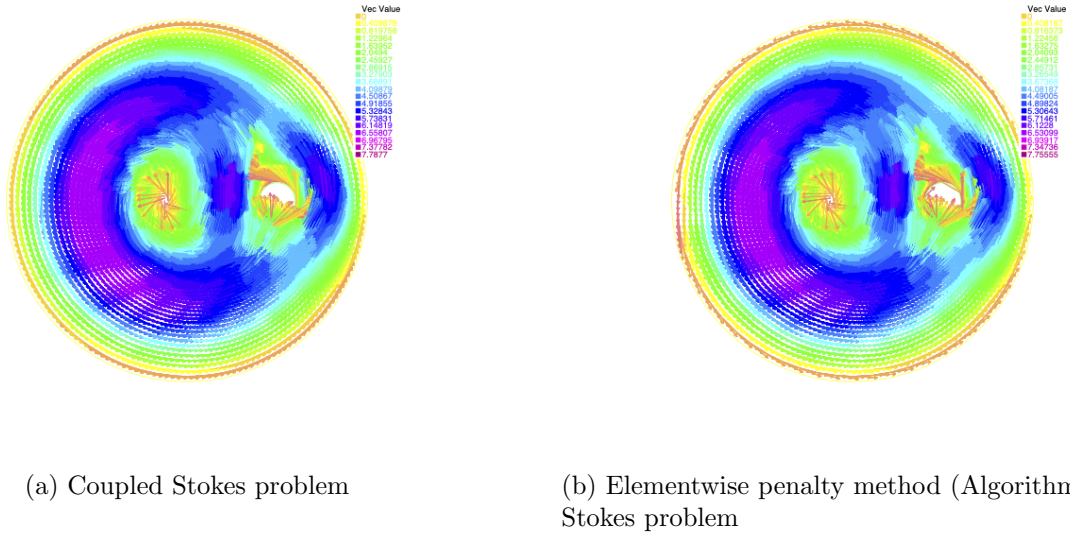


Figure 19: velocity plot of Test 2, comparison between coupled (54) and elementwise penalty system (Algorithm 5)

	constant penalty $\epsilon = 10^{-8}$	elementwise penalty (Algorithm 5)
$\ \nabla \cdot u^h\ ^2$	7.20178e-17	3.7741e-19
average ϵ	1e-8	0.000629366

Table 9: comparison of $\|\nabla \cdot u^h\|^2$ and average value of ϵ between constant penalty and elementwise penalty (Algorithm 1)

3.4.4 Test4: Flow around a cylinder, see Ingram [33], John, Matthies and Rang [40]

This section is an extension of the elementwise penalty method test on the nonlinear Navier-Stokes equation (Algorithm 6). Even though the local condition is only partially satisfied in this test, the global condition is satisfied and well controlled.

The domain Ω is a $[0, 2.2] \times [0, 0.41]$ rectangle. The cylinder S centered at $(0.2, 0.2)$ with

the diameter 0.1 units. The external force $f = 0$, the final time is $T = 8$ and the prescribed viscosity $\nu = 10^{-3}$. The flow has boundary conditions:

$$\begin{aligned} u(x, 0, t) &= u(x, 0.41, t) = u|_{\partial\Omega_S} = (0, 0)^T, \quad 0 \leq x \leq 2.2, \\ u(0, y, t) &= u(2.2, y, t) = 0.41^{-2} \sin(\pi t/8) (6y(0.41 - y), 0)^T, \quad 0 \leq y \leq 0.41. \end{aligned}$$

The mean inflow velocity is $U(t) = \sin(\pi t/8)$ such that $U_{max} = 1$.

Let the initial condition satisfy the steady Stokes problem. The following results using P3 finite element space for velocity. The number of degrees of freedom of velocity is 5091. The mesh is denser near cylinder S, and for this mesh, the shortest edge of all triangles is $min_e h_e = 0.0101291$ and the longest edge $max_e h_e = 0.154404$. The smallest area of element triangle $min_{\Delta} |\Delta| = 3.46846 \times 10^{-5}$ and the largest area of triangle $max_{\Delta} |\Delta| = 0.00773693$. In this test, ϵ lower bound $LowerEps = 10^{-10}$ and global tolerance $TOL = 10^{-5}$. The local tolerance $LocTol_{\Delta} = \frac{1}{2} \frac{TOL^2}{|\Omega|} |\Delta|$ ranges from 10^{-13} to 10^{-15} . Figure 20 is the speed-profile at $T = 2, 4, 5, 6, 7, 8$ for flow with $Re=1000$. We can see the vortex shedding off the back of the cylinder in the test result.

Figure 21 is the plot of $\|\nabla \cdot u^h\|^2$ throughout the whole time interval. The red curve (Algorithm 6 with step repeated) has smaller $\|\nabla \cdot u^h\|^2$ values than the blue curve (without repeating the step). Both global $\|\nabla \cdot u\|$ values are well controlled.

In order to check the local condition, we look at the elementwise value $|\nabla \cdot u^h|_{\Delta}^2 / |\Delta|$ at the final time $T=8$. From Figure 22(a) without repeating the step: $\max \|\nabla \cdot u^h\|_{\Delta}^2 \approx 3 \times 10^{-8} |\Delta| \approx 10^{-11}$ slightly larger than the local tolerance $LocTol_{\Delta}$. From Figure 22(b) with step repeated: $\max \|\nabla \cdot u^h\|_{\Delta}^2 \approx 5 \times 10^{-11} |\Delta| \approx 10^{-14}$ satisfies the local tolerance. For Algorithm 6 with step repeated, the global and local $\|\nabla \cdot u^h\|$ values are smaller but need more computing time compared with Algorithm 6 without retry. For Algorithm 6 without repeating the step, the overall result is satisfying even though the local conditions are only partially satisfied.

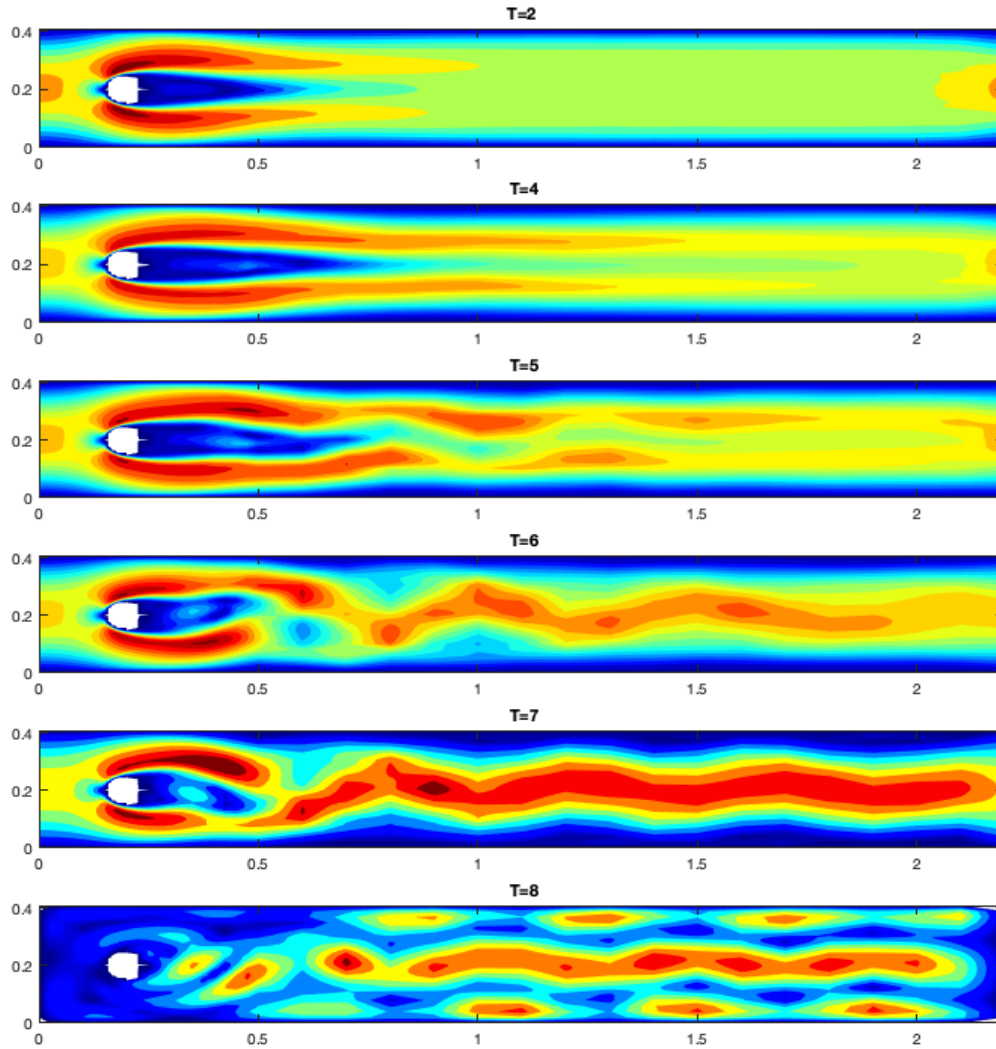


Figure 20: magnitude of velocity field at $T = 2, 4, 5, 6, 7, 8$ of Test 4 Algorithm 6 for NSE, $\Delta t = 0.005$

3.4.4.1 Comparison with constant penalty methods

This section compares Elementwise adaptive penalty (EP) method for the NSE with 1) constant $\epsilon = 10^{-8}\nu$ and 2) constant $\epsilon = k$ penalty methods using the same flow around a

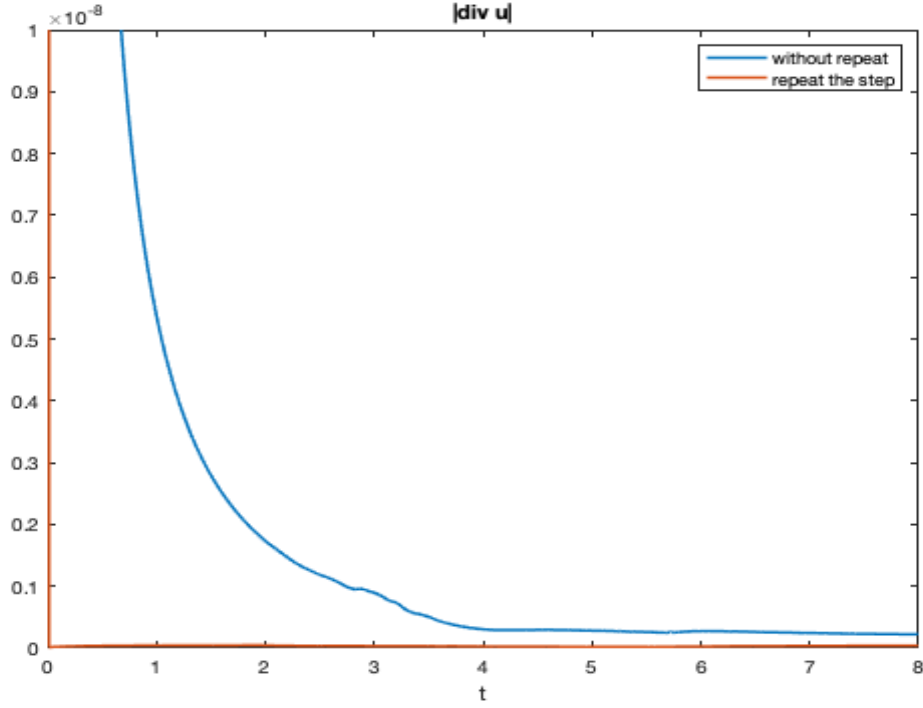


Figure 21: Plot of $\|\nabla \cdot u^h\|^2$ from $T=0$ to $T=8$

cylinder test.

The characteristic values of the flow are the drag coefficient $c_d(t)$, the lift coefficient $c_l(t)$ at the cylinder, and the difference of the pressure between the front and the back of the cylinder at the final time. These coefficients can be computed by

$$\begin{aligned}
 c_d(t) &= -20[(u_t, v_d) + \nu(\nabla u, \nabla v_d) + ((u \cdot \nabla)u, v_d) - (p, \nabla \cdot v_d)], \\
 c_l(t) &= -20[(u_t, v_l) + \nu(\nabla u, \nabla v_l) + ((u \cdot \nabla)u, v_l) - (p, \nabla \cdot v_l)], \\
 \Delta p(T) &= p(0.15, 0.2, T) - p(0.25, 0.2, T),
 \end{aligned}$$

for any function $v_d \in (H^1(\Omega))^2$ with $(v_d)|_S = (1, 0)^T$ and v_d vanishes on all other boundaries and for any test function $v_l \in (H^1(\Omega))^2$ with $(v_l)|_S = (0, 1)^T$ and v_l vanishes on all other boundaries.



(a) $|\nabla \cdot u^h|_{\Delta}^2 / |\Delta|$ at $T_{final} = 8$ without repeating the step (Algorithm 6), the scale is about $10^{-8} \sim 10^{-9}$ (b) $|\nabla \cdot u^h|_{\Delta}^2 / |\Delta|$ at $T_{final} = 8$ with step repeated (Algorithm 6 with retry), the scale is about $10^{-11} \sim 10^{-12}$

Figure 22: result of Test 4 Algorithm 6 for NSE, $\Delta t = 0.005$

According to [38], the reference values for this difference and the maximal values of the drag and lift coefficient are given by:

$$\begin{aligned} t(c_{d,max}) &= 3.93625, & c_{d,max} &= 2.950921575, \\ t(c_{l,max}) &= 5.693125, & c_{l,max} &= 0.47795, \\ \Delta p(8) &= -0.1116. \end{aligned}$$

As in the calculation of drag, lift coefficients, pressure is also an important factor. Here we used two different methods to recover the pressure: 1) by solving the system $\nabla \cdot u^h + \epsilon_{\Delta} p^h = 0$ and 2) by direct calculating $p^h = -1/\epsilon_{\Delta}(\nabla \cdot u^h)$.

Figure 23 is the comparison of $\|\nabla \cdot u^h\|$ using different penalty methods. $\|\nabla \cdot u^h\|$ will not change no matter which pressure recovery methods used. As in the plot, all three penalty methods controlled $\|\nabla \cdot u^h\|$ well and constant $\epsilon = k$ has larger $\|\nabla \cdot u^h\|$ value than both constant penalty $\epsilon = 10^{-8}\nu$ and Elementwise adaptive penalty method (Algorithm 6).

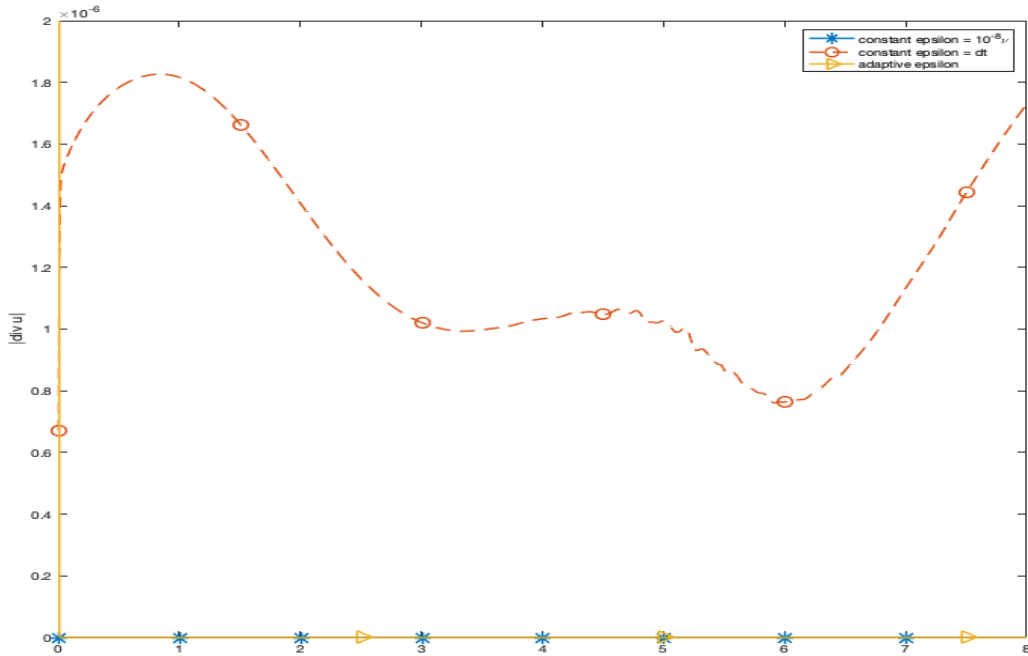


Figure 23: Comparison of $\|\nabla \cdot u^h\|$ using Algorithm 6 and constant penalty methods

Figure 24 is the plot of drag and lift coefficients calculated by solving system $\nabla \cdot u^h + \epsilon_{\Delta} p^h = 0$ and Figure 25 is the plot of drag and lift coefficients calculated by direct calculating $p^h = -1/\epsilon_{\Delta}(\nabla \cdot u^h)$. These two have similar results no matter which pressure recovery methods used. In Figure 24 and Figure 25, constant $\epsilon = k$ and Elementwise adaptive penalty method (Algorithm 6) have similar drag, lift coefficients. The lift coefficient of constant $\epsilon = 10^{-8}\nu$ is very different from the other two penalty methods. And the reason for that is still unknown.

Table 10 is the comparison of values $\Delta p(8)$ calculated using different penalty methods and two different pressure recovery methods. As pressure recovery is still an unknown problem in the penalty method, the results are all not good and far away from the reference value $\Delta p(8) = -0.1116$. For the elementwise adaptive penalty method, pressures recovered by both methods are positive, which could not reflect the pressure drop phenomena we should

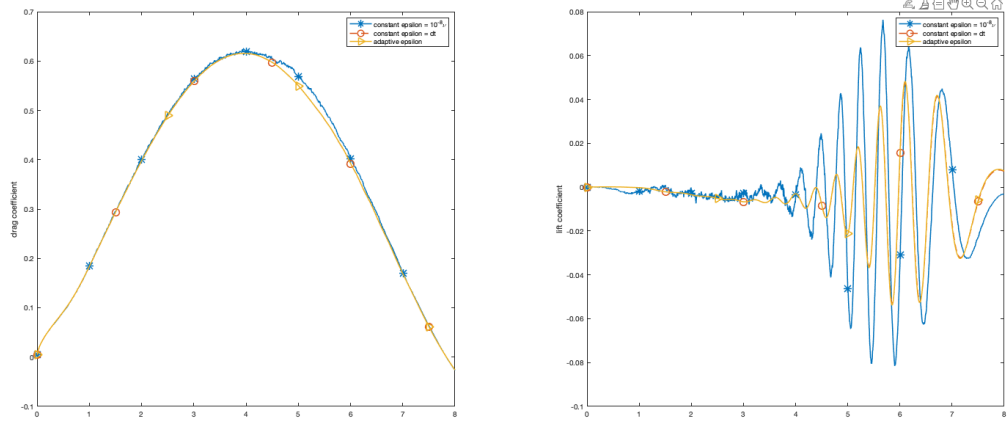


Figure 24: Comparison of drag and lift coefficients, pressure recovery by solving system $\nabla \cdot u^h + \epsilon_{\Delta} p^h = 0$

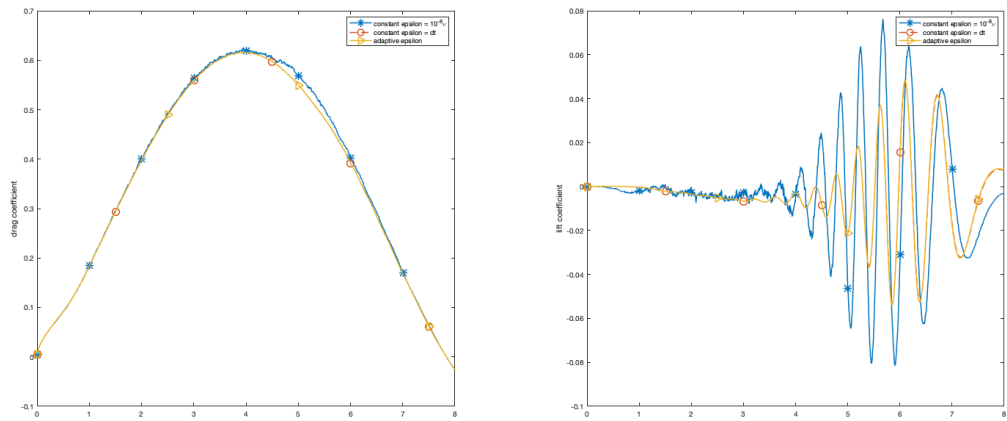


Figure 25: Comparison of drag and lift coefficients, pressure recovery by direct calculating $p^h = -1/\epsilon_{\Delta}(\nabla \cdot u^h)$

observe in this test. The elementwise adaptive penalty method is not accurate in this test.

pressure recovery	constant $\epsilon = 10^{-8}\nu$	constant $\epsilon = k$	Elementwise adaptive penalty
method 1)	-1.20012e-23	-2.86496e-06	2.18002e-11
method 2)	-1.41875e-23	-3.79273e-06	1.89583e-11

Table 10: Comparison of $\Delta p(8)$, method 1) by solving system $\nabla \cdot u^h + \epsilon_{\Delta} p^h = 0$, method 2) by direct calculating $p^h = -1/\epsilon_{\Delta}(\nabla \cdot u^h)$

4.0 Conclusions and future perspectives

The first project presents a stability and error analysis for the adaptive ϵ penalty method. Also, four different algorithms for both constant and variable time-step were introduced. There remain open problems and algorithmic improvements possible in the future. In this thesis, we introduced the adaptive ϵ scheme with a condition from stability analysis that could ensure the stability of the result. It is unclear how sharp this bound is or if the restriction (34) is necessary for all time-steps.

Further, rejecting and repeating steps to guarantee $EST < TOL$ results in violating the restriction (34). The problem has a different optimal ϵ value for different time-step. An algorithm that adapts ϵ and k independently may be inferior to one that relates the step size to the penalty parameter. However, there is no an obvious relation between ϵ and k , so further research may be necessary to find a more efficient doubly adaptive algorithm. The pressure recovered directly from the continuity equation, $\nabla \cdot u + \epsilon p = 0$ (26) is not a good estimate compared with the pressure from the coupled system. We can look into alternate ways to recover the pressure, such as using the Pressure Poisson equation (PPE) see Kean and Schneier [41].

We proposed a new variable ϵ penalty method starting from the Stokes problem in the second project. We proved the stability and derived an error approximation of the new pointwise penalty (PP) (52) on the Stokes problem. Furthermore, at the end we test the algorithm on the Stokes problem and extend it to test the time-dependent nonlinear Navier-Stokes problem using elementwise penalty (EP) (50). This is just the start of this new scheme; there are plenty of improvements possible. Picking the right global tolerance TOL and maximum iteration $MaxIter$ is still a problem to consider. Algorithm 6 is new, and we currently do not know if or not we need to repeat each time-step after setting the new ϵ . We emphasize that our target is the 3d, time-dependent NSE problem for which the method is implemented as Algorithm 6, without appreciable complexity increase over simple, linear constant ϵ penalty methods.

In Chapter 2 and Chapter 3, we focused on the velocity and did not pay much attention

to the accuracy of pressure. Pressure recovery is also a big problem to consider. In Kean and Schneier [41], two different pressure recovery methods are introduced and analyzed. As for the time-dependent problem, only constant time-step schemes are considered in this thesis. To further optimize the algorithm, adding a time filter Guzel and Layton [26] and adapting the time-step is also a promising research direction in the future. Both the stability and error analysis is given based on the assumption that the grad-div term can be replaced by the variational form (51). The numerical analysis based on assumption (49) (i.e. elementwise penalty) is also an interesting problem. Also, other estimators for adjusting $\|\nabla \cdot u\|$ can be considered, e.g. $\|\nabla \cdot u\|/\|u\|$. And here we only develop the adaptive penalty methods based on the Backward Euler method, other higher order time-discretization schemes can be used. Penalty combined with ensemble [36, 35], sparse grad-div [51] or DLN [49, 50] are also some possible directions in the future.

Bibliography

- [1] M. Ainsworth, A. Allendes, G. R. Barrenechea, and R. Rankin. On the adaptive selection of the parameter in stabilized finite element approximations. *SIAM Journal on Numerical Analysis*, 51(3):1585–1609, 2013.
- [2] T. Aubin. *Nonlinear analysis on manifolds. Monge-Ampere equations*, volume 252. Springer-Verlag, 1982.
- [3] J. W. Barrett and W. B. Liu. Finite element approximation of the p-Laplacian. *Mathematics of Computation*, 61(204):523–537, 1993.
- [4] M. Bercovier and M. Engelman. A finite element for the numerical solution of viscous incompressible flows. *Journal of Computational Physics*, 30(2):181–201, 1979.
- [5] C. Bernardi, V. Girault, and F. Hecht. Choix du parametre de pénalisation pour la discrétisation par éléments finis des équations de Navier–Stokes. *Comptes Rendus Mathématique*, 336(8):671–676, 2003.
- [6] C. Bernardi, V. Girault, and F. Hecht. A posteriori analysis of a penalty method and application to the Stokes problem. *Mathematical Models and Methods in Applied Sciences*, 13(11):1599–1628, 2003.
- [7] V. I. Bogachev and M. A. S. Ruas. *Measure theory*, volume 1. Springer, 2007.
- [8] F. Boyer and P. Fabrie. *Mathematical Tools for the Study of the Incompressible Navier-Stokes Equations and Related Models*, volume 183. Springer Science & Business Media, 2012.
- [9] S. C. Brenner and L. R. Scott. *The mathematical theory of finite element methods*, volume 3. Springer, 2008.
- [10] F. Brezzi and M. Fortin. *Mixed and hybrid finite element methods*, volume 3. New York: Springer-Verlag, 1991.
- [11] F. Brezzi and J. Pitkäranta. On the stabilization of finite element approximations of the Stokes equations. In *Efficient solutions of elliptic systems*, pages 11–19. Springer, 1984.

- [12] E. Burman and P. Hansbo. Edge stabilization for the generalized Stokes problem: a continuous interior penalty method. *Computer Methods in Applied Mechanics and Engineering*, 195(19-22):2393–2410, 2006.
- [13] M. A. Case, V. J. Ervin, A. Linke, and L. G. Rebholz. A connection between Scott–Vogelius and grad-div stabilized Taylor–Hood FE approximations of the Navier–Stokes equations. *SIAM Journal on Numerical Analysis*, 49(4):1461–1481, 2011.
- [14] A. J. Chorin. Numerical solution of the Navier-Stokes equations. *Mathematics of computation*, 22(104):745–762, 1968.
- [15] A. J. Chorin. On the convergence of discrete approximations to the Navier-Stokes equations. *Mathematics of computation*, 23(106):341–353, 1969.
- [16] R. Courant. Variational methods for the solution of problems of equilibrium and vibrations. *Lecture notes in pure and applied mathematics*, pages 1–23, 1943.
- [17] V. DeCaria, W. Layton, and M. McLaughlin. A conservative, second order, unconditionally stable artificial compression method. *Computer Methods in Applied Mechanics and Engineering*, 325:733 – 747, 2017.
- [18] V. DeCaria, W. Layton, and H. Zhao. A time-accurate, adaptive discretization for fluid flow problems. *International Journal of Numerical Analysis and Modeling*, 17(2):254–280, 2020.
- [19] H. C. Elman, D. J. Silvester, and A. J. Wathen. *Finite elements and fast iterative solvers: with applications in incompressible fluid dynamics*. Oxford University Press, USA, 2014.
- [20] R. S. Falk. A finite element method for the stationary Stokes equations using trial functions which do not have to satisfy $\operatorname{div} v = 0$. *Mathematics of Computation*, 30(136):698–702, 1976.
- [21] J. A. Fiordilino. On pressure estimates for the Navier-Stokes equations, 2018.
- [22] V. Girault and P. A. Raviart. *Finite element methods for Navier-Stokes equations: theory and algorithms*, volume 5. Springer Science & Business Media, 2012.

- [23] R. Glowinski and A. Marroco. Sur l'approximation, par éléments finis d'ordre un, et la résolution, par pénalisation-dualité d'une classe de problèmes de Dirichlet non linéaires. *ESAIM: Mathematical Modelling and Numerical Analysis - Modélisation Mathématique et Analyse Numérique*, 9(R2):41–76, 1975.
- [24] P. Gresho and R. Sani. *Incompressible flow and the finite element method. Volume 2: Incompressible flow and finite element*. John Wiley and Sons, Inc., New York, NY (United States), 1998.
- [25] M. D. Gunzburger. *Finite element methods for viscous incompressible flows: a guide to theory, practice, and algorithms*. Elsevier, 2012.
- [26] A. Guzel and W. Layton. Time filters increase accuracy of the fully implicit method. *BIT Numerical Mathematics*, 58(2):301–315, 2018.
- [27] Y. He. Optimal error estimate of the penalty finite element method for the time-dependent Navier-Stokes problem. *Math. Comput.*, 74:1201–1216, 07 2005.
- [28] Y. He and J. Li. A penalty finite element method based on the Euler implicit/explicit scheme for the time-dependent Navier–Stokes equations. *Journal of Computational and Applied Mathematics*, 235(3):708 – 725, 2010.
- [29] N. D. Heavner. Locally chosen grad-div stabilization parameters for finite element discretizations of incompressible flow problems. *SIURO*, 7:SO1278, 2017.
- [30] J. G. Heywood and R. Rannacher. Finite element approximation of the nonstationary Navier–Stokes problem. I. regularity of solutions and second-order error estimates for spatial discretization. *SIAM Journal on Numerical Analysis*, 19(2):275–311, 1982.
- [31] J. G. Heywood and R. Rannacher. Finite-element approximation of the nonstationary Navier–Stokes problem. Part IV: Error analysis for second-order time discretization. *SIAM Journal on Numerical Analysis*, 27(2):353–384, 1990.
- [32] T. J. R. Hughes, W. K. Liu, and A. Brooks. Finite element analysis of incompressible viscous flows by the penalty function formulation. *Journal of Computational Physics*, 30(1):1–60, 1979.
- [33] R. Ingram. A new linearly extrapolated Crank-Nicolson time-stepping scheme for the Navier-Stokes equations. *Math. Comp.*, 82(284):1953–1973, 2013.

- [34] E. W. Jenkins, V. John, A. Linke, and L. G. Rebholz. On the parameter choice in grad-div stabilization for the Stokes equations. *Advances in Computational Mathematics*, 40(2):491–516, 2014.
- [35] N. Jiang. A higher order ensemble simulation algorithm for fluid flows. *Journal of Scientific Computing*, 64(1):264–288, 2015.
- [36] N. Jiang and W. Layton. An algorithm for fast calculation of flow ensembles. *Int. J. Uncertain. Quantif.*, 4(4):273–301, 2014.
- [37] V. John. *Large eddy simulation of turbulent incompressible flows: analytical and numerical results for a class of LES models*, volume 34. Springer Science & Business Media, 2003.
- [38] V. John. Reference values for drag and lift of a two-dimensional time dependent flow around a cylinder. *Int. J. Numer. Methods Fluids*, page 777–788, (2004).
- [39] V. John. *Finite element methods for incompressible flow problems*. Springer, 2016.
- [40] V. John, G. Matthies, and J. Rang. A comparison of time-discretization/linearization approaches for the incompressible Navier-Stokes equations. *Comput. Methods Appl. Mech. Engrg.*, 195(44-47):5995–6010, 2006.
- [41] K. Kean and M. Schneier. Error analysis of supremizer pressure recovery for POD based reduced-order models of the time-dependent Navier–Stokes equations. *SIAM Journal on Numerical Analysis*, 58(4):2235–2264, 2020.
- [42] K. Kean, X. Xie, and S. Xu. A doubly adaptive penalty method for the Navier Stokes equations. *arXiv preprint arXiv:2201.03978*, 2022.
- [43] H. Kheshgi and M. Luskin. Analysis of the finite element variable penalty method for Stokes equations. *mathematics of computation*, 45(172):347–363, 1985.
- [44] H. S. Kheshgi and L. E. Scriven. Variable penalty method for finite element analysis of incompressible flow. *International journal for numerical methods in fluids*, 5(9):785–803, 1985.

- [45] A. Labovsky, W. J. Layton, C. C. Manica, M. Neda, and L. G. Rebholz. The stabilized extrapolated trapezoidal finite-element method for the Navier–Stokes equations. *Computer Methods in Applied Mechanics and Engineering*, 198(9-12):958–974, 2009.
- [46] O. A. Ladyzhenskaya and N. N. Uraltseva. *Linear and Quasilinear Elliptic Equations*. Academic Press, New York, London, 1968. MR0244627 (39:5941).
- [47] W. Layton. *Introduction to the Numerical Analysis of Incompressible Viscous Flows*. Society for Industrial and Applied Mathematics, Philadelphia, PA, 2008.
- [48] W. Layton and M. McLaughlin. Doubly-adaptive artificial compression methods for incompressible flow. *Journal of Numerical Mathematics*, 28(3):175–192, 2020.
- [49] W. Layton, W. Pei, Y. Qin, and C. Trenchea. Analysis of the variable step method of Dahlquist, Liniger and Nevanlinna for fluid flow. *Numerical Methods for Partial Differential Equations*, 2021.
- [50] W. Layton, W. Pei, and C. Trenchea. Refactorization of a variable step, unconditionally stable method of Dahlquist, Liniger and Nevanlinna. *Applied Mathematics Letters*, 125:107789, 2022.
- [51] W. Layton and S. Xu. Unconditional stability in 3d of a sparse grad-div approximation of the Navier-Stokes equations. *arXiv preprint arXiv:2112.07062*, 2021.
- [52] W. Layton and S. Xu. Conditioning of linear systems arising from penalty methods. *arXiv preprint arXiv:2206.06971*, 2022.
- [53] W. J. Layton. A nonlinear, subgridscale model for incompressible viscous flow problems. *SIAM Journal on Scientific Computing*, 17(2):347–357, 1996.
- [54] M. Olshanskii and A. Reusken. Grad-div stabilization for Stokes equations. *Mathematics of Computation - Math. Comput.*, 73:1699–1718, 01 2004.
- [55] A. P. Oskolkov. A small-parameter quasi-linear parabolic system approximating the Navier-Stokes system. *Journal of Soviet Mathematics*, 1(4):452–470, 1973.
- [56] A. Prohl. *Projection and quasi-compressibility methods for solving the incompressible Navier-Stokes equations*. Springer, 1997.

- [57] H.-G. Roos, M. Stynes, and L. Tobiska. *Robust numerical methods for singularly perturbed differential equations: convection-diffusion-reaction and flow problems*, volume 24. Springer Science & Business Media, 2008.
- [58] J. Shen. On error estimates of some higher order projection and penalty-projection methods for Navier-Stokes equations. *Numerische Mathematik*, 62(1):49–73, 1992.
- [59] J. Shen. On error estimates of the penalty method for unsteady Navier–Stokes equations. *SIAM Journal on Numerical Analysis*, 32(2):386–403, 1995.
- [60] H. Sohr. *The Navier-Stokes equations: An elementary functional analytic approach*. Springer Science & Business Media, 2012.
- [61] R. Temam. Une méthode d’approximation de la solution des équations de Navier-Stokes. *Bulletin de la Société Mathématique de France*, 96:115–152, 1968.
- [62] R. Temam. Sur l’approximation de la solution des équations de Navier-Stokes par la méthode des pas fractionnaires (I). *Archive for Rational Mechanics and Analysis*, 32(2):135–153, 1969.
- [63] R. Temam. Sur l’approximation de la solution des équations de Navier-Stokes par la méthode des pas fractionnaires (II). *Archive for Rational Mechanics and Analysis*, 33(5):377–385, 1969.
- [64] R. Temam. *Navier-Stokes equations: theory and numerical analysis*, volume 343. American Mathematical Soc., 2001.
- [65] X. Xie. On adaptive grad-div parameter selection. *arXiv preprint arXiv:2108.01766*, 2021.